

**STRUCTURAL AND STRATIGRAPHIC EVOLUTION OF SHIRA
MOUNTAINS, CENTRAL UCAYALI BASIN, PERÚ**

A Thesis

by

JAIME ORLANDO SANCHEZ ALVAREZ

Submitted to the Office of Graduate Studies of
Texas A&M University
in partial fulfillment of the requirements for the degree of

MASTER OF SCIENCE

December 2007

Major Subject: Geology

**STRUCTURAL AND STRATIGRAPHIC EVOLUTION OF SHIRA
MOUNTAINS, CENTRAL UCAYALI BASIN, PERÚ**

A Thesis

by

JAIME ORLANDO SANCHEZ ALVAREZ

Submitted to the Office of Graduate Studies of
Texas A&M University
in partial fulfillment of the requirements for the degree of

MASTER OF SCIENCE

Approved by:

Chair of Committee,	John R. Hopper
Committee Members,	Wayne M. Ahr
	Walter B. Ayers, Jr.
Head of Department,	John H. Spang

December 2007

Major Subject: Geology

ABSTRACT

Structural and Stratigraphic Evolution of Shira Mountains, Central Ucayali Basin, Perú.

(December 2007)

Jaime Orlando Sanchez Alvarez, B.S., Universidad Industrial de Santander

Chair of Advisory Committee: Dr. John R. Hopper

The Ucayali Basin is a Peruvian sub-Andean basin that initially formed during the extensive tectonics of the Early Paleozoic. Originally, the Ucayali Basin was part of a larger basin that extended east of the current Andean chain along the Peruvian territory. Subsequently, this large basin was divided into many smaller sub-Basins during the Andean Orogeny. Today, the basin covers an area of about 140,000 km², and it is morphologically defined by two well-differentiated structural features: the sub-Andean fold and thrust belt (SFTB) to the west and the Amazon plain and Brazilian shield to the east. It is limited to the north and south by the Contaya and Fitzcarrald Arches respectively, the Andes to the west and the Brazilian Shield to the east. These structural features acted as favorable elements to add sediments and to contribute to the structural development of this basin. The sedimentary section of the basin varies in thickness from 1 to 10 km, with ages of strata ranging from the Paleozoic to Quaternary. The strata were deposited in deep and shallow marine as well as transitional and fluvial continental environments. The most important phase of marine sedimentation was initiated with the transgression of the Cretaceous sea (Aptian –

Albian) over the irregular paleogeography defined by morphologic highs and peneplains.

Tectonic features of the basin show structural deformations parallel to the Andean front, where overturned structures are observed. These are commonly cut by thrusts and laterally displaced by strike-slip faults.

To better understand the development of the Shira Mountains in the central part of the Ucayali Basin, the structural and stratigraphic relationships were mapped out using a dense grid of 2D seismic reflection data and well log control. Three regional E-W cross sections were constructed and restored to the top of the Cretaceous to determine the nature of deformation and faulting during the Paleozoic and Mesozoic.

The reconstructions show that Shira Mountains fault was initially a major normal fault bounding a half graben. The fault was reactivated by later compression as a thick-skinned thrust fault that detaches between 21 and 24 km depth. Reactivation occurred during Upper Miocene between 7.2 and 5.3 Ma, corresponding to the Quechua 3 compressive phase of Andean Orogeny. The shortening of the central Ucayali Basin determined by the reconstructed cross sections ranges between 3 and 5.5%.

DEDICATION

This thesis is dedicated to
my mom Odilia,
the memory of my dad Hernando,
my beloved wife Adriana,
my sweet and intelligent son, Diego Alejandro,
my brothers and sisters, Javier, Cristina, Nestor and Claudia, and
my beautiful niece Maria Camila

ACKNOWLEDGMENTS

I would like to thank the chair of my committee, Dr. John Hopper for his guidance, and help through my research. It is an honor to be his first student at Texas A&M University. Thanks also to my committee members, Dr. Walter Ayers and Dr. Wayne Ahr for the time invested reviewing my proposal and my thesis final document.

I would also like to thank the Integrated Ocean Drilling Program IODP for the financial support throughout my master's degree and for the opportunity to be part of this great scientific program for two years and to Perupetro S.A. for providing the data and information for this research. I want to express my appreciation to all the faculty and staff of the Department of Geology and Geophysics of Texas A&M University, especially to Dr. John Spang for serving as my committee member for my thesis defense and for all his support during my studies at this amazing University as well. Thanks to my friends and classmates particularly to Fernando Rodriguez for teaching me how to use 2DMove and for his help and suggestions to refine some of my thesis models.

Finally, thanks to my mother for her encouragement, to my wife and son for their love and for being always with me and to my brother Javier for all his support at those moments when I truly needed him.

TABLE OF CONTENTS

	Page
ABSTRACT	iii
DEDICATION	v
ACKNOWLEDGMENTS	vi
TABLE OF CONTENTS	vii
LIST OF FIGURES	ix
 CHAPTER	
I INTRODUCTION	1
Objectives	4
Data Available	5
II BACKGROUND	10
Regional Tectonic Setting	10
Stratigraphy and Sedimentary Environments	19
III METHODOLOGY	26
Loading and Interpretation of Seismic Data and Well Logs	26
Model Construction and Interpretation of Results	31
IV RESULTS	32
Stratigraphic Evolution	32
Structural Evolution	47
V CONCLUSIONS	79
REFERENCES CITED	82

	Page
APPENDIX 1	92
APPENDIX 2	93
APPENDIX 3	94
APPENDIX 4	95
APPENDIX 5	96
APPENDIX 6	97
APPENDIX 7	98
APPENDIX 8	99
APPENDIX 9	100
APPENDIX 10	101
APPENDIX 11	102
APPENDIX 12	103
APPENDIX 13	104
VITA	105

LIST OF FIGURES

FIGURE		Page
1	Location of the Central Ucayali Basin and Shira Mountains, Perú	2
2	Seismic Lines and Wells Location.....	9
3	Regional Morpho-Structural Units Map	11
4	Schematic Model of Extensional Tectonic in Central Andes During the Late Permian to Early Tertiary	14
5	Composite Diagram Showing Deformation Episodes in Relation to Sedimentation and Magmatism in Central Perú (10°30'S to 13°S lat.)	17
6	Generalized Stratigraphic Section of the Central Ucayali Basin	21
7	Mesozoic–Cenozoic Stratigraphic Synopsis of the Central Andes from 10°S to 8°30'S.....	24
8	Seismic Line NP31	28
9	3D “Type” Model	29
10	Well Log Correlations Location	30
11	Geologic Map Central Ucayali Basin	33
12	Well Correlation 2.....	36
13	Well Correlation 3.....	37
14	Flattened Seismic Line G609.....	39
15	Well Correlation 1.....	41
16	Seismic Line W74-53	43

FIGURE		Page
17	Seismic Line G609.....	45
18	Copacabana Group Time-Structure Map	49
19	Copacabana Group 3D Time Structure Model	50
20	Base of Cretaceous Time-Structure Map	51
21	3D Time-Structure Model of Top of Copacabana Group Pinching-out Towards the Base of the Cretaceous	52
22	Base of the Cretaceous 3D Time-Structure Model	53
23	Top of Mesozoic Time-Structure Map	54
24	Top of Mesozoic 3D Time-Structure Model	55
25	Permian Isochore Map	56
26	Cretaceous Isochore Map.....	57
27	3D Geologic Map and Seismic Lines NP31, G603, G450 and W74-29.....	61
28	Balanced Structural Profile A-A'	62
29	Balanced Structural Profile A-A' With Vertical Exaggeration	63
30	3D Geologic Map and Seismic Lines G609 and W75-89.....	65
31	Balanced Structural Profile B-B'	66
32	Balanced Structural Profile B-B' With Vertical Exaggeration.....	67
33	3D Geologic Map and Seismic lines 96ENE01, 96ENE12 and HIS15	69
34	Balanced Structural Profile C-C'	70
35	Balanced Structural Profile C-C' With Vertical Exaggeration.....	71
36	Epicentres and Hypocentres of Earthquakes in Central Perú	73

FIGURE		Page
37	Seismic Line W74-29	76
38	Self-Similar Folding Model	77
39	Seismic Line W74-66	78

CHAPTER I

INTRODUCTION

The Ucayali Basin is located in the central Andes in a region known as sub-Andean foothills or sub-Andean basins in central-east Perú (Figure 1). It is 250 km wide, extending from the Andean fold and thrust belt in the west to the Brazilian Shield in the east and is 650 km in length from the Contaya Arch in the north to the Fitzcarrald Arch in the south (Perupetro, 2003). This study focuses on the central area of the Ucayali Basin where the Shira Mountains form a prominent structural high that plays a key but poorly understood role in the development of the basin. The region experienced a complex structural evolution as a consequence of multiple regional extensional and compressional tectonic events that began in the early Paleozoic, or earlier (Gil, 2001).

From the morpho-structural point of view, the Ucayali Basin is complicated as a result of the emplacement of the Shira Mountains which divides the basin into two sub-basins: the Pachitea sub-Basin to the west and the Ucayali Basin to the east (Martinez, 1975).

In southern Perú and northern Bolivia, the sub-Andean foothills are dominated by thrust systems that are clearly observed in the study area (Baby et al., 1997, 1999, 2005; Gil et al., 1999, 2001). The basin contains major basement-involved thrust faults that in many cases are thought to be reactivated Paleozoic normal faults. These thrust systems dip west, toward the Pachitea sub-Basin (Gil, 2002).

This thesis follows the style of American Association of Petroleum Geologist Bulletin.

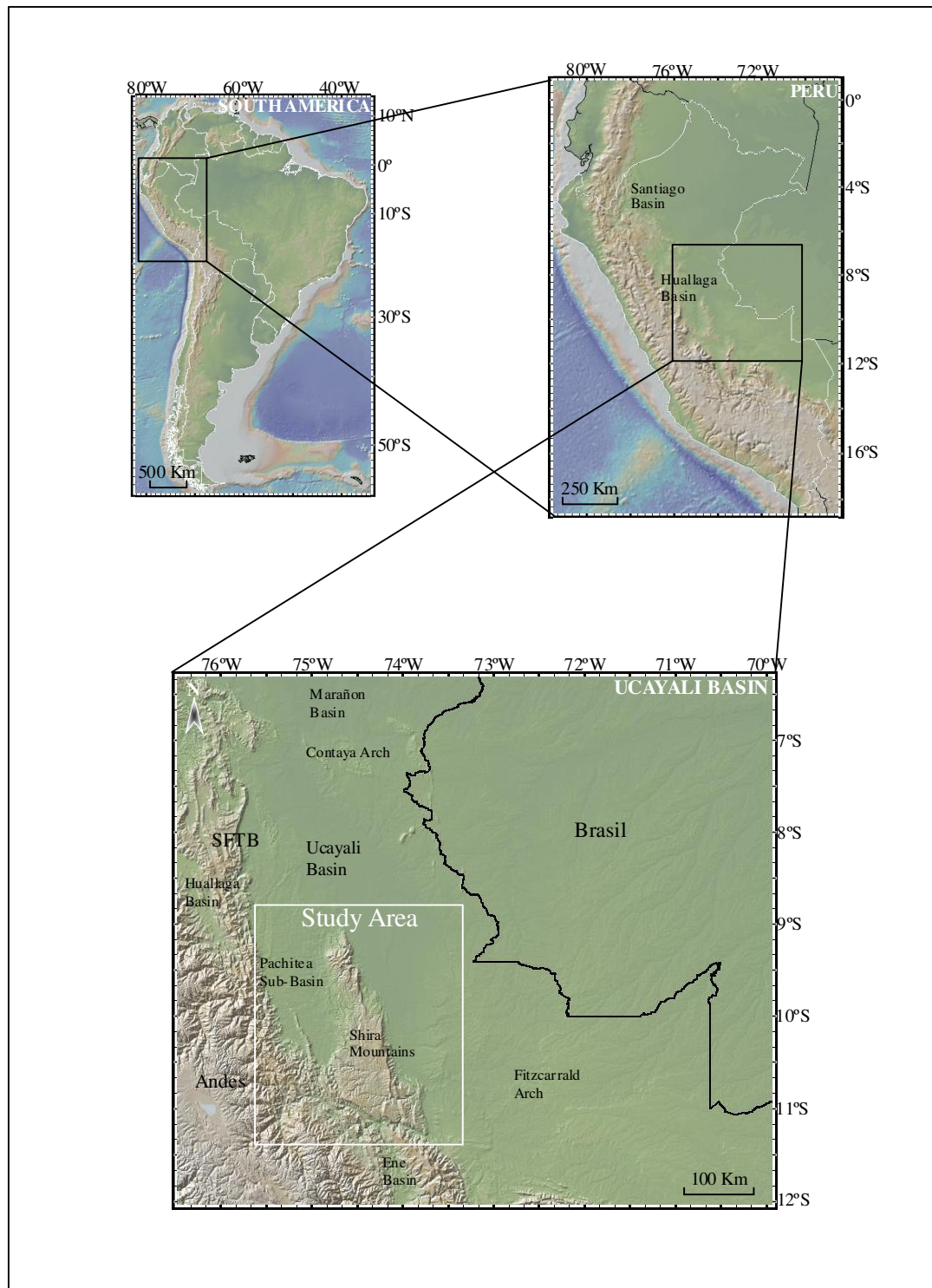


Figure 1. Location of the central Ucayali Basin and Shira Mountains, Perú. (Digital Elevation Model, DEM from GeoMapApp)

The Ucayali Basin includes thick sedimentary sequences that also occur in the Marañón Basin north of Perú and the Acre and Solimoes Basins of Brazil. These sedimentary sequences pinch-out onto the Brazilian and Guiana Shields (Martinez, 1975). Seismic and well data indicate that a fairly complete Paleozoic, Mesozoic and Cenozoic sedimentary succession was deposited in the basin. However, a discontinuous preservation of the pre-Cretaceous sedimentary section overlying the crystalline basement in some areas, for instance the central eastern Ucayali Basin demonstrates an irregular tectonic evolution that involved the pre-Andean deformation from the Ordovician to the Middle Jurassic (Megard, 1984 and Perupetro, 2003).

The main hydrocarbon source rocks are the Pucara Formation to the north and Tarma- Copacabana Groups in the south. The reservoirs are mostly Upper Permian lacustrine, eolian, and marine sandstones and Cretaceous continental and marine sandstones (<http://mirror.perupetro.com.pe/Library/Ucayali%20C.pdf>). Hydrocarbon exploration began in the 1930's and the first well drilled in the Ucayali Basin was Ganso Azul #1 in 1937 to test the Agua Caliente structure located north of the study area. Since then this basin has been continuously explored and exploited by a diverse group of national and international oil companies although work was suspended during the 1960's and 1970's for political reasons. In the late 1970's, oil companies renewed their interest in the region, and hydrocarbon exploration and exploitation has been under continuous since then (Perupetro, 2003).

OBJECTIVES

There are few published studies of the Shira Mountain range and its influence on both the structural development and the petroleum systems of the Ucayali Basin. Most previous studies focused on the hydrocarbon potential and many are not available in the public domain.

Geologic and geophysical data were interpreted to understand the structural and stratigraphic development of the Shira Mountains and the different factors involved in its evolution. The main purpose of this study was to determine the structural framework and to understand the stratigraphy of the Shira Mountains and its relationship with the development of the Ucayali Basin. The objectives in this study are to: 1) understand the structural and stratigraphic evolution of Shira Mountains and Central Ucayali Basin; 2) present geological evidence for the most important tectonic phases that affected the development of the Shira Mountains and Central Ucayali Basin, especially the tectonic inversion; 3) associate the stratigraphy identified in this area with the major marine regressions and transgressions from the Permian to the Paleogene previously identified in different studies; 4) determine the depth of the detachment of the main thrust faults in the study area.

DATA AVAILABLE

This project is possible thanks to the cooperation of Perupetro S.A., the Peruvian national petroleum company. Perupetro S.A. provided the seismic data, well logs, and field reports, as well as other scientific reports and information.

The first step was to load the 2D seismic survey and well log data into KINGDOM Suite. This software was used to interpret horizons and structures and for well log correlations. Stratal patterns indicating growth structures and deformation such as sediment folding were identified. Where possible the well logs were tied to the seismic data using synthetic seismograms. This permitted the identification of key geologic formations and time boundaries on the seismic lines and enabled us to establish the stratigraphic and structural evolution of the basin in relation to the Shira Mountains. The data and information available for this study are listed below.

1. 2D Seismic data (available in SEG-Y format, approximately 110 lines, 0 phase with about 7,000 km of total length) (Table 1 and Figure 2)
2. Data for logs, 17 Wells (available in LAS format) and well final reports (including lithologic logs, well tests, etc.) for Ucayali Basin, Pachitea basin and Ene basin (Figure 2).
3. Fieldwork reports from the western and eastern flank of Shira Mountains and Ucayali Basin (Perupetro S.A, OXY and others.)
4. Detailed geologic maps from Ucayali Basin (Perupetro S. A. and INGEMMET)
5. Satellite images and DEMs from Shira Mountains (NASA and GeoMapApp)

Table 1. 2D Seismic lines list

Line Name	Line Length (m)	Process	Datum (m)	Rep. Velocity m/s
AC-90-02	28527	Migrated	200	2000
AC-90-04	23440	Migrated	200	2000
AC-90-06	18946	Migrated	200	2000
G-413E	8097	Migrated	200	2000
G-414	33604	Migrated	200	2000
G-448S	21747	Migrated	200	2000
G-450	54975	Migrated	200	2000
G-459	22674	Migrated	200	2000
G-601	76208	Migrated	200	2000
G-602	73942	Migrated	200	2000
G-603	64103	Migrated	200	2000
G-604W	53235	Migrated	200	2000
G-604E	67003	Migrated	-	-
G-605E	34355	Migrated	200	2000
G-605W	52619	Migrated	200	2000
G-606E	28511	Migrated	200	2000
G-606W	49445	Migrated	200	2000
G-607E	40634	Migrated	200	2000
G-607W	18642	Migrated	200	2000
G-608E	34856	Migrated	200	2000
G-608W	23505	Migrated	200	2000
G-609	53642	Migrated	200	2000
G-610	49699	Migrated	200	2000
G-611	55224	Migrated	200	2000
G-612	130121	Migrated	200	2000
G-613N	48233	Migrated	-	-
G-613S	64762	Migrated	200	2000
G-618	33969	Migrated	-	-
G-619	31572	Migrated	-	-
G-620	36113	Migrated	-	-
G-622	34144	Migrated	-	-
G-1056	13571	Migrated	200	2000
G-1084	13634	Migrated	200	2000
MP01-97	16006	Migrated	-	-
MP02-97	10503	migrated	-	-
MP03-97	15428	migrated	-	-
MP06-97	11497	migrated	-	-
NP-28	14448	Migrated	-	-
NP-30	13254	Migrated	200	2000
NP-34	29436	Migrated	200	2000
NP-36	38078	Migrated	200	2000

Table 1 (continued)

Line Name	Line Length (m)	Process	Datum (m)	Rep. Velocity m/s
35-REP99-101	36065	Migrated	350	2000
35-REP99-126	48079	Migrated	350	2000
35-REP99-128	48074	Migrated	350	2000
82-UBA-01	42876	Migrated	350	2000
82-UBA-02	41173	Migrated	-	-
82-UBA-03A	41302	Migrated	350	2000
82-UBA-06	50972	Migrated	350	-
85-UB-59	52457	Migrated	350	2000
85-UB-595	19828	Migrated	-	-
85-UB-61	105413	Migrated	350	2000
85-UB-615	19984	Migrated	-	-
85-UB-62	83623	Migrated	350	2000
85-UB-64	58747	Migrated	350	2000
85-UB-108	75565	Migrated	350	2000
W74-29	58877	Stack	-	-
W74/75-30	37957	Migrated	-	-
W74-31	61985	Migrated	-	-
W74-32	60438	Stack	-	-
W74-33	61233	Migrated	-	-
W74-34	44549	Migrated	-	-
W74-35	41710	Stack	-	-
W74-36E	81441	Stack	-	-
W74-53	50811	Stack	-	-
W74-66	40358	Migrated	-	-
W74-68	13378	Migrated	-	-
W74-75	20021	Stack	-	-
W74-75A	16176	Stack	-	-
W75-67	16701	Migrated	-	-
W75-74	16229	Stack	-	-
W75-76A	15419	Migrated	-	-
W75-77	26779	Migrated	-	-
W75-87A	20197	Migrated	-	-
W75-89	30878	Migrated	-	-
W75-91	44118	Migrated	-	-
W75-92	19897	Migrated	-	-
W75-94A	15181	Stack	-	-
W75-95	42198	Migrated	-	-
W75-96	34546	Migrated	-	-
W75-100	21412	Migrated	-	-

Table 1 (continued)

Line Name	Line Length (m)	Process	Datum (m)	Rep. Velocity m/s
W75-101	7838	Migrated	-	-
W75-102	8764	Migrated	-	-
W75-103	30231	Migrated	-	-
96ENE01	23284	Migrated	400	-
96ENE02	34955	Migrated	400	-
96ENE03	23178	Migrated	400	-
96ENE05	34349	Migrated	400	-
96ENE07	31052	Migrated	400	-
96ENE09	34659	Migrated	400	-
96ENE12	12132	Migrated	400	-
96ENE105	35372	Migrated	400	-
HIS9	116217?	Migrated	-	-
HIS11	115412?	Stack	-	-
HIS15	76961	Stack	-	-
HIS20	79930	Migrated	-	-
HIS21	70015	Migrated	-	-
HIS23	46496	Migrated	-	-
HIS27SW	19105	Migrated	-	-
HIS33	50535	Migrated	-	-
HIS35	51550	Migrated	-	-
HIS8A	19172	Migrated	-	-
HIS8B	54897	Migrated	-	-
87-18	42205	Migrated	350	2000
87-18E	63510	Migrated	350	2000
87-20.4	21970	Migrated	350	2000

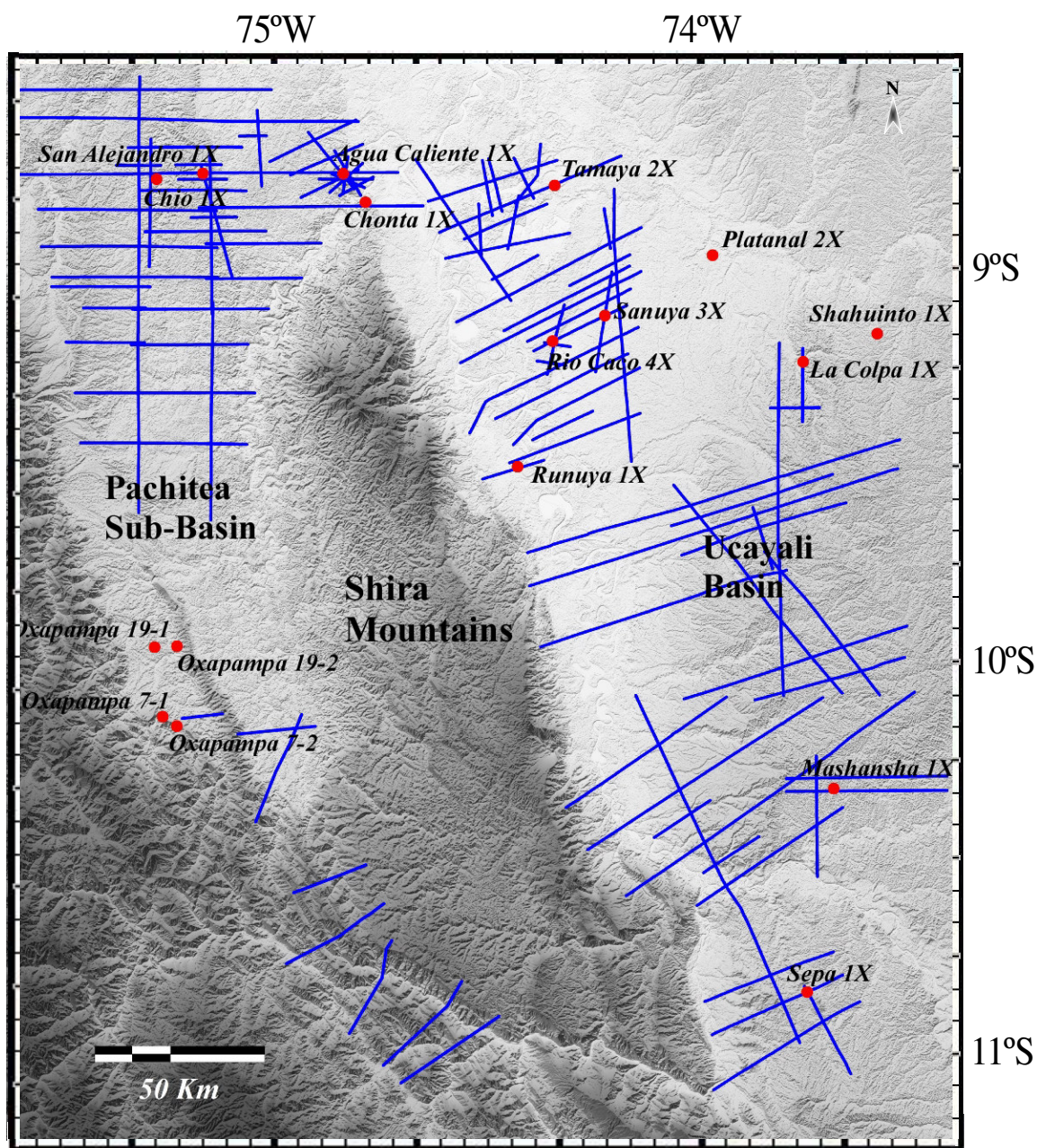


Figure 2. Seismic lines and wells location. (DEM from ftp://e0srp01u.ecs.nasa.gov/srtm/version2/SRTM3/South_America)

CHAPTER II

BACKGROUND

REGIONAL TECTONIC SETTING

The present tectonics of the Ucayali Basin and the Shira Mountains are directly related to the development of the Andean Mountain Belt. The Andean Chain is the major morphological feature of the South American Continent. It runs 8000 km along the western border of the South American Plate. At the plate scale, the Andes resulted from compression related to the eastward subduction of the Nazca plate beneath the western South American margin (Jacques, 2003a). The mountain belt can be divided into three segments of distinct orientation separated by two major bends.

The NNE-SSW trending Colombian-Ecuadorian segment (12°N - 5°S) is 2000 km long and includes part of northernmost Perú and westernmost Venezuela. It is bounded to the south by the Huancabamba Bend, which separates it from the Peruvian segment (Megard, 1984). The Peruvian segment (5°S - 18°S) is 2000 km long and trends NW-SE. It includes central and southern Perú and northern Bolivia, and it is separated from the Chilean segment by the Arica Bend. The Chilean segment (18°S-56°S) is 4000 km long and trends N-S (Jaillard, et. al., 2000). The Peruvian segment exhibits five main longitudinal morpho-structural units. These are, the coastal area, Western Cordillera, Eastern Cordillera, the sub-Andean Zone and Eastern Lowlands

(Figure 3) (Jaillard et al., 2000). This study focuses on the sub-Andean Zone and Eastern Lowlands, where the Ucayali Basin and the Shira Mountains are located.

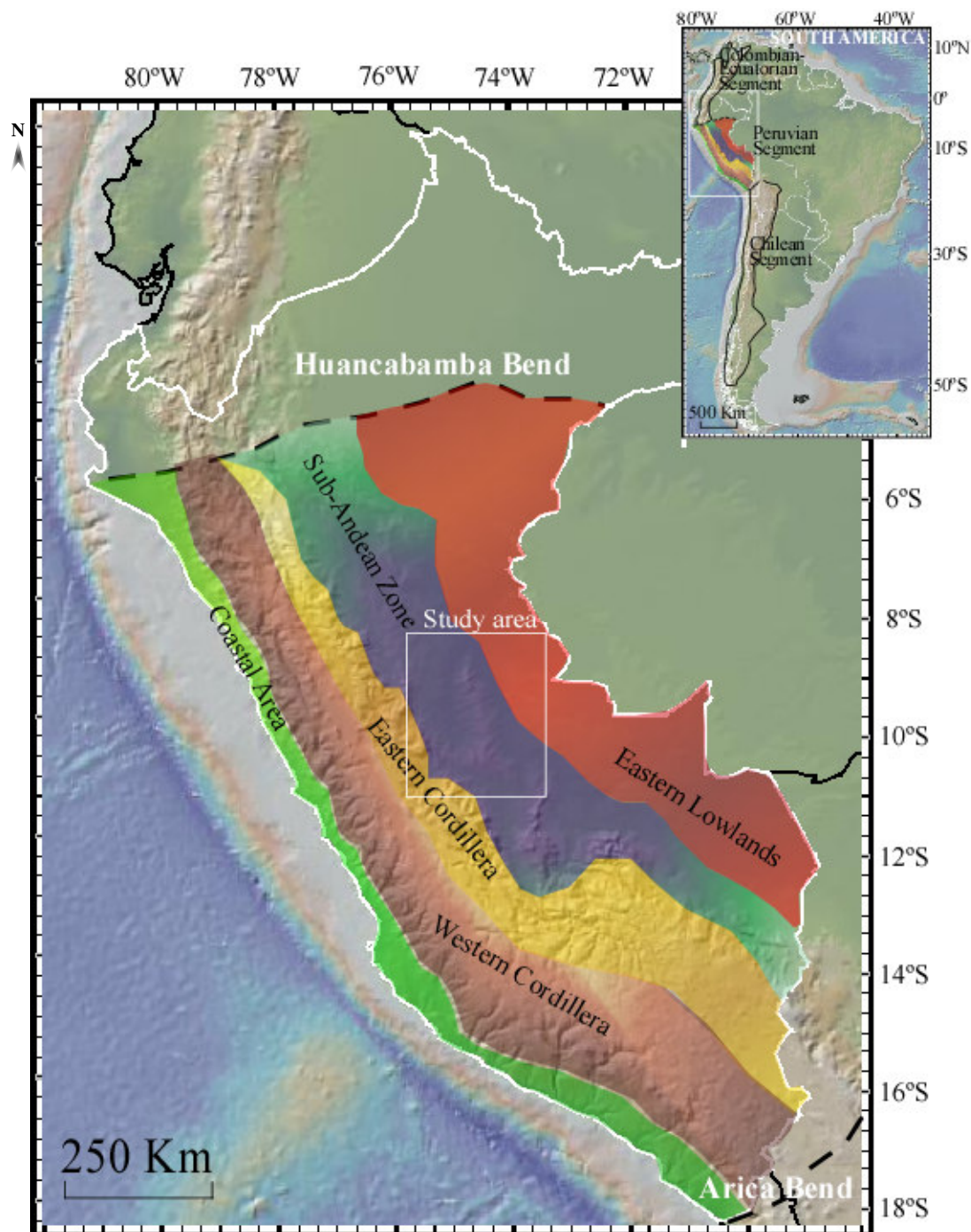


Figure 3. Regional morpho-structural units map. (Based on Jaillard et al., 2000, DEM from GeoMapApp)

The Ucayali Basin is one of several sub-Andean basins located to the east of the SFTB. They are a series of foreland style basins with individual characteristics but genetically related by the major tectonic events that took place along the South American continent. The Ucayali Basin has a complex tectonic history with several extensional and compressional episodes from the Paleozoic to the present as summarized below.

Within the central Ucayali Basin, the Shira Mountains represent the most prominent tectonic element. These mountains divide the southern basin into a larger eastern portion, and a western portion that includes the Oxapampa/Ene fold and thrust belt and the Pachitea sub-Basin. Perupetro (2003) and Elf (1996) interpreted the Shira Mountains as forming from an ancestral horst block that was part of a Paleozoic rifting event. The internal structure of the Shira Mountains is not well documented; however, previous studies have suggested that is a very large flower structure (Perupetro, 2003). This thesis has been built on testing the various hypotheses about the structure of the Shira Mountains and central Ucayali Basin; results are discussed in the chapters IV and V.

The alternation between magmatic, tectonic and depositional periods led to complex lateral disparity, both from east to west and north to south and resulted in a wide range of regimes for the development of mineral deposits (Fornari and Hérail, 1991) and hydrocarbon generation and accumulation (Tankard et al., 1995).

According to Carlier et al. (1982), during the Late Permian to the Early Triassic, intense magmatic activity took place along the eastern area of Perú (Eastern Cordillera

region) associated with extensional and transtensional conditions as a consequence of the Pangaea break-up (arc-related wrench and retro-arc extensional regimes) affecting most of the Peruvian territory including the sub-Andean basins. The main axis of the rift system appears to coincide with the axis of the Eastern Cordillera (Debelmas and Trottereau, 1967). This period included significant brittle deformation, basement-involved faulting and block movements (Jaillard et al., 2000). This tectono-magmatic event is related to the volcanic series of the Mitu Group and it is known as the Mitu rifting.

The extensive felsic magmatism that characterizes this cycle was originally interpreted to be the product of crustal extension (Audebaud, 1976). Later studies showed that the felsic magmatism is the result of an early cycle of subduction during the Carboniferous (Figure 4.a), followed by acid-non-orogenic magmatism associated with active extensional faulting between the Permian and Triassic (Figure 4.b, Ramos, 2000 and Holth, 2005).

The development of a subduction zone during late Permian to early Triassic times is supported by geological information along the Peruvian eastern Range, where a Permo-Triassic continental volcanic arc has been mapped. The Triassic rift system has a general NW-SE trend that was controlled by basement fabrics. The rifts were filled with red-beds and volcanic rocks of different composition (Gutiérrez-Marco et al., 1992).

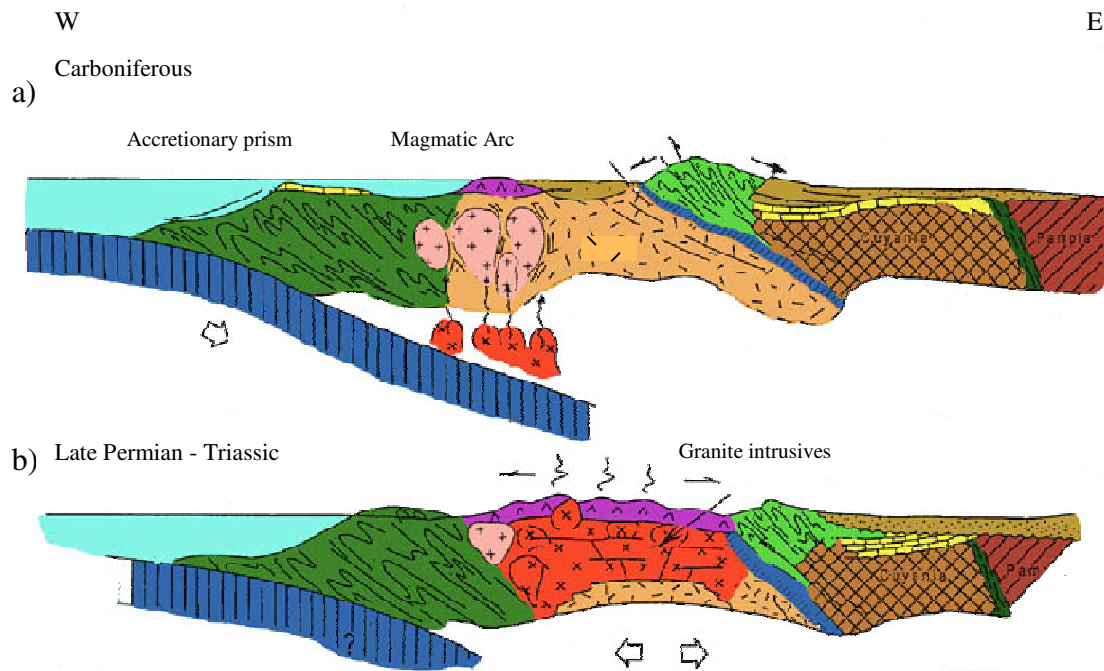


Figure 4. Schematic model of extensional tectonic in central Andes during the Late Permian to Early Tertiary. a) The early subduction of the Nazca Plate beneath the South American Plate occurred during the Carboniferous creating an accretionary prism. b) An Extensional tectonic phase associated with magmatism occurred during the Late Permian to Early Triassic. (Modified from Mpodozis and Ramos, 1990 in <http://www.geo.arizona.edu/geo5xx/geo527/Andes/tectonicandes.html>)

The period from Late Triassic (Norian) to the Early Jurassic (Sinemurian) was characterized by relative tectonic and magmatic quiescence (Barros et al., 1991), followed by active subduction of the Pacific plate beneath the western Peruvian margin, related magmatism and sinistral wrenching movements along NW-SE faults from Early Jurassic (Sinemurian) and the Early Cretaceous (Gerbault et al., 2005). Sempere and others, (2002) show that syn-rift and probably thermal sag deposition related with retro-arc extension must have occurred in the Eastern Cordillera domain during this time as a consequence of lithospheric thinning and consequent pluton emplacement. The absence

of Late Triassic –Jurassic sequences as well as onlap of Early Cretaceous sediments on Paleozoic units demonstrates that this area was uplifted and eroded over this time interval resulting in regional basin inversion.

The Andean tectonic system was initiated in the upper Early Cretaceous (Albian) with the subduction of the Nazca plate beneath the South American plate along the western margin of Perú (Soler, et al., 1989; Jaillard, et al., 1990 and Jacques, 2003a), which occurred at the same time as Pangaea breakup (Barros and Carneiro, 1991).

The Andean orogenic period consisted of at least 6 distinct compressional phases from Albian to late Miocene. Deformation migrated progressively toward the Amazonian foredeep. The major Andean structures in central and northern Perú are related to the Eocene (Incaic), early Miocene (Quechua **1**) and late Miocene (Quechua **3**) phases. The SFTB is related to the Quechua 3 phase. In the SFTB imbricate thrusts merge at depth in large decollement faults. Gravity sliding does not play a dominant role, for these faults have to be rooted westward in the pre-Andean basement (Mégard, 1984). The corresponding crustal shortening played a significant part in the creation of the sialic root of the Andes

The kinematic evolution of the South American orogenies resulted from a combination of factors (Jacques, 2003b). According to Jaillard et al. (2000) these include: a westward shift of the overriding South American continental plate, driven by South Atlantic ridge push from the Albian onwards and resulting in Andean crustal shortening and slab retreat; the age of subducted oceanic crust; an increase in convergence rate between the Nazca oceanic and South American continental plates and

its relationship to subsidence rates in both the fore-arc and foreland regions; changes in the convergence direction of the colliding plates; the angle of dip of the subducting slab and its potential for basal erosion of the overriding plate; the “choking” of the subduction system by the arrival of continental crustal fragments, aseismic ridges and seamounts.

The first phase of compression occurred in the Late Albian and folded the west Peruvian basin where syntectonic gabbros were emplaced (Cobbing, et al., 1981). This period is called the Mochica phase, to be consistent with the nomenclature used in Perú since Steinmann’s work in 1929 (Mégard, 1984).

The second phase of compression is called the Peruvian phase and occurred during the Santonian, and is the first episode of widespread deformation that took place in the Peruvian territory. During this period marine sedimentation was replaced by continental red bed sedimentation (Figure 5). In the eastern Cordillera, the Peruvian folding affected an isolated area with a NW-SE trend where the aggregate thickness of Paleozoic and Mesozoic sediments may be locally as much as 9000 m (Mégard, 1979).

The third phase, called the Incaic phase, is the main period of shortening in the Peruvian and Bolivian Andes and occurred during the Middle to Late Eocene. The highly deformed north-eastern belt of the western Cordillera in central and northern Perú developed at this time (Mégard, 1984). These structures were eroded and unconformably overlain by coarse clastic and volcanic rocks dated at about 40 Ma (Farrar, et al., 1988).

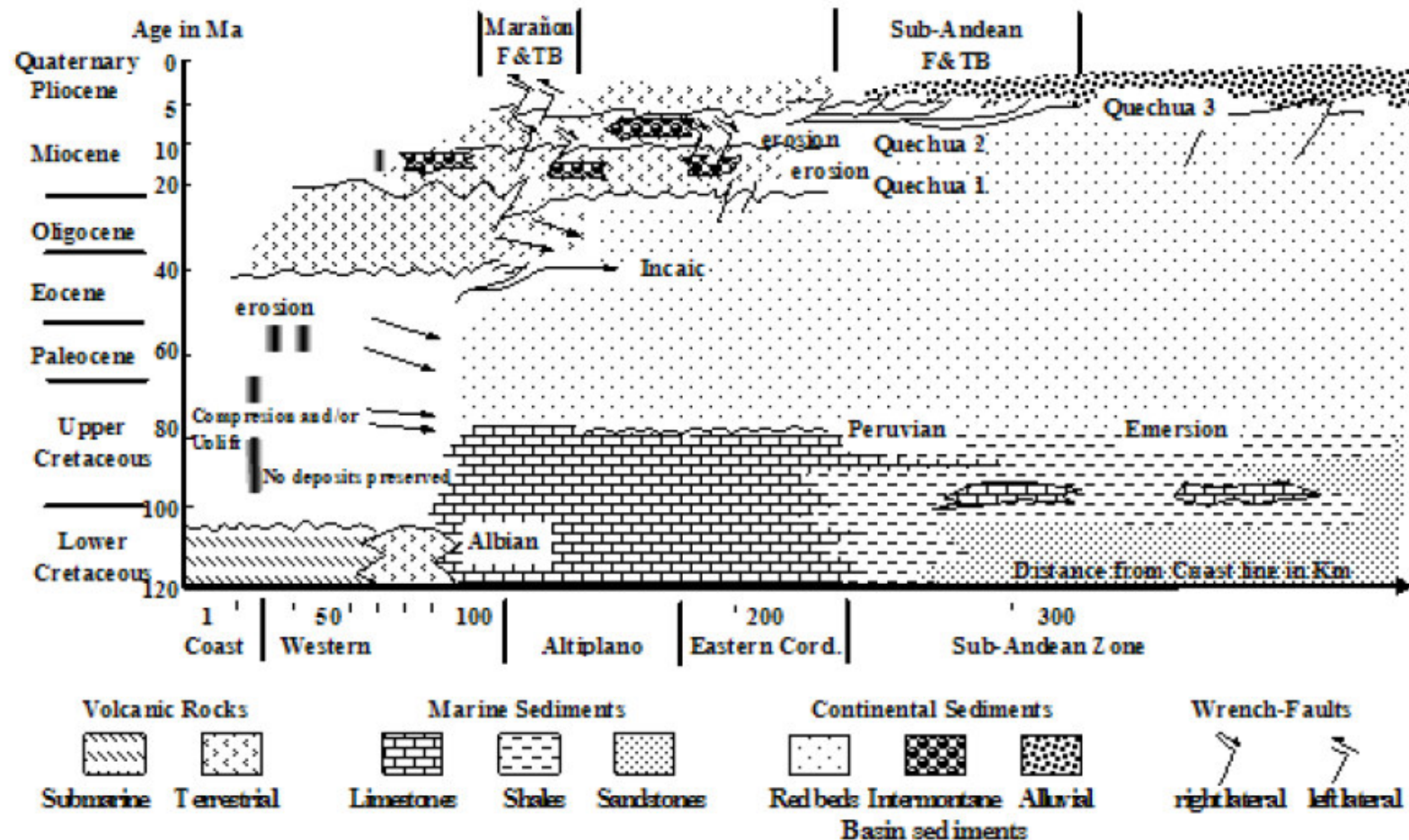


Figure 5. Composite diagram showing deformation episodes in relation to sedimentation and magmatism in central Perú (10°30'S to 13°S lat.). Ages of batholithic intrusions and part of the data concerning the volcanic units of the coast and the western Cordillera are from Cobbing et al. (1981). Age scale for period 0-10 Ma is x2. The solid rectangles denote both the location and the time of emplacement of the batholithic intrusions. Arrows indicate the source areas of the clastics; they are directed toward the sedimentary basins. (Modified from Mégard, 1984)

The last compressive event in the Andes was the Neogene Quechua phase, which has been subdivided into three discrete phases: Quechua 1, 2 and 3 (Jacay, 2002). The timing of the Quechua phase 1 is not known exactly but is thought to be between 20 and 12.5 Ma approximately. This phase affected the western Cordillera, the Altiplano and the eastern Cordillera where Incaic structures were reactivated. Like the previous phases, the Quechua 1 phase involved NE-SW compression (Mégard, 1984). According to Mégard et al., (1984), the Quechua 2 phase caused dextral slip along mainly longitudinal NE-SW trending faults. The age of this pulse is constrained to be between 9.5 and 8.5 Ma. During the Quechua 3 phase the Peruvian Andes were subjected to shortening in a nearly E-W direction. It is considered to be Late Miocene-Pliocene in the Sub-Andean zone where it gave rise to the SFTB (Figure 5, Soulas, 1977).

The Quechua tectonic phases are directly responsible for the current structural configuration of the Ucayali Basin and the Shira Mountains.

STRATIGRAPHY AND SEDIMENTARY ENVIRONMENTS

Diverse sedimentary environments during the evolution of the central Ucayali Basin resulted in a wide range of stratigraphic signatures. The central Ucayali Basin contains a thick sedimentary sequence that also occurs in the Marañón Basin north of Perú and the Acre and Solimoes Basins in Brazil. These sedimentary sequences pinch out onto the Brazilian and Guiana Shields. The Precambrian basement in the study area is composed mainly of a light grey and/or pink gneissic granite and a lesser proportion of grey, gneissic diorite. A grey to green, unmetamorphosed diorite cuts this sequence (REPSOL YPF, 2001a). The gneissic basement is covered by Paleozoic units and could be the product of an ancient Proterozoic substratum uplifted by tectonism of the Amazonian basement or the eastern Cordillera where it is frequently observed with the metamorphic series (Sempere, et al., 2002).

Outcrops of Precambrian rocks are observed to the west of the Pachitea sub-Basin in the eastern cordillera as well as in the southern part of the Ene basin (Gil, 2001) and the eastern flank of Shira Mountains (REPSOL YPF, 2001b). In addition, the Cuchabatay High and Contaya Arch are Precambrian in age (Lauren and Pardo, 1974).

Seismic and well data indicate that an almost complete composite sedimentary section of Paleozoic, Mesozoic and Cenozoic sediments were deposited in the Ucayali Basin (Perupetro, 2003). Paleozoic strata are primarily marine sediments. Seismic lines show that the early Paleozoic units are thickest to the southwest and pinch out toward the Brazilian shield (Velarde et al., 1978). The oldest pre-Andean sequence found in central

Ucayali Basin are the Ordovician siliciclastic sediments of the Contaya Formation, which was deposited in littoral and deltaic environments and are characterized by an intercalation of sandstones and mudstones (Petróleos del Perú, 1962). Unlike the Marañón basin, Devonian sediments are quite extensive in the Ucayali Basin, particularly in the south. The Cabanillas Group (Newell, 1945 from Gil, 2001) is composed of intercalations of argillites (carbonates with silica nodules), silts and sandstones deposited in a shallow marine to a littoral setting (Figure 6, Hermoza, 2004).

Carboniferous sedimentary rocks occur in Ambo and Tarma Groups. The lithology of the Ambo Group consists of sandstone intercalated with limestone and siltstone as well as a few thin coal layers that were deposited in a deltaic system (Rojas, 2002). The Tarma Group concordantly overlies the Ambo Group and is mainly characterized by an intercalation of limestones with sandstone layers deposited in a shallow marine to littoral environment.

The Copacabana Group and the Ene Formation are Permian sedimentary successions (Leight and Rejas, 1966). The Copacabana Group is from a shallow marine platform, and is composed of limestone and dolomitic limestone with some layers of shales and shaly claystones intercalated with dolomite. The Ene Formation consists mainly of detritic sedimentation probably associated with the Late Permian compressional tectonics. It contains interbedded dolomite grading to dolomitic limestone, and some intercalations of claystones and siltstones derived from a shallow marine to flood plain setting (Jacques, 2003b).

ERA	PERIOD	EPOCH	AGE	GROUP/FM	LITHOLOGY	DER. ENVIR	TEC. EVENT	
CENOZOIC	NEOGENE		Holocene	Alluvial Deposits			Quechua3 Quechua2 Quechua1 Incaic phase	
			Pleistocene	Ucayali Fm		Fluvial		
			Pliocene	Ipururo Fm		Continental/Fluvial		
			Miocene	Chambira Fm		Continental		
	PALEOGENE		Oligocene					
			Eocene	Pozo Fm		Marine		
			Paleocene	Yahuarango Fm		Continental		
MESOZOIC	CRETACEOUS	Upper	Maastrichtian	Casablanca Fm		Fluvial	Peruvian phase	
				Hudspayacu Fm		Continental		
			Campanian	Cachiyacu Fm		Marine		
				Vivian Fm		Deltaic		
				Chonta Fm				Marine
		Lower	Albian	Agua Caliente Fm		Fluvial/Coastal	Modica phase Andean tectonics/ Nazca subduction	
				Raya Fm		Marine/Restricted marine		
			Aptian	Cuchabaty Fm		Fluvial		
			Barremian					
			Hauterivian					
			Valanginian					
	Barmanian							
	JURASSIC	Upper		Sarayaquillo Fm		Fluvial	Subduction-related magmatism	
		Middle				Sprattalsabla		
		Lower		Pucara Gr		Deep water/		
	TRIASSIC	Upper				Carbonate platform	Triassic rifting	
Middle								
Lower								
PERMIAN	Lopingian		Mitu Gr		Lacustrine/Fluvial	Mitu rifting/ Hercynian Orogeny		
	Guadalupian		Ene Fm		Shallow marine/Fluvial			
	Cisuralian		Copacabana Gr		Shallow marine platform			
PALEOZOIC	CARBONIFER	Pennsylvanian		Tarma Gr		Shallow marine/ Littoral	Interior sea/ Subduction/ Uplift	
		Mississippian		Ambo Gr		Deltaic plain/ Shallow marine		
	DEVONIAN	Upper		Cabanillas Gr			Uplift/ erosion	
		Middle				Shallow marine/ Littoral		
		Lower						
	SILURIAN						Rifting/ Magmatic activity	
	ORDOVICIAN	Upper		Contaya Gr				Uplift
		Middle						
		Lower				Littoral/Deltaic		
	CAMBRIAN						Early rifting/ plate collision/ uplifting erosion	
PRE-CAMBRIAN				Basement			Rifting/ Magmatism?	

Figure 6. Generalized stratigraphic section of the central Ucayali Basin. (based on Gil, 2001; Perupetro, 2003 and Leight & Rejas, 1966)

Rocks from the Late Permian – Early Triassic occur in the Mitu Formation, which is composed of conglomerates attributed to a process of orogenic collapse following the late Hercynian Orogeny (Rivadeneira and Baby, 1999), the deposition environment of this formation is continental, lacustrine, and fluvial (REPSOL YPF, 2001b). The Mesozoic sequence contain a combination of marine and continental sedimentary rocks. This includes the Pucara Group which was deposited in a carbonate platform environment and it is characterized by deep water shales, limestones and cherts (Quintana Minerals, 1998). This formation contains calcareous facies in the Pachitea sub-Basin and dolomites and evaporites to the east. The Pucara Group has been dated as Late Triassic – Middle Jurassic (Muller, 1982). The top of the Pucara sequence is characterized by evaporite deposits identified in outcrops, wells and seismic images (Fernandez et al., 2002). This evaporite level acted as a decollement during the Neogene compressive deformation (Navarro, 2005).

The Late Jurassic is represented by the Sarayaquillo Formation (Kummel, 1946, Mégard, 1979). A regional supratidal sabkha environment developed at the transition between the Pucara Group and Sarayaquillo Formations and marks a change from shallow marine to continental deposition. The evaporitic unit associated with the sabkha is an important stratigraphic marker horizon in the western Ucayali/Ene basin area. In the Peruvian fold and thrust belt, it can be traced over a distance of at least 700 km. These deposits were penetrated by the Oxapampa 7-1 and Chio 1X wells in the central part of Ucayali Basin (Figure 2) (Perupetro, 2003). The Sarayaquillo Formation is

composed of intercalated sandstones, claystones and siltstones and was deposited in a continental fluvial environment (Figure 7) (Rojas, 2002).

The Aptian-Albian Cuchabatay Formation appears to be tectonically controlled by the Shira Mountains (Gil, 2001). This unit forms a fining upwards sequence of sandstones that unconformably overlies the Sarayaquillo formation (Elf, 1996b). It consists of a thick, amalgamated and braided to low-sinuosity channel belt sandstones. This broad, laterally continuous sandstone unit body is overlain by the marine to restricted marine shales of the Raya Formation. Perupetro (2003) interprets this formation as the end of a broad transgressive trend recorded by the Cuchabatay Formation.

Overlying the Raya Formation, the Agua Caliente Formation includes the entire Cenomanian sequence (Müller, 1982). This formation contains fluvial and coastal sandstones that thin northward. Above the Agua Caliente Formation is the Chonta Formation which was penetrated by all the wells drilled in the central Ucayali Basin. This formation was dated as Turonian to Coniacian using cores from the Oxapampa 7-1 well (Gutiérrez, 1982). It is characterized by shales amalgamated with limestones and dolomites. The base is marked by red mudstones and the top is marked by green mudstones (Velarde et al., 1978).

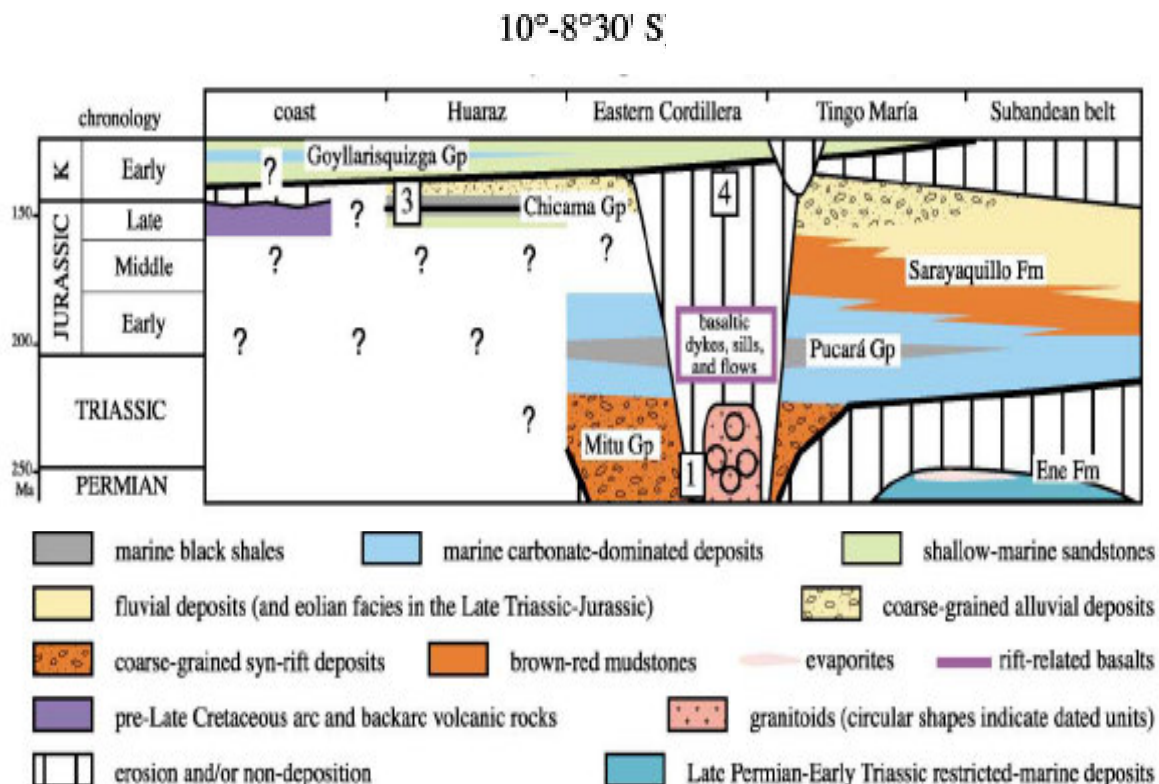


Figure 7. Mesozoic – Cenozoic stratigraphic synopsis of the Central Andes from 10° S to $8^{\circ}30'$ S. Overall decrease of the marine influence from W to E. Framed numbers 1= Late Permian – Triassic rifting; 3= Downwarping of Chicama basin; 4= latest Jurassic – Early Cretaceous uplifts. (Modified from Sempere et al., 2002)

The Campanian Vivian Formation in central Ucayali Basin is a sandstone complex subdivided into 3 units, with two sand sequences, the upper and lower Vivian, (Jaillard, 1996). The sands are white quartz arenites, very fine to very coarse-grained. The upper Vivian typically has authigenic kaolinite, whereas the Lower Vivian sandstone has a much cleaner sand character (Jaillard et al., 2005). The Cachiyacu Formation represents the end of a Late Cretaceous transgressive cycle (fining upward sequence) that begins with the deposition of Lower Vivian sands (Perupetro, 2003). This last cycle is characterized by a period of considerable stratigraphic variability due

to the sea level fluctuations. It contains numerous shales and discontinuous sands that were protected from fresh water flushing. This is in contrast to main Vivian sections where fresh water flushing was common (Elf, 1996c).

The end of the Cretaceous is marked by the deposition of the Huchpayacu Formation and the base of the Casa Blanca Formation. The Huchpayacu Formation is characterized by intercalated coarse grained continental sands with fine to medium sandstones (Velarde et al., 1978). The fluvial Casa Blanca Formation consists of medium to coarse grained yellow quartz sandstones and can be identified in all the wells in the Ucayali Basin (Quintana Minerals, 1998).

The Tertiary section forms of a wedge-shaped foredeep deposit of red bed cycles with poor hydrocarbon potential interbedded with the Pozo Shale and Sand of Eocene - Oligocene age (Perupetro, 2003). It is widely distributed throughout the basin especially in the eastern flank. The Late Paleocene – Early Eocene is represented by the continental red beds of the Yahuarango Formation (Rojas, 2002). After the Middle Eocene isostatic rebound, a generalized orogenic loading stage in the Andes induced subsidence in the foreland area, resulting in a marine incursion and the deposition of the Pozo Shale formation. Variations in orogenic loading during the Late Oligocene to Middle Miocene controlled the deposition of the continental Chambira red beds (Hermoza, 2004).

CHAPTER III

METHODOLOGY

The present study was divided into two main phases: The first phase involved getting seismic and well log data into the KINGDOM Suite software package to identify and map key seismic horizons and structures within the basin. The last phase involved the refining of the basic interpretation and constructing models to determine the history of motion along the major faults bounding the Shira Mountains to establish their importance during the evolution of the Ucayali Basin. This last step included use of the software packages 2DMove, Canvas, Strater and the GIS MapInfo.

LOADING AND INTERPRETATION OF SEISMIC DATA AND WELL LOGS

The seismic and well data for this project were provided by Perupetro S.A. and consist of 110 seismic lines in SEG-Y format and 17 well logs in LAS format. The seismic data were processed through time migration (with a few exceptions that are unmigrated) and are all zero phase (Figure 2. Table 1). All data were loaded into KINGDOM Suite and the wells were tied to the seismic using time-depth charts based on nine sonic logs (DT) located throughout the central Ucayali Basin: Chio, Mashansha, San Alejandro, Sanuya, Tamaya, Runuya, Rio Caco, La Colpa and Sepa (Figure 2). Nine synthetic seismograms were generated from the sonic and density logs and convolved with a seismic wavelet derived from the coincident seismic line (Appendixes

1-9). This enabled the key formations to be properly identified in the seismic so that they could be mapped throughout the region.

Six key Seismic horizons were identified on the seismic and picked throughout the study area. These were chosen based on their relative importance for determining the tectonic and depositional events from the Upper Devonian (Cabanillas Gr.) to the Eocene-Oligocene (Pozo Fm.) (Figure 8). A large number of faults were also identified with different origins, ages and characteristics. For example, basement-involved normal faults associated with rifting events were identified in the Paleozoic section and thrust faults related to Cenozoic and Mesozoic compressive periods are common. To establish a time framework for the basin inversion, growth stratal patterns were identified and mapped on the seismic lines.

The final product of the seismic interpretation includes three color-grid, time-structure maps of the top of the Copacabana Gr. (Middle Permian), the base of the Cretaceous and the top of Chonta Fm. (Upper Cretaceous). Time-structure maps help to define structural controls on deposition at both flanks of the Shira Mountains (central Ucayali Basin to the east and Pachitea sub-Basin to the west) and the relationship with the development of this mountain chain as well. 3D structure maps were also generated using VuPack in order to show the relationship between the picked horizons, the main faults and the Shira Mountains (Figure 9). Isochore maps of key Paleozoic and Mesozoic units (Tarma-Copacabana Groups, and Cushabatay-Chonta Formations) were generated as well, in order to establish the main depocenters by showing where the units are thickest to see their relation to the main faults.

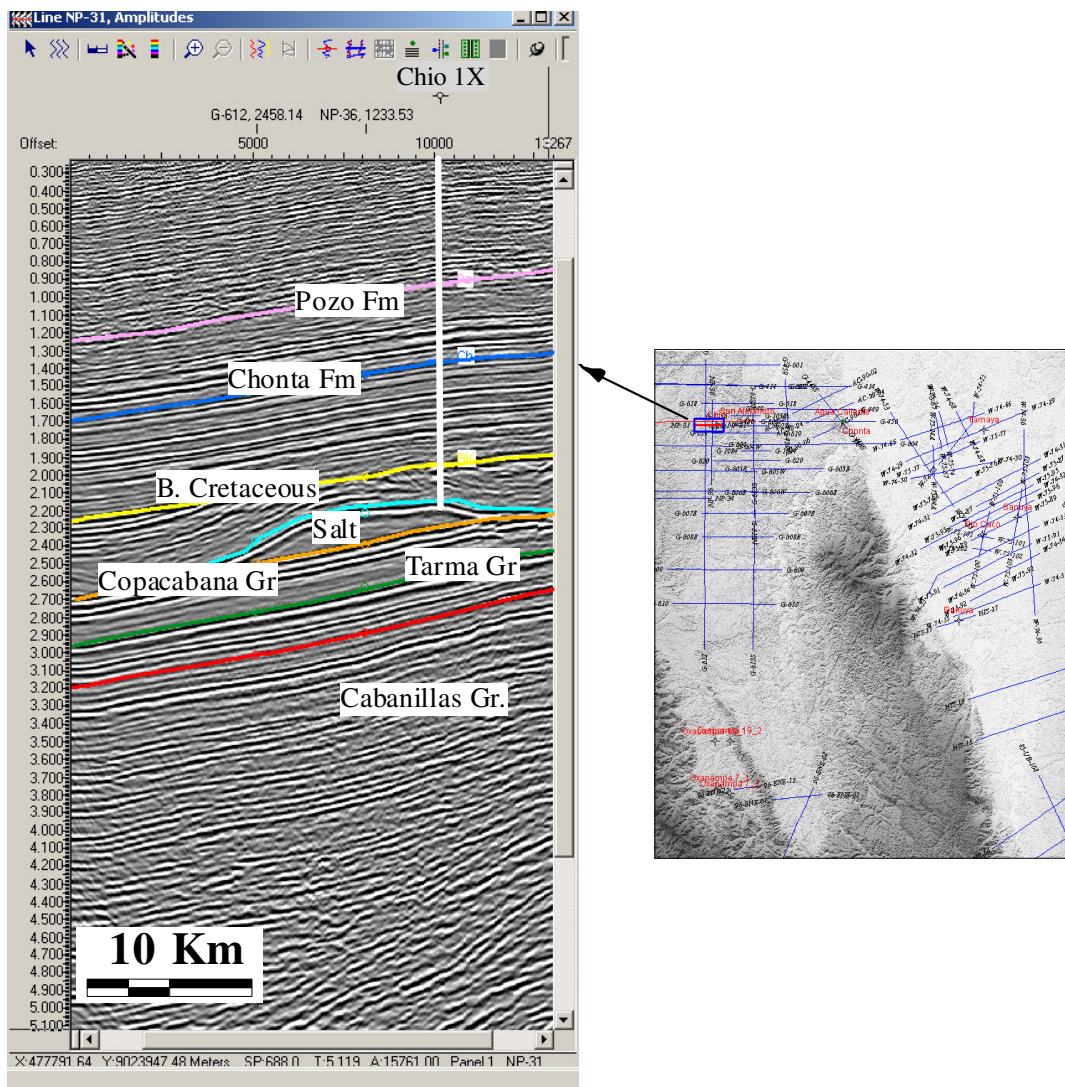


Figure 8. Seismic line NP31. Example of a seismic “type” line with all the horizons interpreted and Chio 1X well northwestern Shira Mountains, also the base map showing the line location in a blue square.

Generating the regional maps involved gridding and interpolating the horizons which is complicated by major data gaps over the Shira Mountains and San Matias Cordillera where no seismic data has been collected. Most of the key formations, however, crop out in these mountain chains and their contacts have been mapped, facilitating the extrapolation between the eastern and western lines. Although this

process is not very accurate because of large regions with sparse data and lack of proper velocity control, it is nevertheless a useful exercise to better establish how the structures are segmented the basin. To correlate the geologic mapping data to the seismic sections, which are in two-way travel time (TWT), the DEM was converted from meters to seconds using an assumed replacement velocity with MapInfo Vertical Mapper. The geologic map was superposed on the DEM to get the outcropping formation points in seconds. The resulting polygons were exported as ASCII files and then imported into KINGDOM Suite and merged with picked horizons. Negative travel times thus correspond to regions where the units crop out in the elevated areas

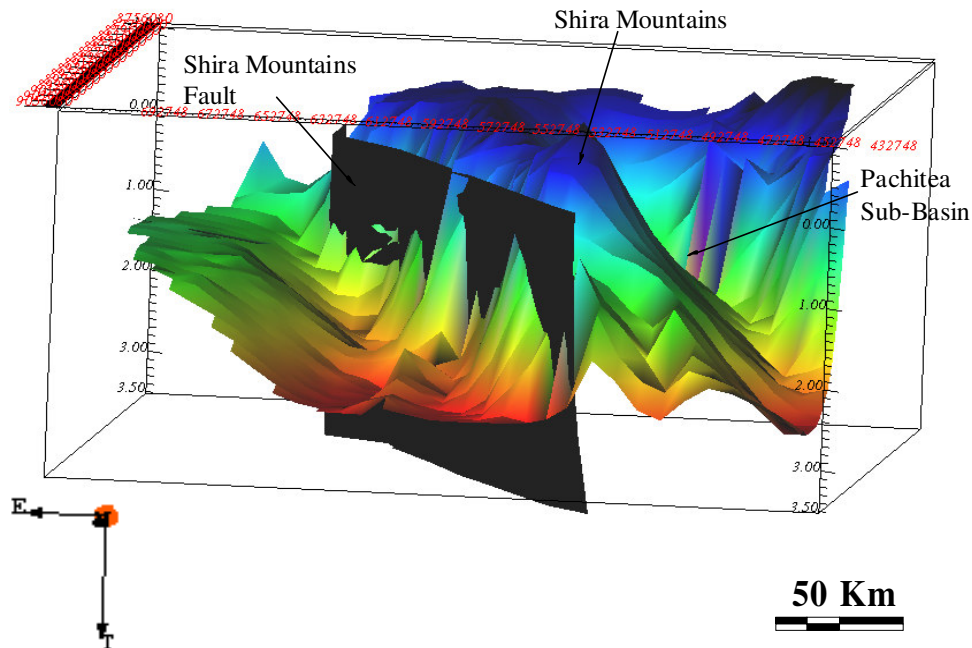


Figure 9. 3D “type” model.

Well log correlations were constructed using KINGDOM Suite, Strater and Canvas. Every well log was interpreted to corroborate the previous interpretation by

Perupetro. Three general well log correlations were generated showing the main characteristics in terms of stratigraphy (pinch-outs, unconformities, truncations, etc.) (Figures 12, 13 and 15). These are located in the northern, center and southern central Ucayali Basin (Figure 10). Twelve wells were used in the construction of the correlations.

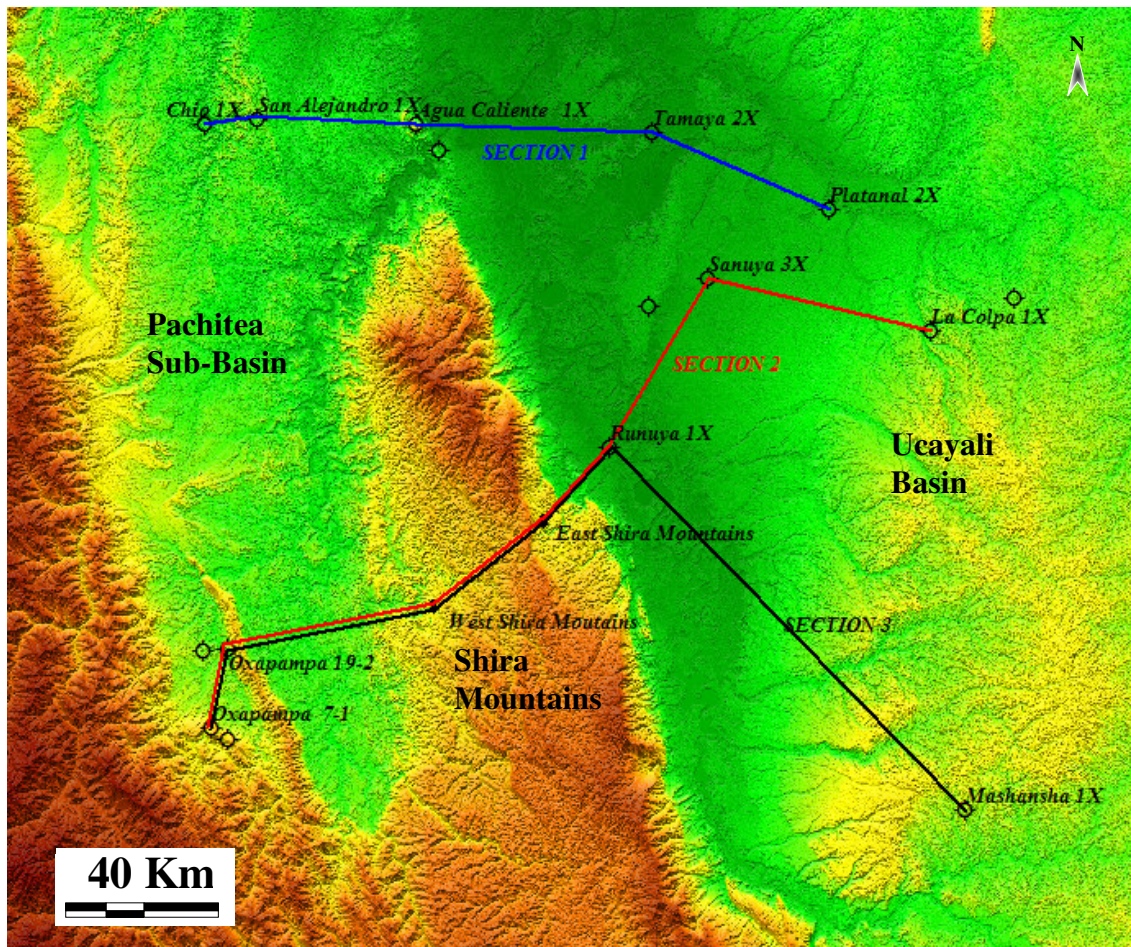


Figure 10. Well log correlations location. (DEM from ftp://e0srp01u.ecs.nasa.gov/srtm/version2/SRTM3/South_America)

MODEL CONSTRUCTION AND INTERPRETATION OF RESULTS

The last phase of the research involved constructing models and to place the interpretation in regional tectonic context. Thirteen composite logs were generated in order to determine the relationship between the gamma ray (GR), spontaneous potential (SP) and caliper (CALI) logs with the lithology and seismic data. Synthetic seismograms were constructed for nine of the composite logs (Appendixes 1 to 13). Composite log refers to the model generated using the combination of data (lithology, GR, SP, CALI logs, seismic and synthetic seismograms)

A detailed geologic structural map in DXF format was constructed using Canvas based on 24 geologic quadrangles 1:100,000 scale (18-M to 23-O) from Instituto Geológico Minero Metalúrgico del Perú (INGEMMET, Figure 11). 2D Move was used to develop and balance three detailed cross sections in depth. To convert the interpreted seismic lines utilized in the cross section construction from TWT to depth, time-depth charts previously developed from the sonic logs were used taking an average velocity for all the geologic formations and basement from every well included in the cross sections construction. Each cross section uses at least 1 well to check the accuracy of the time-depth conversion.

CHAPTER IV

RESULTS

STRATIGRAPHIC EVOLUTION

The stratigraphic evolution of the central Ucayali Basin and the Shira Mountains was affected by many tectonic events from the Permian through the Neogene. Key markers show dramatic changes in the origin and nature of sediment, tectonic activity (uplift or subsidence) and sea level fluctuations. The study area contains sedimentary sequences ranging in age from Ordovician to Quaternary (Figure 11).

Three major tectonostratigraphic units have been identified that represent different tectonic settings: syn-rift deposits, post-rift deposits with limited evidence for compression and later primary inversion-related deposits. The syn-rift sequences were deposited during extensional faulting and rift-basin infill, primarily during Paleozoic. Post-rift sequences were deposited after the cessation of the extensional faulting. These sequences may include unconformities that removed part of the syn-rift sequence (Williams et al., 1989). The syn-inversion sequences were deposited more recently during compressional episodes that invert the basin structures.

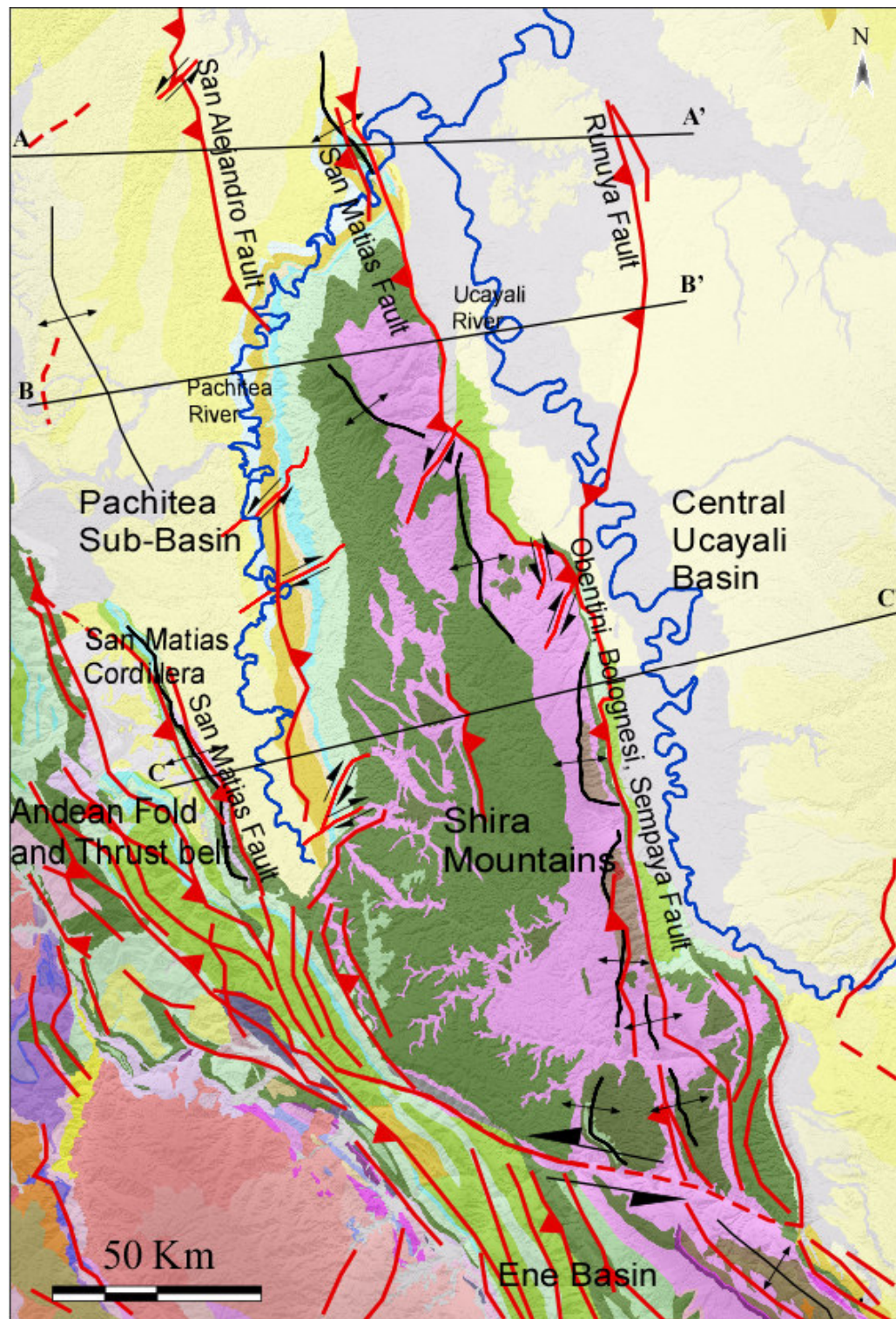


Figure 11. Geologic map central Ucayali Basin. (Modified from INGEMMET, 1984-1997)

LEGEND

ERA	PERIOD	EPOCH	LITHOSTRATIGRAPHIC UNITS		
			Sedimentary	Igneous	Methamorphic
CENOZOIC	Neogene	Holocene	Qh-al Alluvial Dep.		
		Pleistocene	NQ-rp Rio Picha Fm		
		Pliocene	NQ-u Ucayali Fm		
		Miocene	N-i Ipururo Fm		
		Oligocene	KsP-ch Chambira Fm		
	Paleogene	Eocene	P-p Pozo Fm		
		Paleocene	P-y Yahuarango Fm		
			Ks-cb Casa Blanca Fm		
			Ks-ca-h Cachiyacu-Huchpaycu		
			Ks-v Vivian Fm		
MESOZOIC	Cretaceous	Upper	Kis-ch Chonta Fm		
		Lower	Ki-c Oriente Gr		
	Jurassic	Upper	Js-s Sarayaquillo Fm		
		Lower	Ji-c Condorsinga Fm		
	Triassic	Upper	Ji-a Aramachay Fm	TJ-sa San Antonio To-GD	
			TJ-pu Pucara Gr	Tr-sr San Ramon MG-SG	
		Lower	Ts-ch Chambará Fm	Tr-ca Carrizal Qz-MG	
			PT-e Ene Fm	PT-ro Rocadura Tonal.	
PALEOZOIC	Permian	Upper	Ps-m Mitu Gr	PT-ta Tarma Granodiorite	
			Pis-rt Rio Tambo Fm	PT-su Suchamichay MG-GD	
		Lower	Pi-c Copacabana Gr	Pi-mgd Diorite - Mon-granite	
	Carboniferous	Upper	Cs-l Tarma Gr		
			Cs-a Ambo Gr		
	Devonian	Upper	D-e Excelsior Gr		
		Lower	Di-c Cabanillas Gr	Pal-gd Granodiorite	
	Ordovician	Upper	Os-c Contaya Fm		
PROT	Neo-Proterozoic			Pr-gr Granito	Pr-cm Met. Complex
	Meso-Proterozoic				PE-ma Maraysha Gr.
					PE-hu Huaytapayana Gneiss

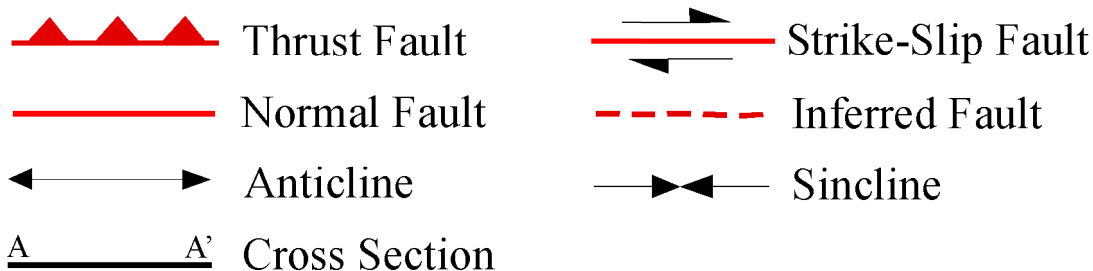


Figure 11 continued

Syn-Rift-Related Deposits

Between the Devonian and Early Triassic several tectonic events occurred. These were dominated by extensional tectonics (rifting), although there may have been some short compressive events. The stratigraphic units deposited during this period are the Cabanillas, the Ambo, the Tarma, the Copacabana, the Mitu Groups and Ene Formation.

From the Devonian to the Early Carboniferous, the Cabanillas and Ambo Groups were deposited in deltaic and shallow marine environments. In the eastern central Ucayali Basin, the Cabanillas Group is absent from the La Colpa and Mashansha wells, and the Ambo Group directly overlies basement rocks. The Runuya well, located farther west near the Shira Mountains, contains the Cabanillas Group, which overlies the crystalline basement, and the Ambo Group is missing. This may indicate that the Runuya well area was in a deeper water setting than the region to the east (La Colpa and Mashansha area). During the Ordovician-Silurian and Early Carboniferous, the Runuya well area appears to have been locally uplifted; as indicated by the absence of the Contaya Formation and Ambo Group (Figures 12 and 13).

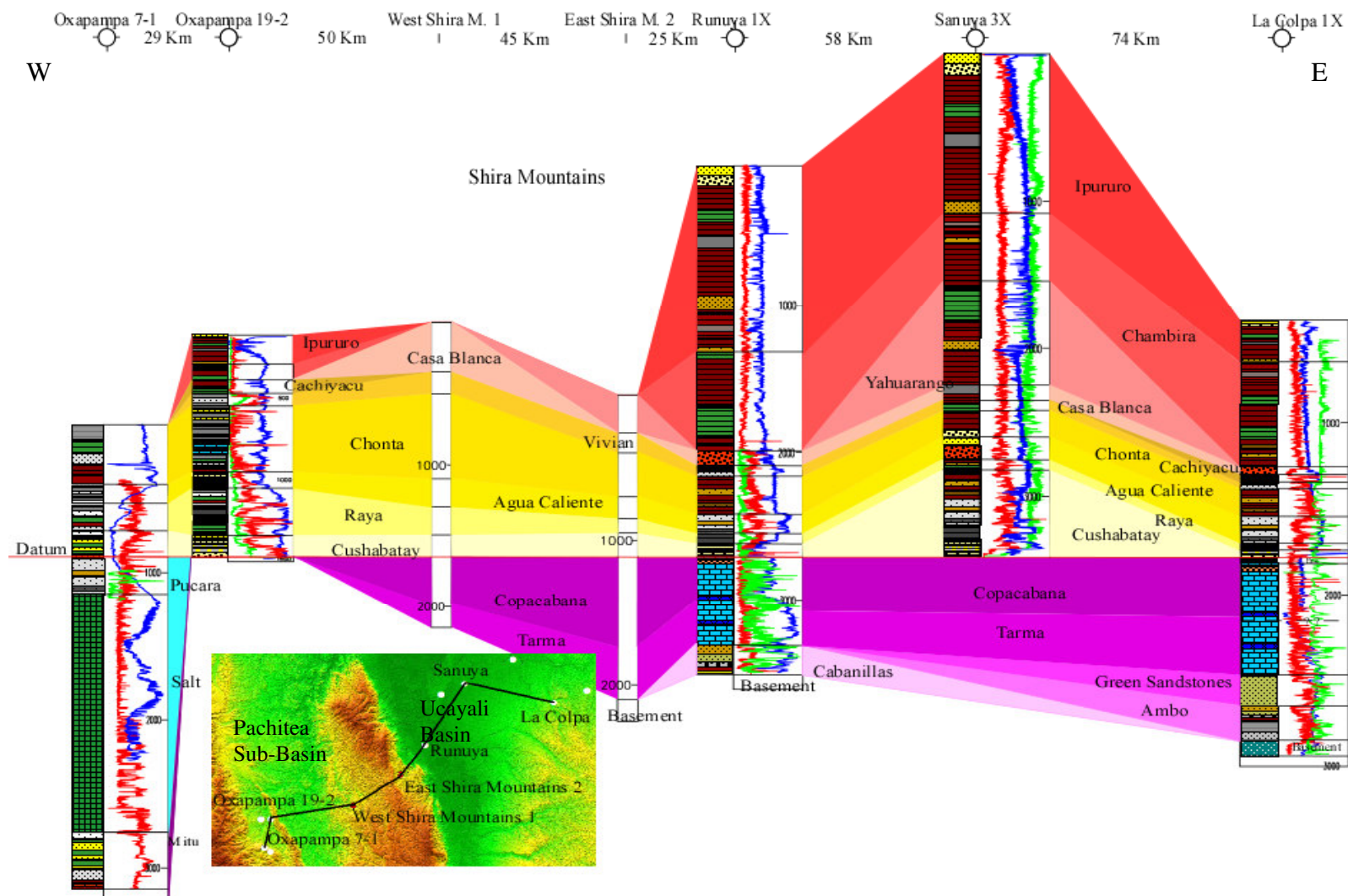


Figure 12. Well correlation 2. Datum at the base of Cretaceous (Cushabatay Formation) Shows a fairly complete Mesozoic unit western Ucayali Basin (Pachitea sub-Basin) and the Pucara and Mitu Groups truncated by base of Cretaceous erosive unconformity. A quite complete sedimentary column can be recognized eastern Ucayali Basin with a very thick Cenozoic sequence (depth in meters).

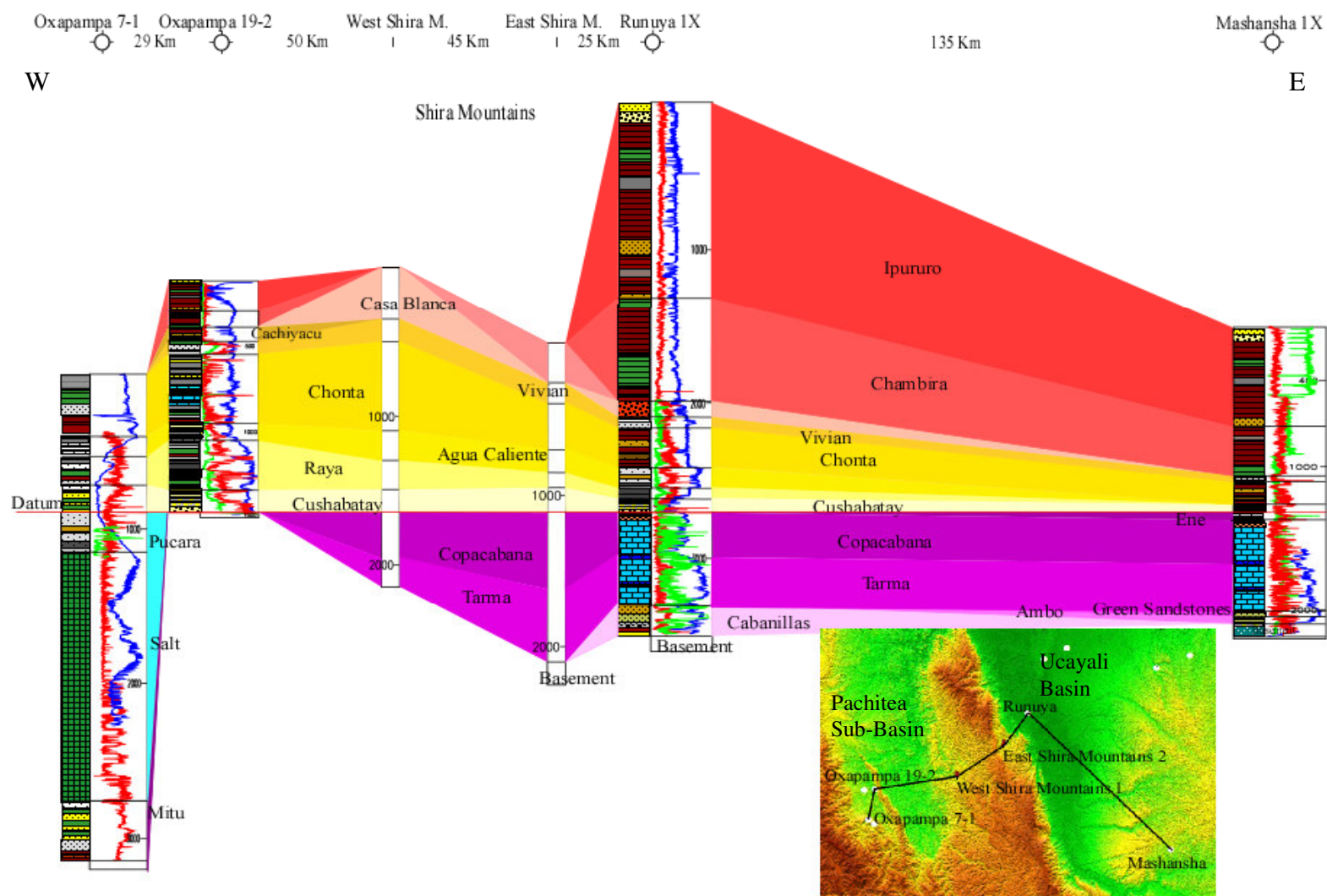


Figure 13. Well correlation 3. Datum at the base of Cretaceous shows a quite complete Mesozoic sedimentary unit in the western Ucayali Basin (Pachitea sub-Basin) and post-Paleozoic pinch-out towards the Brazilian Shield and Fitzcarrald Arch. Fairly complete pre-Cretaceous section can be recognized eastern study area as well as a very thick Cenozoic unit (depth in meters).

Deposition of the Pennsylvanian Tarma Group started with basal green sandstones, indicating a transgression of an Upper Permian Sea into the central Ucayali Basin. This sedimentary succession is recognized in most of the study area. One important exception is that the entire Carboniferous section appears to be missing in the Agua Caliente field area (Figure 15). Pre-Mesozoic units are truncated eastward in the Pachitea sub-Basin by the base of Cretaceous unconformity (Figure 14) and northern Shira Mountains, perhaps indicating that the Agua Caliente dome can be interpreted as a paleohigh that was uplifted at this time.

Continued eastward transgression, during the Permian resulted in a shallow marine carbonate platform represented by the Copacabana Group. This stratigraphic unit is sampled by all the wells in the study area except for the Oxapampa wells, presumably because they did not drill deep enough. Thus, the central Ucayali Basin was completely covered by the Permian sea during this time.

The Ene Formation was deposited during Middle to early Late Permian in a shallow marine and flood plain environment. This formation is present in the eastern central Ucayali Basin and was drilled at the Platanal, Mashansha and La Colpa wells, possibly indicating that the eastern flank was partially covered by a shallow sea in this interval of time with the shoreline migrating west.

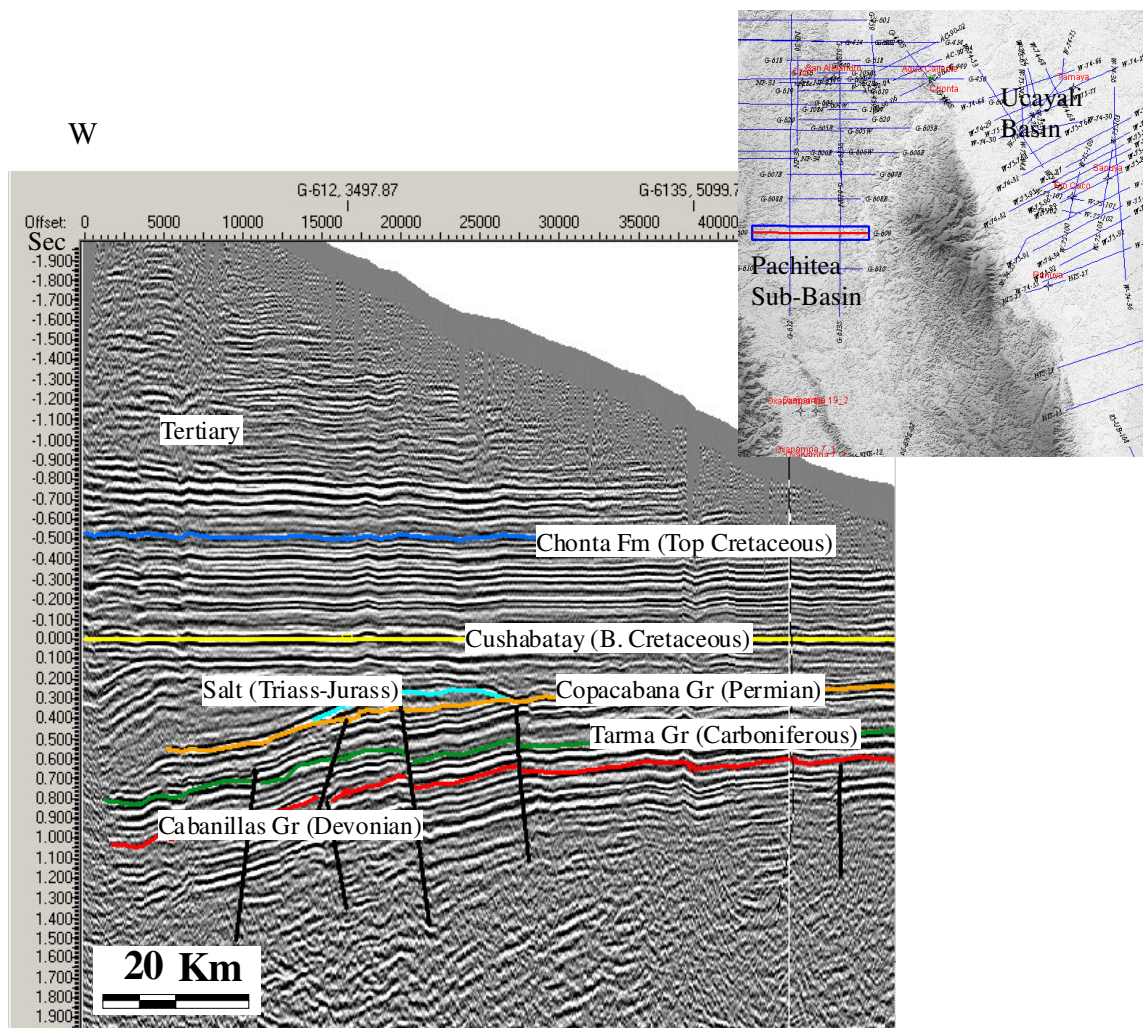


Figure 14. Flattened seismic line G609. Located in the Pachitea sub-Basin (blue square, red line) pre-Cretaceous units truncated eastward by the base of the Cretaceous Unconformity shows the presence of Tarma Group in this area.

Late Permian (Lopingian?) time was marked by a major regression of the sea caused by uplift of the west of the present day Huallaga Basin, located northwestern Ucayali Basin (Figure 1) and restringing access to the open ocean (Quintana Minerals, 1998). This regression resulted in the deposition of the lacustrine and fluvial sediments of the Mitu Group. Magmatic activity thought to be rift related occurred at this time and affected the Western and part of the Eastern Cordillera as well. Mitu strata are missing

in the eastern and most of the western part of the central Ucayali Basin except for the Oxapampa area (Figure 12, 13 and 15). Thus most of the region may have experienced erosion due to the uplift, resulting in a widespread unconformity. During this period of sub-aerial exposure, the Copacabana carbonates could have developed secondary porosity, which is also indicated by karst features in outcrops of the Copacabana near the San Matias Cordillera (Marksteiner and Aleman, 1997).

Post-Rift-Related Deposits

Deposition of Triassic and Jurassic units marks renewed transgression in the study area, mostly in Pachitea sub-Basin. Near to the end of the Middle Triassic, uplift with associated volcanic activity occurred west of the Huallaga and Santiago Basins, (Figure 1) coincident with a rapidly sinking basin eastern the present SFTB (Tassara, 2005). This basin, filled with thick deep water shales, limestones and cherts of Pucara Group. Oxapampa, Chio and San Alejandro wells confirm deposition of Pucara Group in this area (Figure 12, 13 and 15). As the sea transgressed eastward, shallow water shelf carbonates and minor amounts of shelf sands were deposited. The depositional environment of the Pucara Group continued through Early Jurassic. The Pucara Group is not present in outcrops on the Shira Mountains as evidence by the fact that none of the wells in these areas penetrated this unit. This indicates that the area was already uplifted during this period.

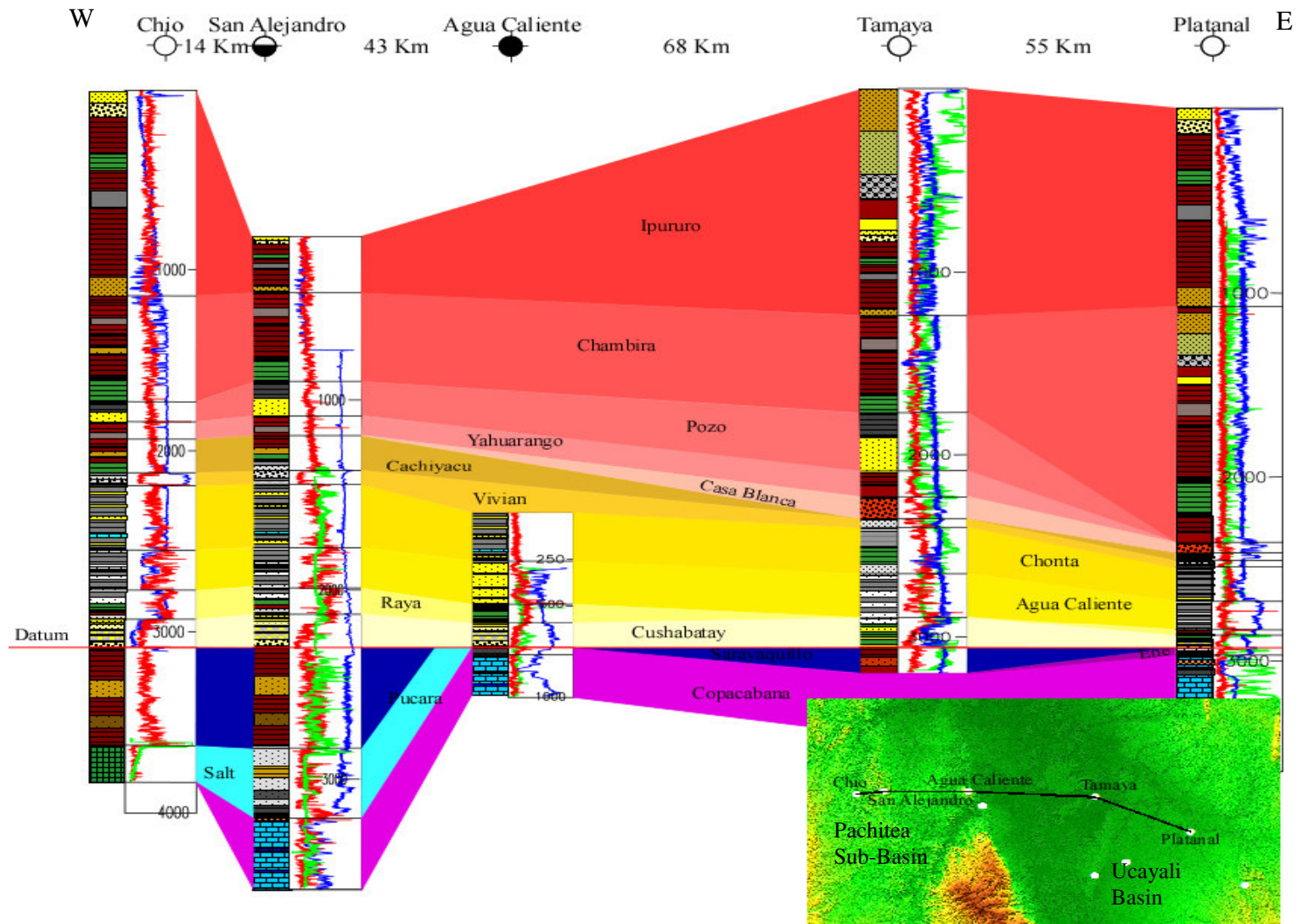


Figure 15. Well correlation 1. Datum at the base of Cretaceous shows a heterogeneous pre-Cretaceous sedimentary unit. Pucara Group and Sarayaquillo Formation are truncated by the base of the Cretaceous unconformity in the Agua Caliente area. A continuous and very thick Cenozoic section can be recognized as well as Mesozoic sequence pinch out towards the Brazilian Shield (depth in meters).

During the Middle Jurassic, renewed uplift of the Eastern Cordillera initiated a new regression, restricting the connection to an open seaway and creating an ideal environment for salt deposition in the Huallaga, Santiago and western Ucayali Basins (Dunbar, et al., 1990). These salt deposits were penetrated by the Oxapampa and Chio wells and can be recognized in some of the seismic lines in the northern Pachitea sub-Basin (Figures 10 and 16).

As the uplift in the western central Ucayali Basin continued, a thick wedge of red beds of the Sarayaquillo Formations was deposited. The Sarayaquillo Formation is absent from the Agua Caliente – Shira Mountains trend as well as from the eastern flank of the study area. With the available data can not be determined if this is because of non-deposition or subsequent erosion. If it was eroded away, the presence of the Sarayaquillo Formation in the Tamaya well demonstrates that this region was not sufficiently exposed to remove it completely. Seismic and well data suggest that the Sarayaquillo Formation is quite thick in the Pachitea sub-Basin. Eventually, however, the formation became thick enough that the salt deposits mobilized to form mounds and cause non-tectonic deformation. But this salt related deformation ended before the beginning of the Cretaceous as evidenced by flat lying beds above the salt mounds.

In the Early Cretaceous, a major regional erosional unconformity developed that separates the Sarayaquillo Formation from the Cushabatay sandstones (Figure 14 and 16). The Cushabatay Formation can be found consistently over the entire central Ucayali Basin and therefore the base of this unit was chosen as a key datum for correlations and reconstructions.

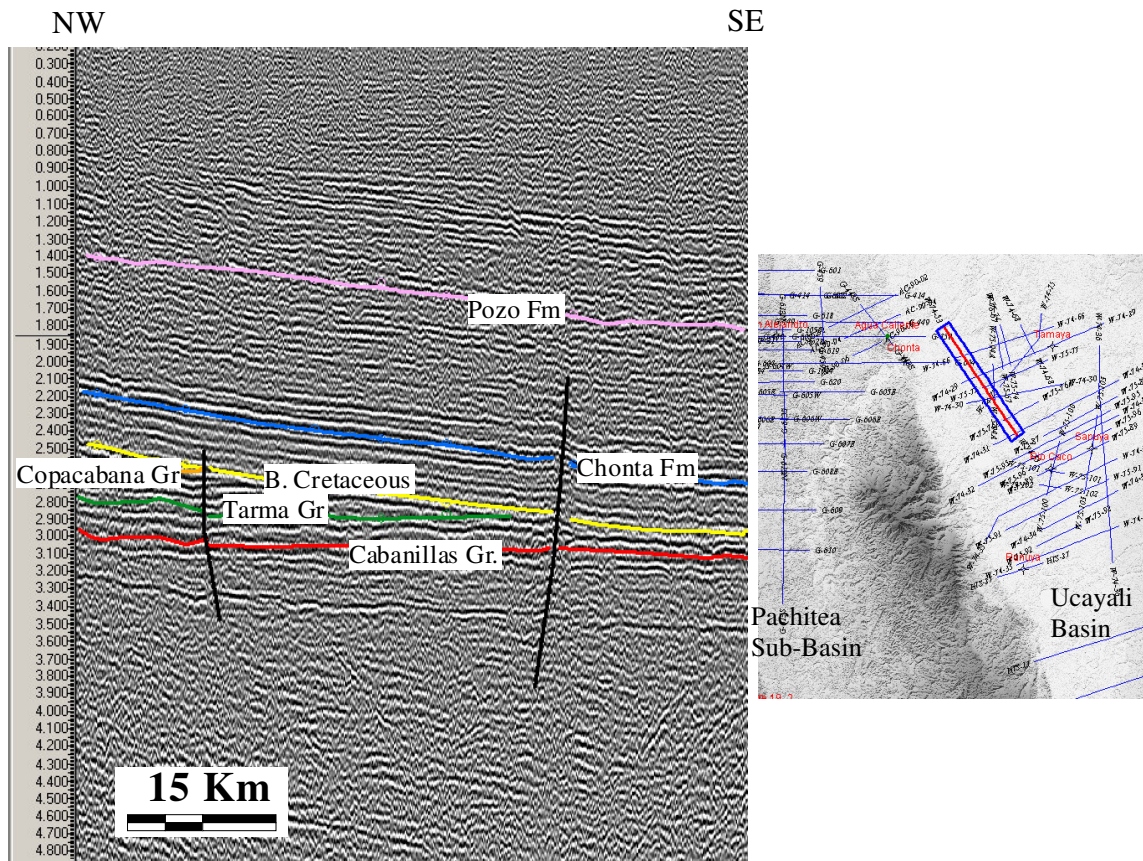


Figure 16. Seismic line W74-53. Shows pre-Cretaceous stratigraphic units truncating on the Base of Cretaceous angular unconformity.

The Early Cretaceous was marked by continental fluvial deposition evenly distributed over the region. However, marine sedimentation was reinitiated with transgression of the Cretaceous sea during the Aptian – Albian. During this period the Raya Formation was deposited in the Pachitea sub-Basin and Shira Mountains, as well as in the eastern and northern central Ucayali Basin (Figures 12, 13 and 15). This depositional phase is considered to be one of the most important oceanic sedimentation periods in the study area and lasted almost 50 My from the Early Aptian to the Late Campanian. The Raya Formation is missing in the La Colpa, Mashansha, Tamaya and

Platanal wells, where the Agua Caliente Formation directly overlies the Cushabatay Formation, possibly indicating that the depositional system was confined to the western part of the basin.

The Agua Caliente Formation consists primarily of shallow marine to deltaic and fluvial coastal sediments of late Albian age (Perupetro, 2003). This formation was drilled in all the wells in the Pachitea sub-Basin, northern Shira Mountains, and in the eastern central Ucayali Basin, except for the Mashansha well,. In addition, it crops out within the Shira Mountains. Thus, the central Ucayali Basin was covered by a shallow Albian sea, probably restricted by the uplifting eastern most part of the basin as well as the Andes, this last as a result of the subduction of the Nazca plate underneath the South American plate and the resultant Andean Orogeny (Elf Petroleum Perú, 1996a). Shallowing of the broad Albian Sea resulted in a transition to a coastal-deltaic environment at the top of the Agua Caliente Formation (Gutierrez, 1982).

Marine sedimentation continues through the Santonian during the deposition of Chonta Formation. This formation was penetrated in all the wells, crops out in the Shira Mountains, and has a fairly uniform thickness over the region (Figure 12, 13, 15). This indicates that this period was characterized by a long tectonic quiescence. This is seen in the seismic data where Cretaceous sediments appear unaffected by faulting or any significant deformations (Figure 17). The Chonta Formation is capped by a strong seismic reflection probably due to the contrast between lithologies. This formation can be correlated across the entire study area. By the Campanian, renewed uplift of the region is indicated by the deposition of the Vivian Formation.

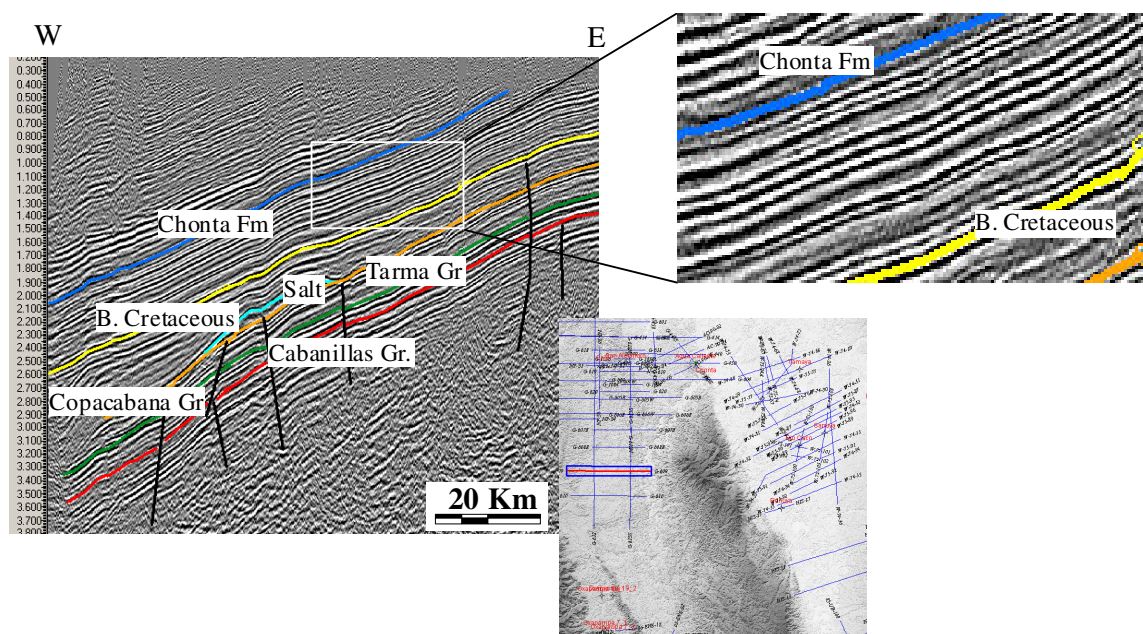


Figure 17. Seismic line G609. Illustrates a homogeneous practically undeformed and unfaulted Cretaceous sedimentary interval. This characteristic can be observed on all seismic lines in central Ucayali Basin.

Deposition of the Cachiyacu Formation defines the end of a long oceanic sedimentation period that lasted most of the Cretaceous. From the well log correlation, it can be concluded that this formation was deposited on the flank of the northern and western Shira Mountains forming wedges that pinch out toward the mountains (Figures 12, 13 and 15). This shows that uplift associated with the formation of the Shira Mountains began at this time and coincides with the compressive episode of the Peruvian phase of Andean orogeny.

The thin continental Huchpayacu Formation was deposited concordantly on the Cachiyacu Formation, but it is observed in just three of the wells: the Chio and San Alejandro wells to the north and the Rio Caco eastern flank Shira Mountains (Appendixes 1, 3 and 5).

The Casa Blanca Formation is distributed uniformly across the central Ucayali Basin but it was not found in northern Chio and San Alejandro wells or cropping out in the Shira Mountains. This indicates that uplift in the Shira Mountains continued through the Paleocene during the pre-Incaic phase. Sediments were sourced mainly by the Brazilian Shield, Fitzcarrald Arch, the Andes (Roddaz, et al., 2005) and possibly by the Shira Mountains. This transition to localized continental deposition indicates continuing uplift and erosion in the region

Primary Inversion-Related Deposits

While some basin inversion began during the Cretaceous, the main Andean compressive phase that affected the basin is associated with the Incaic phase, which began in the Paleogene. This is also when the Shira Mountains fault and the Runuya fault became active as thrust surfaces (Figure 11). For this reason, we distinguish deposits of Cenozoic ages as the primary inversion related deposits.

The Yahuarango Formation is distributed uniformly in the northern area but is not present in the eastern central Ucayali Basin and Pachitea sub-Basin. It is a thin unit of continental deposits overlain by an erosional unconformity, indicating continued uplift of the region. The Sanuya well is somewhat enigmatic because shows this unit to be 800 m thick, indicating a highly localized deep basin, or perhaps has been misidentified in the well log. The seismic data in this area does not show evidence of a

thickness change, or any other characteristic that can be associated with an irregular local stratigraphic or structural event.

The Middle and Upper Paleogene sequence consists of the Eocene to Middle Oligocene Pozo Formation which is characterized by thin marine sandstones and shales identified in the northern wells (Chio, San Alejandro and Tamaya). This formation is also recognized along the western edge of the Shira Mountains as well as the Agua Caliente structure (Figure 11). Therefore, a Late Paleogene sea covered these areas at the base of the Shira Mountains.

After this brief marine episode, the Incaic compressive phase resulted in uplift of the region that brought it to its present elevation. All the deposits overlying the Pozo Formation are continental. The Chambira and Ipururo Formations can be correlated across the central Ucayali Basin. The Ipururo and the Ucayali Formations are the last strata deposited in this region. The Ipururo Formation can be recognized in all the wells except the Sepa well (Higley, 2004).

STRUCTURAL EVOLUTION

To establish the structural evolution of the area, major stratigraphic horizons and sedimentary layers were mapped using the seismic data, resulting in time structure, isochore maps and 3D models as well as composite cross sections that were palinspastically reconstructed. As it was noted in the Chapter III, time-structure maps were made of the top of Copacabana Group (Permian), base of the Cretaceous (regional

unconformity) and the Upper Cretaceous Chonta Formation previously calibrated with the well logs. Isochore maps were also made to determine the thickness of the geologic sections and consequently the main depocenters in relation to the location of the Shira Mountains Fault. The balanced cross sections were restored to the Late Cretaceous aged Chonta Formation. This enabled me to evaluate the nature of the Shira Mountains fault during the Paleozoic and Mesozoic and further permitted estimation of the present depth of detachment to be estimated.

Time-Structure Maps

Copacabana Group time-structure map

The area of the time-structure maps can be divided into two structural provinces separated by the Shira Mountains fault: the Pachitea sub-Basin – Shira Mountains province and the eastern central Ucayali Basin province. In the western province the Permian aged Copacabana Group dips westward toward the SFTB (Figure 18). The main thrust faults in this area dip to the west with the exception of the Shira Mountains back-thrust which dip eastward.

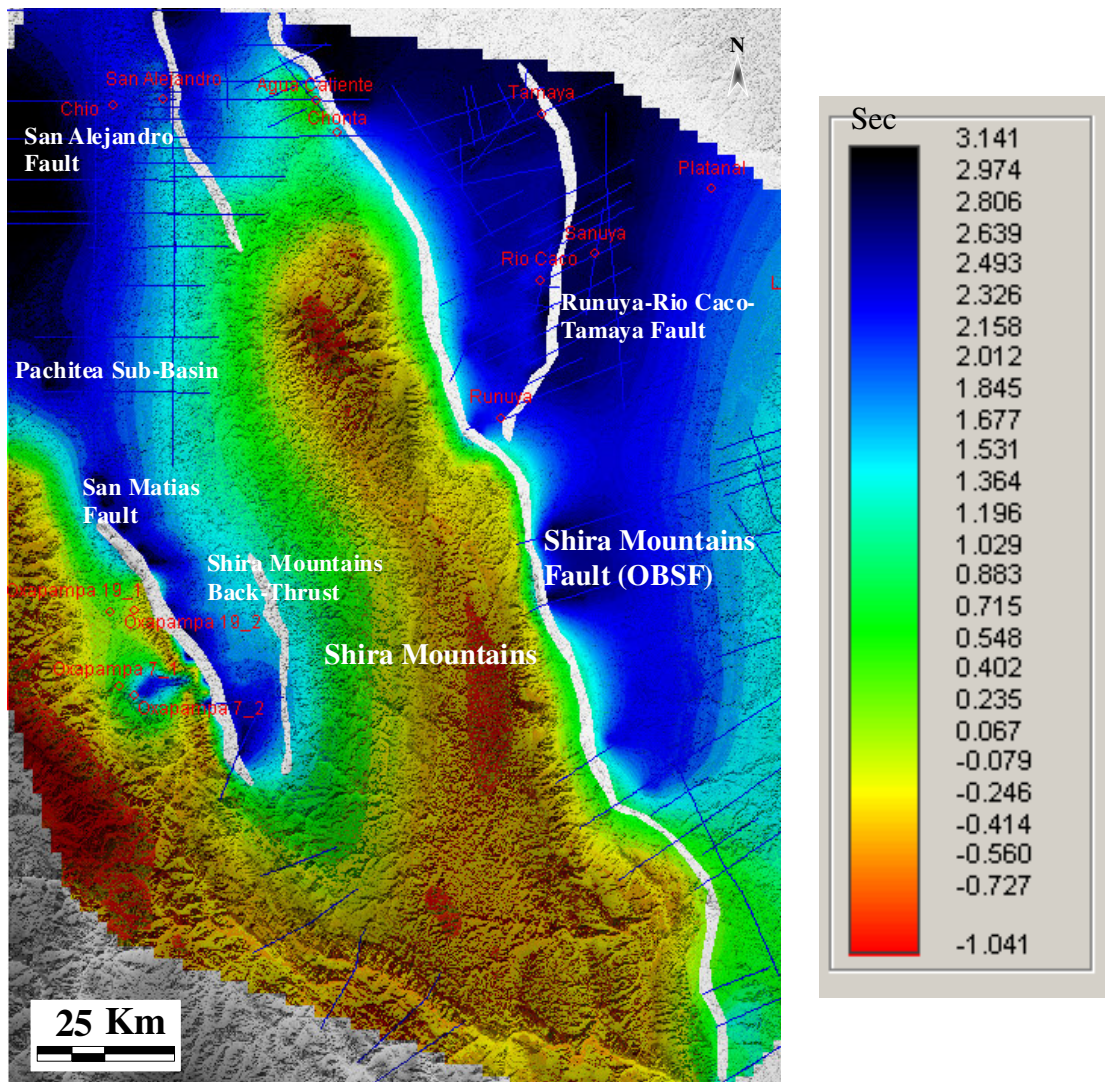


Figure 18. Copacabana Group time-structure map.

Major faults and anticline structures that have been the subject of exploration and drilling by oil companies are easily recognized (e.g. the San Alejandro and Runuya-Rio Caco-Tamaya faults and anticlines and Agua Caliente anticline). The latter is the main hydrocarbon structure in the study area closed by the Shira Mountains Fault (Figure 19).

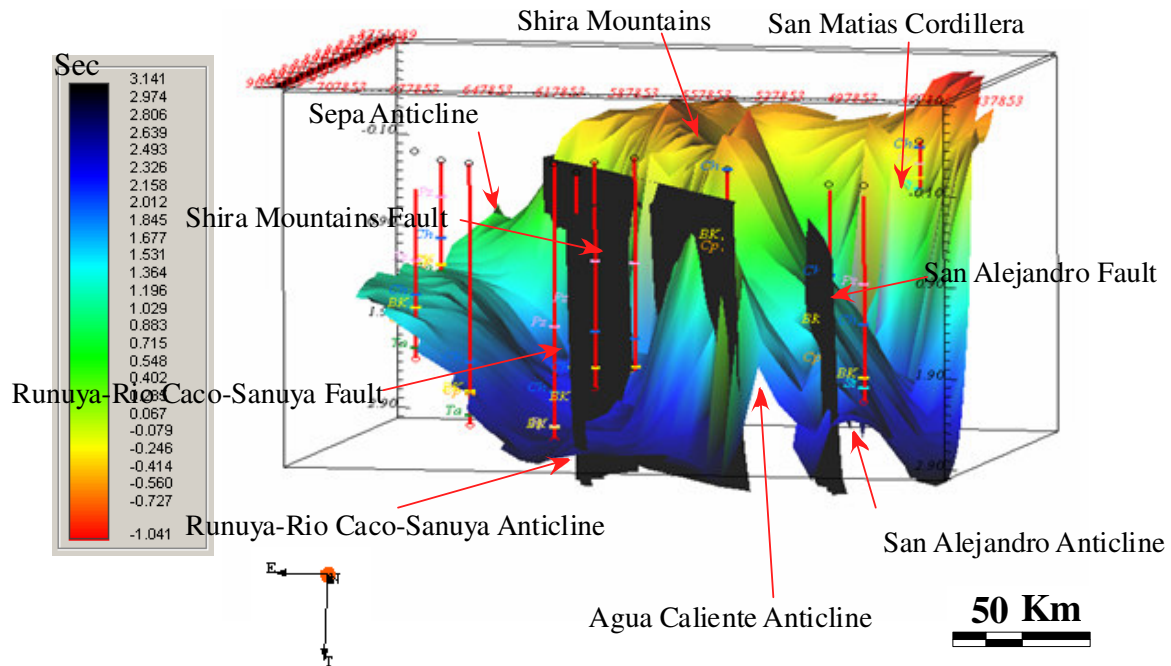


Figure 19. Copacabana Group 3D time-structure model. Illustrates the main faults and their relationship with the anticline structures.

Base of Cretaceous time-structure map

The major structural features identified are the Shira Mountains Fault, the San Alejandro Fault and anticline, the Runuya Fault and anticline, the San Matias Fault, the Sepa anticline and the Shira Mountains back-thrust fault. The base of the Cretaceous dips consistently west in the Pachitea sub-Basin structural province whereas in the eastern central Ucayali Basin it appears to follow the same structural tendency of the underlying Copacabana Group (Figure 20).

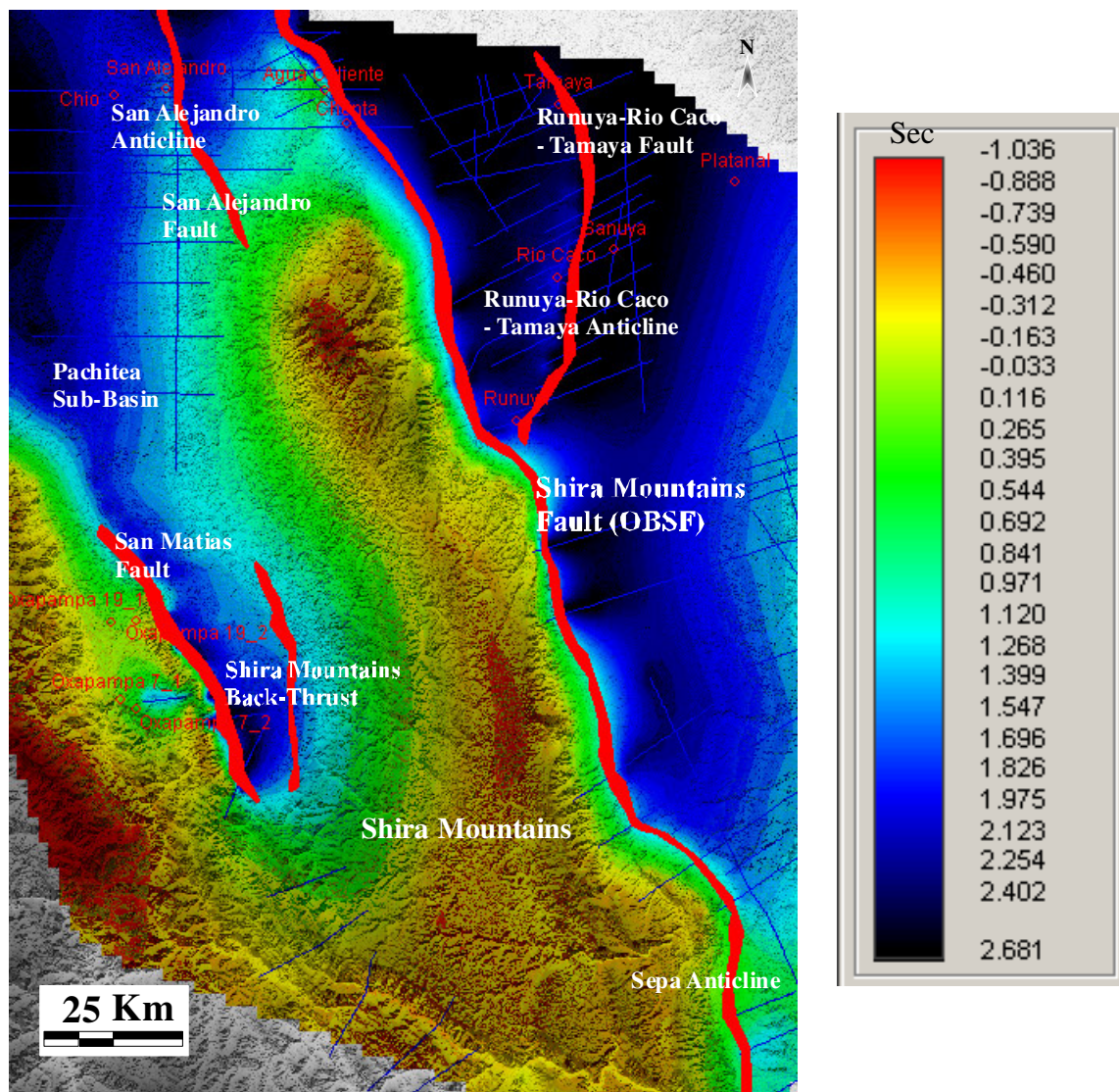


Figure 20. Base of Cretaceous time-structure map.

The base of Cretaceous time-structure map is very similar to the top of the Copacabana time-structure map. However there are two key differences. First, in the Pachitea sub-Basin the pre-Cretaceous units are steeper than the Cretaceous sequence (Figure 21). Second, the Copacabana Group truncates onto the Cretaceous unconformity in the northeastern area (Figure 16). Using the time-structure 3D model the main

characteristics of the base of Cretaceous are easier to visualize. The relationship between the faults in conjunction with the structures can be observed from different points of view facilitating the interpretation (Figure 22).

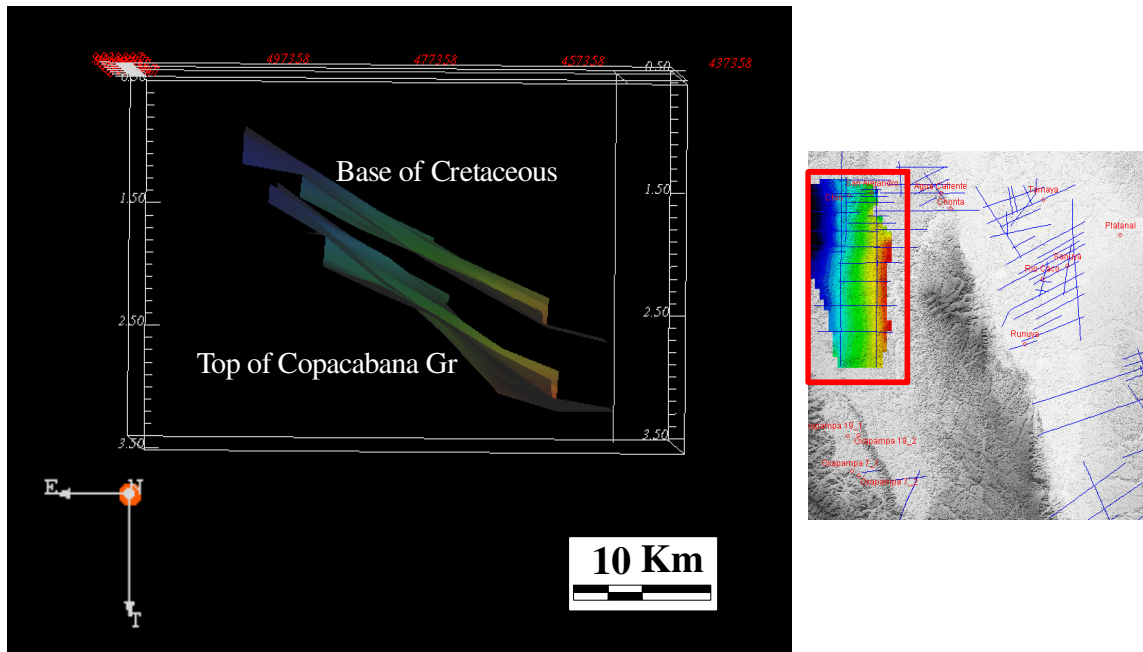


Figure 21. 3D time-structure model of top of Copacabana Group pinching-out towards the base of the Cretaceous.

Top of the Mesozoic time-structure map

The top of the Mesozoic time-structure map shows essentially the same features observed in the base of the Cretaceous and top of Copacabana time-structure maps. Thus, the Mesozoic interval was not greatly affected or disturbed by faulting from the early episodes of compressional tectonics related to Andean subduction. Some differences are nevertheless clear. Overall the area was shallower at this time and the basin shape is less elongated.

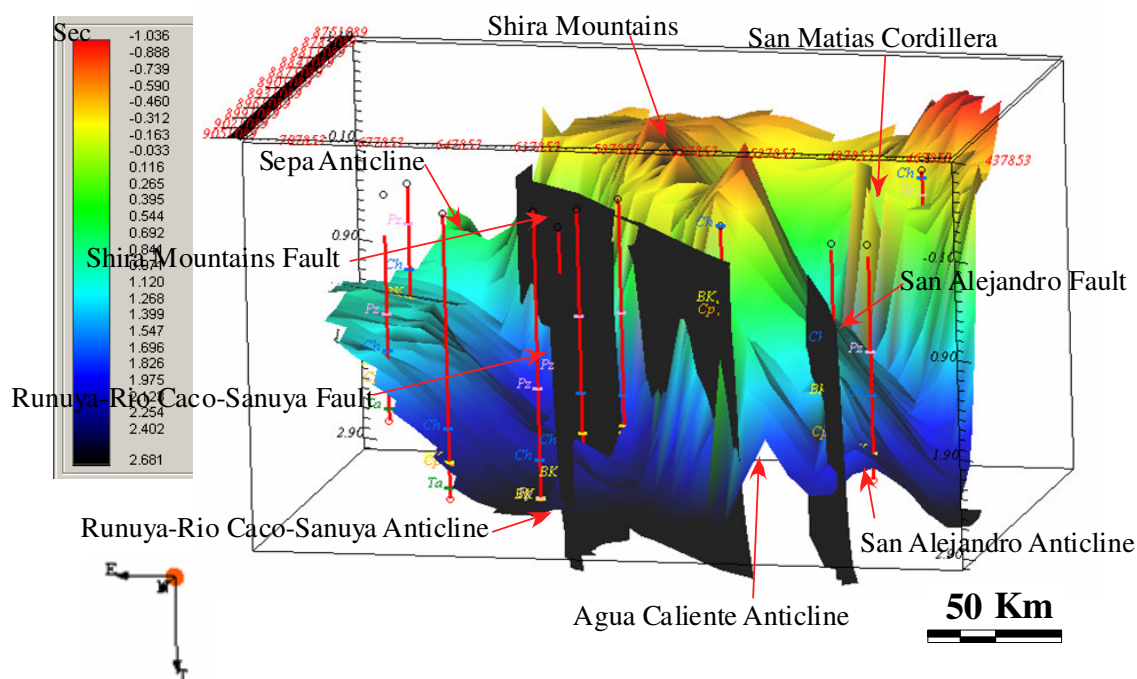


Figure 22. Base of the Cretaceous 3D time-structure model. Illustrates the relationship between faults and structures as well as some of the wells in the study area.

The structures located in the eastern central Ucayali Basin are better defined and easier to identify compared to the previous time structure maps. For example, the Runuya-Rio Caco and Agua Caliente anticline structures are readily apparent for example (Figure 23). The eastern part of this horizon shallows toward the Brazilian Shield as observed on the previous time-structure maps. To better understand the configuration of the top of the Mesozoic in the central Ucayali Basin a 3D time-structure model has been also generated (Figure 24).

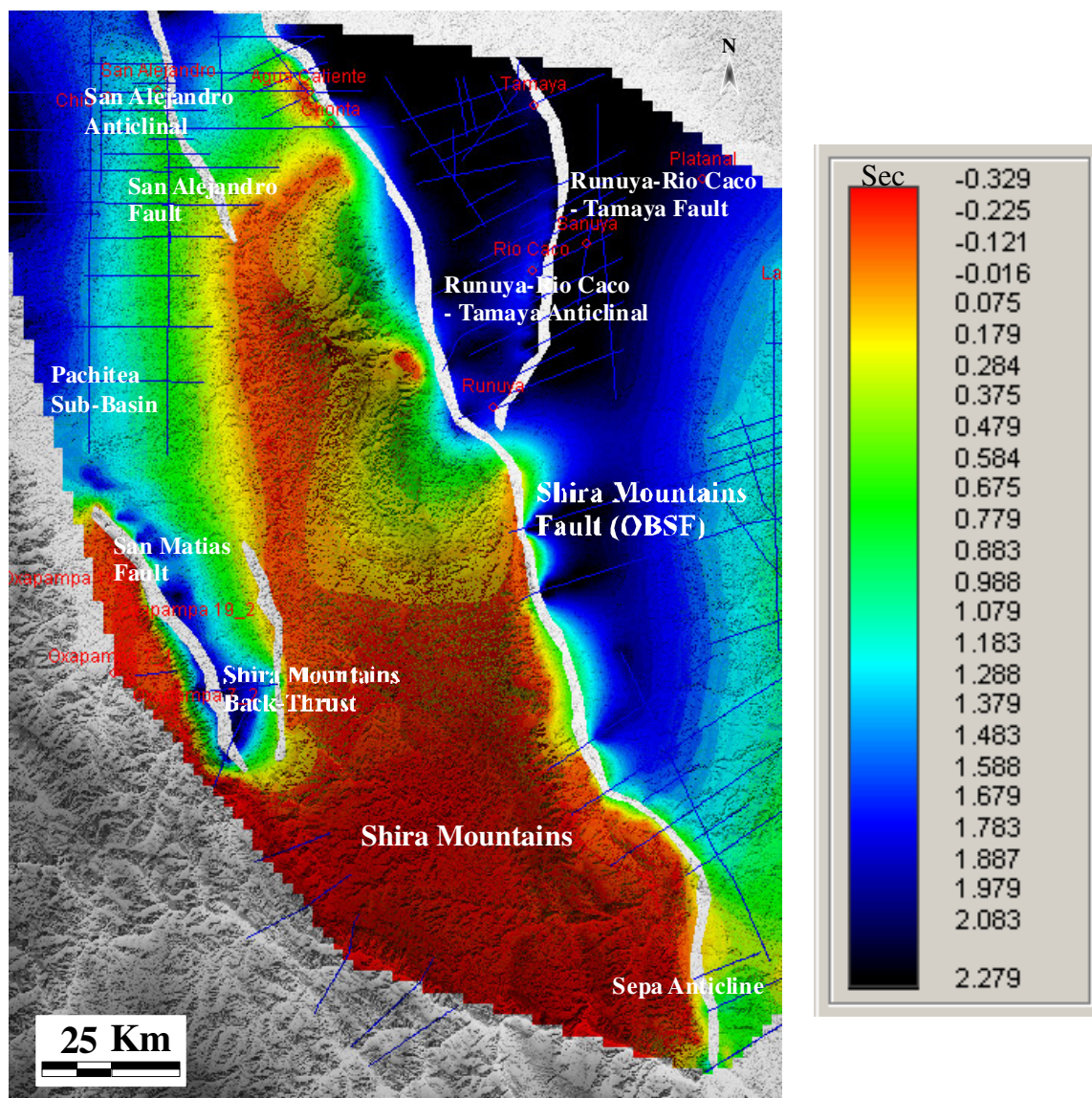


Figure 23. Top of the Mesozoic time-structure map.

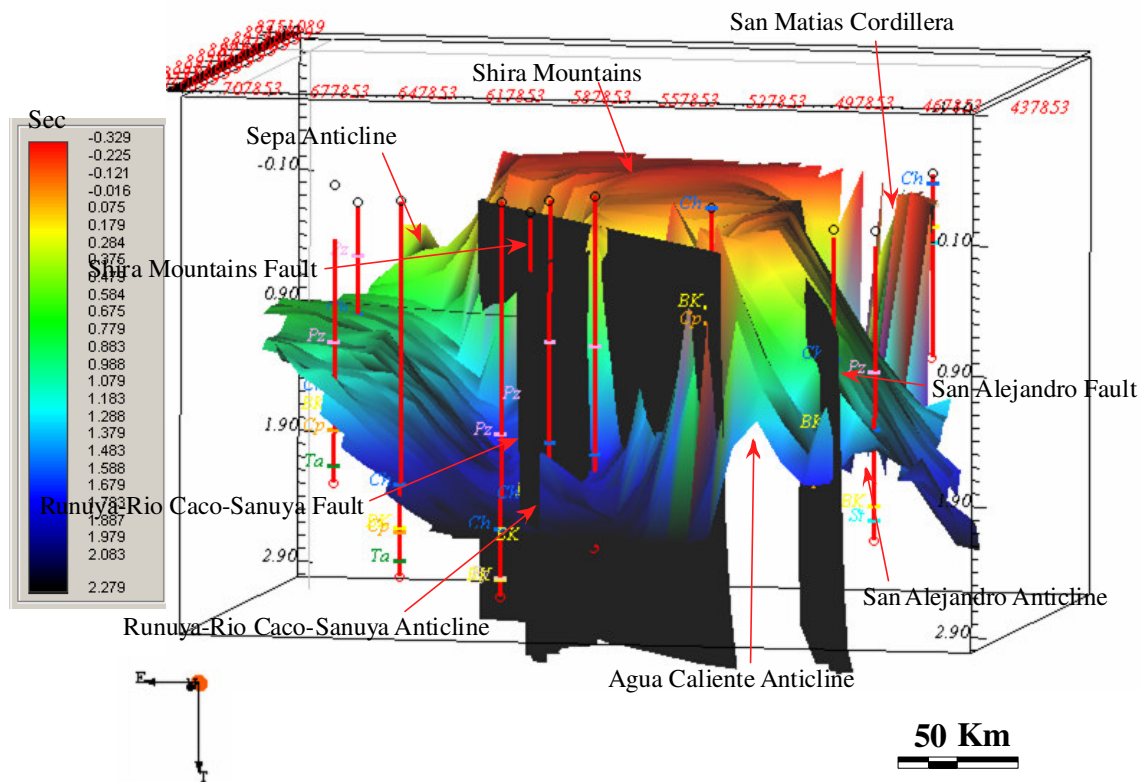


Figure 24. Top of Mesozoic time-structure 3D model.

Isochore Maps

Two isochore maps of the Permian and the Cretaceous were generated to identify the thickness of these sequences and recognize where the main depocenters were located to establish the nature of the faults in the study area at that geologic time. The Permian map shows a maximum thickness in the Pachitea sub-Basin. It can be seen clearly as the thickness decreases toward the Shira Mountains. However, in the eastern central Ucayali Basin the overall thickness is less (Figure 25).

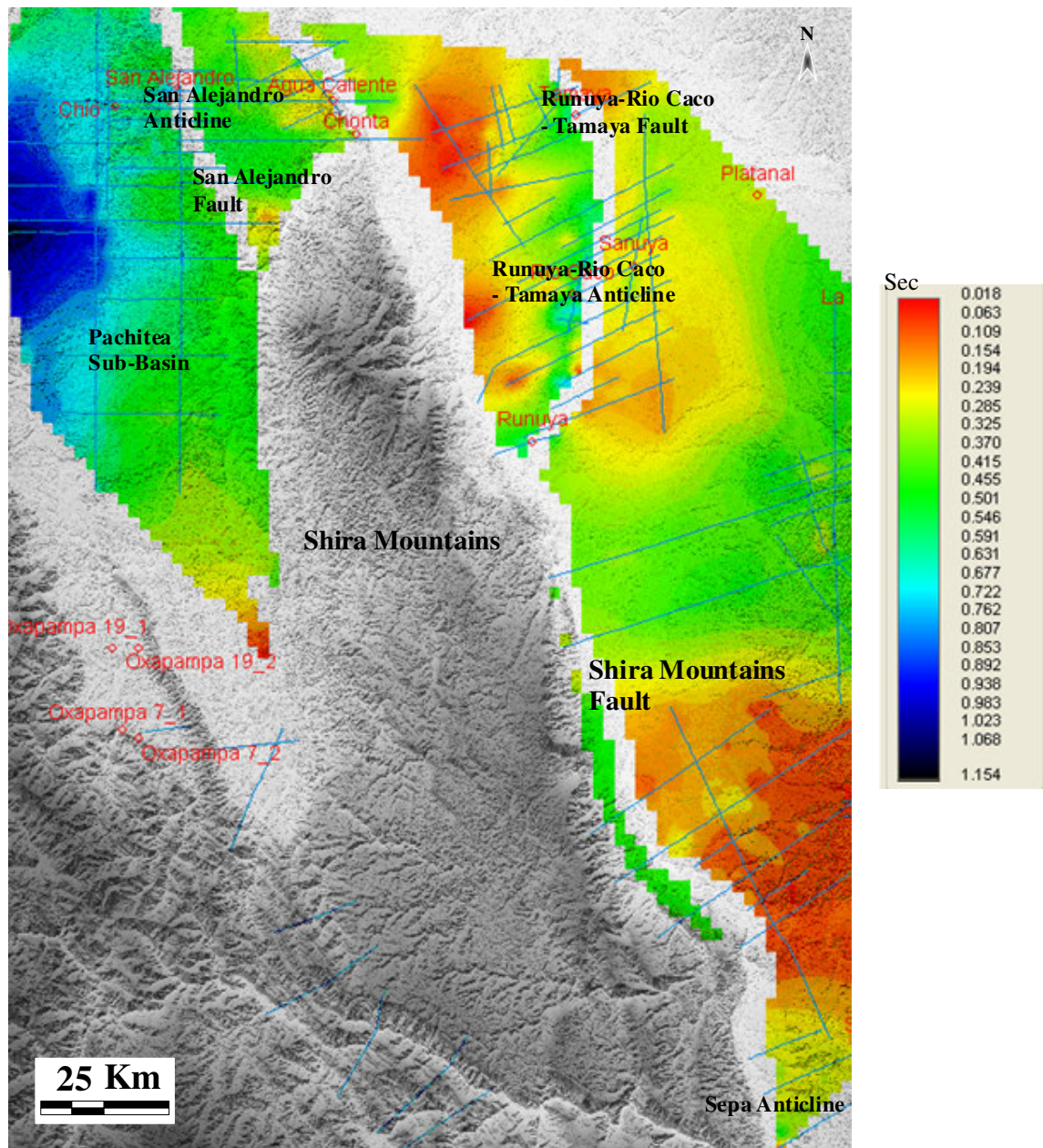


Figure 25. Permian isochore map. Clearly shows maximum thickness in the Pachitea sub-Basin.

The Cretaceous isochore map shows maximum thickness in the Pachitea sub-Basin, decreasing towards the Shira Mountains and the Agua Caliente Anticline. The eastern central Ucayali Basins indicates a fairly regular thickness of the Cretaceous sequence except in the central part where it decreases probably as a consequence of a local uplift resulting from the Andean orogeny (Figure 26).

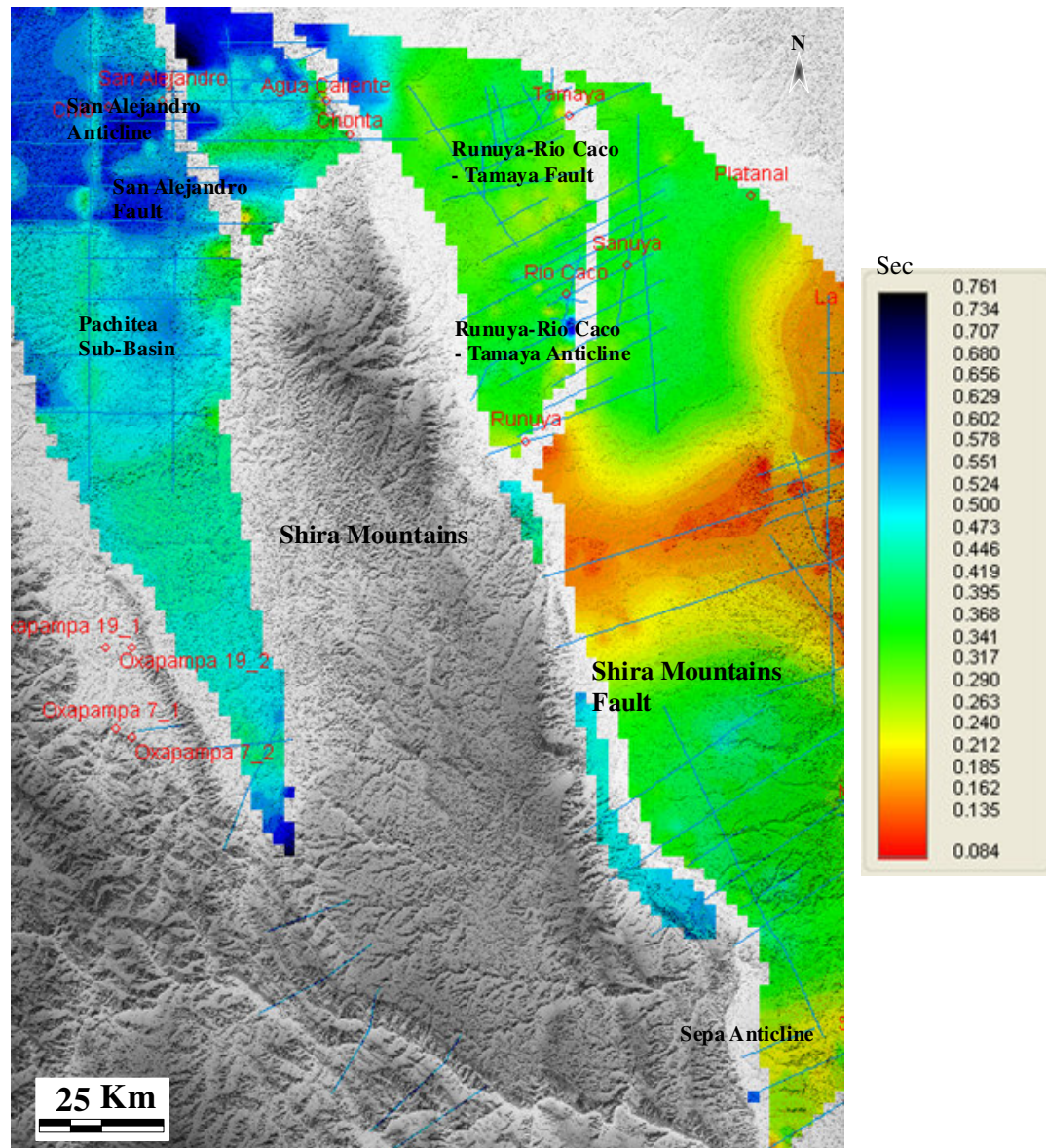


Figure 26. Cretaceous isochore map. Maximum thickness in the Pachitea sub-Basin.

These results show that the main depocenter during the Permian and Cretaceous times was located in the Pachitea sub-Basin, consistent with interpreting the Shira Mountains Fault probably as normal fault during this times with the hanging wall located in the Pachitea sub-Basin.

Depth Cross Sections

To establish the nature of the main faults, especially the Shira Mountains Fault three cross sections were generated and balanced to the Chonta Formation, the upper most regional reflector in the Cretaceous. These cross sections further allow us to identify the geologic time when the Shira Mountains Fault was inverted and the beginning of the development of this mountain chain. The structural profiles constructed in this project cover the entire central Ucayali Basin (Figure 11).

Cross Section A-A': Chio-San Alejandro-Agua Caliente-Tamaya

This 181.52 km profile crosses several important structural features. From west to east these include: Early Mesozoic salt swells, the San Alejandro Fault and anticline, the Agua Caliente anticline, the Shira Mountains Fault, the Runuya-Rio Caco-Tamaya Fault and south north trending anticline. The balanced profile length is 189.04 km therefore the amount of shortening in this area is 7.53 km, which is equivalent to 3.98%. The data used in the construction of this structural profile were:

- Seismic lines: NP31, G603, G450 and W74-29 (Figure 27)

- Wells: Chio, San Alejandro, Agua Caliente and Tamaya (Figures 27, 28a and 29a)
- Geological maps: Geologic quadrangles 18M-23O INGEMMET
- Field reports

The Agua Caliente anticline is a dome-like structure trending SE-NW and, bounded by the west dipping Shira Mountains thrust (Bolaños and Wine, 2003). Hydrocarbons have been produced from this structure since the 1930s (Hermoza, et al., 2005). Post-Paleozoic sediments are characterized by almost horizontal bedding in the eastern central Ucayali Basin whereas the whole sedimentary infill in the western flank is dipping between 15° to 35°, with the steeper horizons localized between the San Alejandro and Agua Caliente anticlines. The pre-Mesozoic sequence appears to have been a large half-graben structure that has been subsequently inverted by compression (Figure 28).

The Shira Mountains Fault is observed on line G450 where it is seen as a very steep thrust associated with the Incaic or Quechua tectonic phases in the Cenozoic. The reconstruction indicates detachment of this fault at 20 km depth.

The balanced cross section further shows that the Shira Mountains and Runuyar-Rio Caco-Tamaya Faults were originally normal faults associated with the Paleozoic rifting events and remained so through Late Cretaceous – Early Paleocene times. A pre-Cretaceous half graben structure can be observed in the Tamaya area of eastern central Ucayali Basin (Figures.28b and 29b). The San Alejandro Fault, however, shows thrusting and inversion as early as Upper Cretaceous compressive Peruvian phase.

The reconstructed profile also shows that significant erosion of Mesozoic and Tertiary sequences occurred primarily between the Agua Caliente anticline and the San Alejandro anticline. Thus, the northern central Ucayali Basin was exposed during the Cretaceous and Cenozoic.

Cross Section B-B': Pachitea-Shira Mountains-Rio Caco-Sanuya

The cross section B-B' is 167.23 km long and crosses the Pachitea sub-Basin, the northern Shira Mountains and the Runuya-Rio Caco-Tamaya and Sanuya faults and anticlines. The length of the balanced profile is 177.02 km for a total shortening of 9.79 km or 5.53%. The data used in the construction of this structural profile were:

- Seismic lines: G609 and W75-89 (Figure 30)
- Wells: Rio Caco and Sanuya (Figures 30, 31a and 32a)
- Geological maps: Geologic quadrangles 18M-23O INGEMMET
- Field reports

The Shira Mountains are the most prominent structural feature and are the main sediment source for the present day central Ucayali Basin. They are bounded by the west dipping Shira Mountains Fault, the major thrust fault in the study area. The Mesozoic sedimentary units dip west between 15° to 20°, whereas, the Paleozoic sequence dips west, between 25° to 35°, pinching out towards the Shira Mountains in the Pachitea sub-Basin (Shira Mountains fault hanging wall).

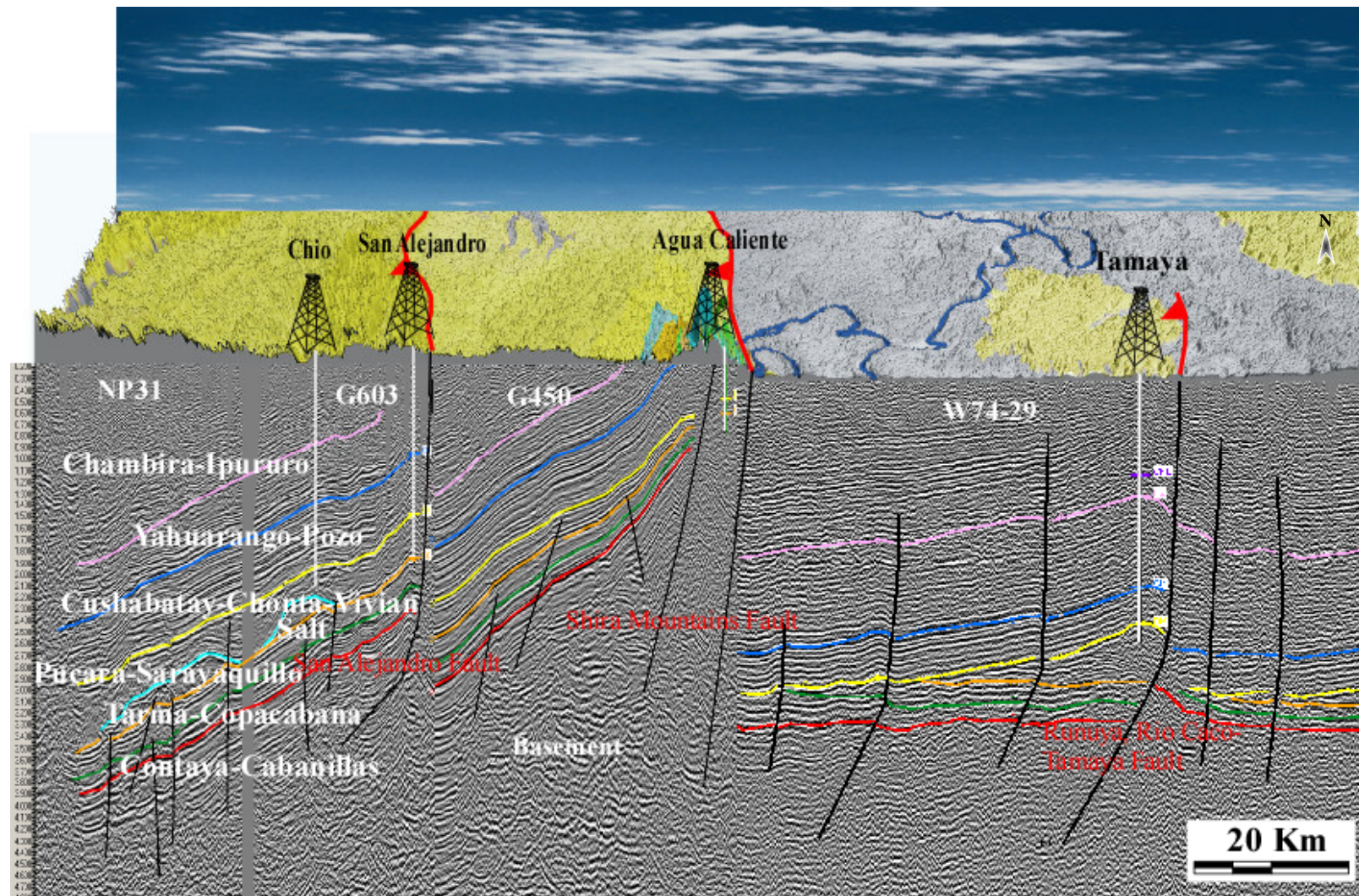


Figure 27. 3D Geologic map and seismic lines NP31, G603, G450 and W74-29. Used for the construction of the structural profile A-A'.

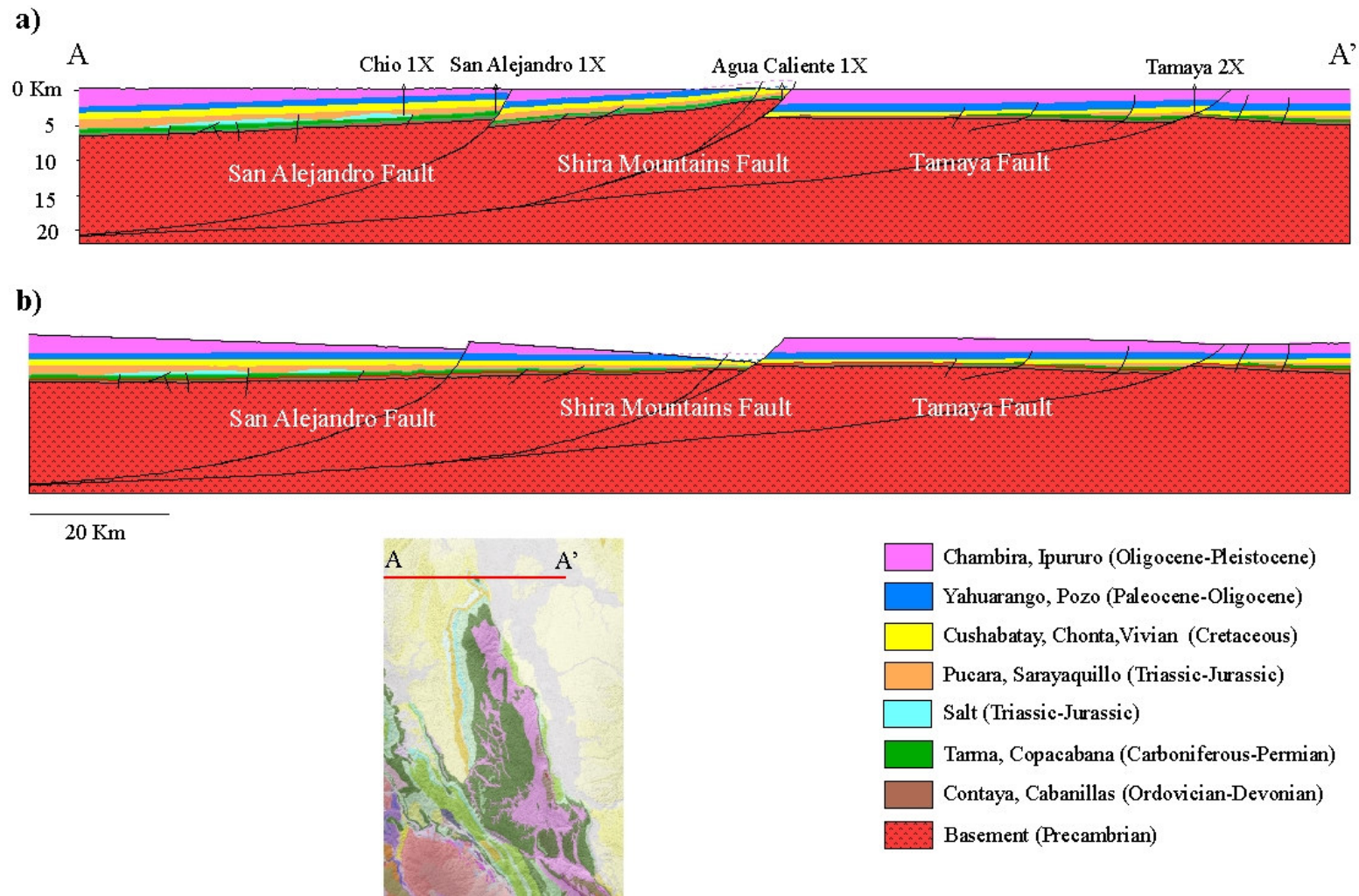


Figure 28. Balanced structural profile A-A'. a) Structural profile A-A'; b) balanced cross section to the top of Cretaceous. Illustrates the still extensional nature of the Shira Mountains Fault as well as Tamaya Fault and the beginning of the San Alejandro Fault inversion.

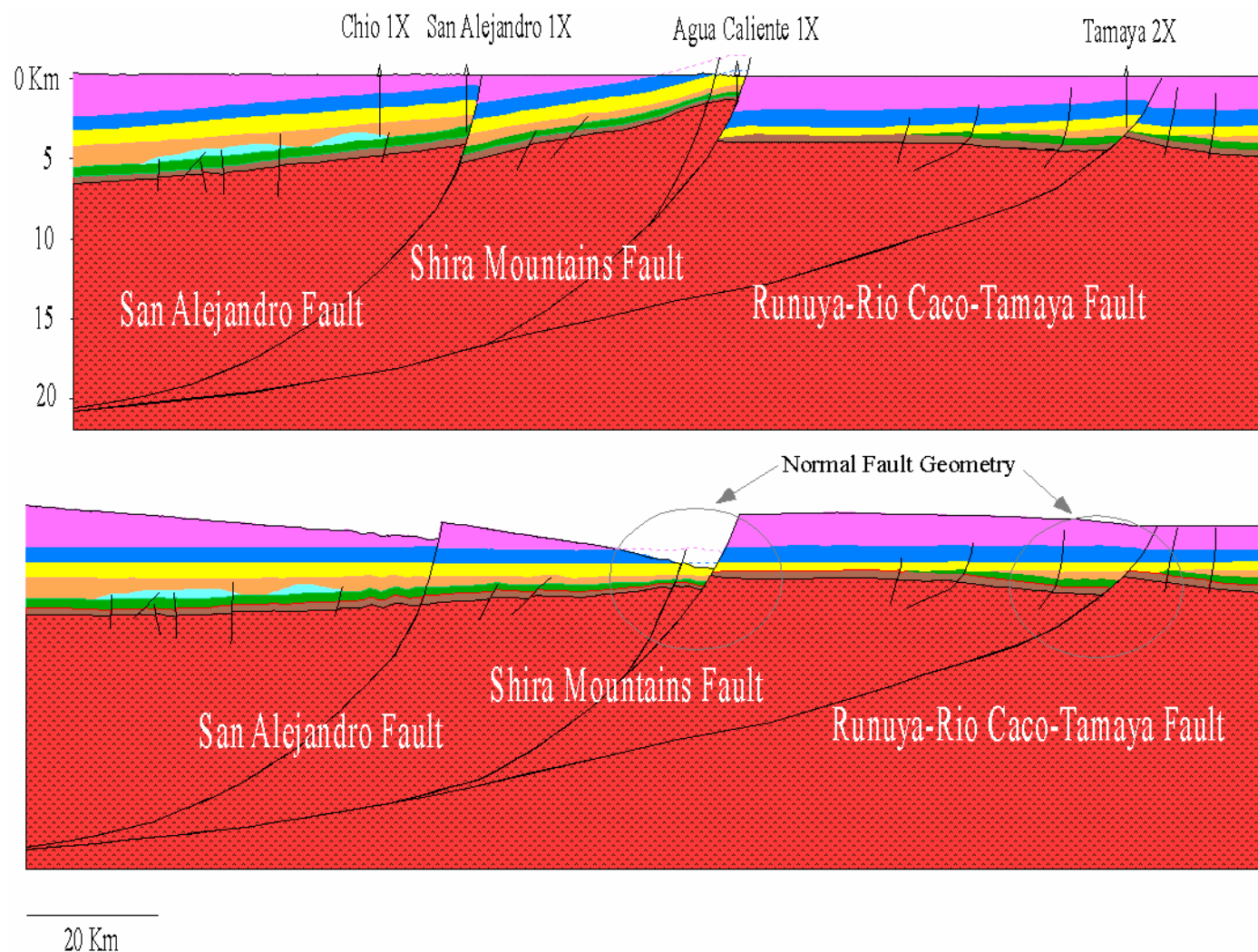


Figure 29. Balanced structural profile A-A' with vertical exaggeration. a) Structural cross section A-A'; b) balanced cross section.

The reconstruction balances if the Shira Mountains fault detaches at ~ 25 km depth. In the eastern central Ucayali Basin an inverted half graben is clear along strike from the Tamaya region on profile B-B'. This structure is covered by almost horizontal Mesozoic and Cenozoic sediments (Figures 31a and 32a). The Sanuya anticline is a SW-NE trending structure bounded to the east by the Sanuya Fault. The hanging wall contains pre-Cretaceous sequences that pinch-out to the west, indicating normal fault growth during Paleozoic.

The Sanuya Fault cuts all the sedimentary infill. However, the vertical displacement is not as great as the other faults. This may indicate very recent inversion. In the western portion of the section, Paleozoic normal faults show no sign of inversion. The balanced cross section shows the early extensional nature of the faults at top of the Cretaceous in conjunction with the structural profile A-A'' (Figure 31b and 32b). The entire sedimentary infill is almost completely eroded from the top of the Shira Mountains

Cross Section C-C': Oxapampa-Shira Mountains-Eastern Central Ucayali Basin

The structural profile C-C' is 186.4 km long and crosses the following structural features: the Early Mesozoic salt swells (drilled by Oxapampa 7-2), the San Matias Cordillera, the San Matias fault, the Shira Mountains back thrust, the Shira Mountains and the Shira Mountains fault.

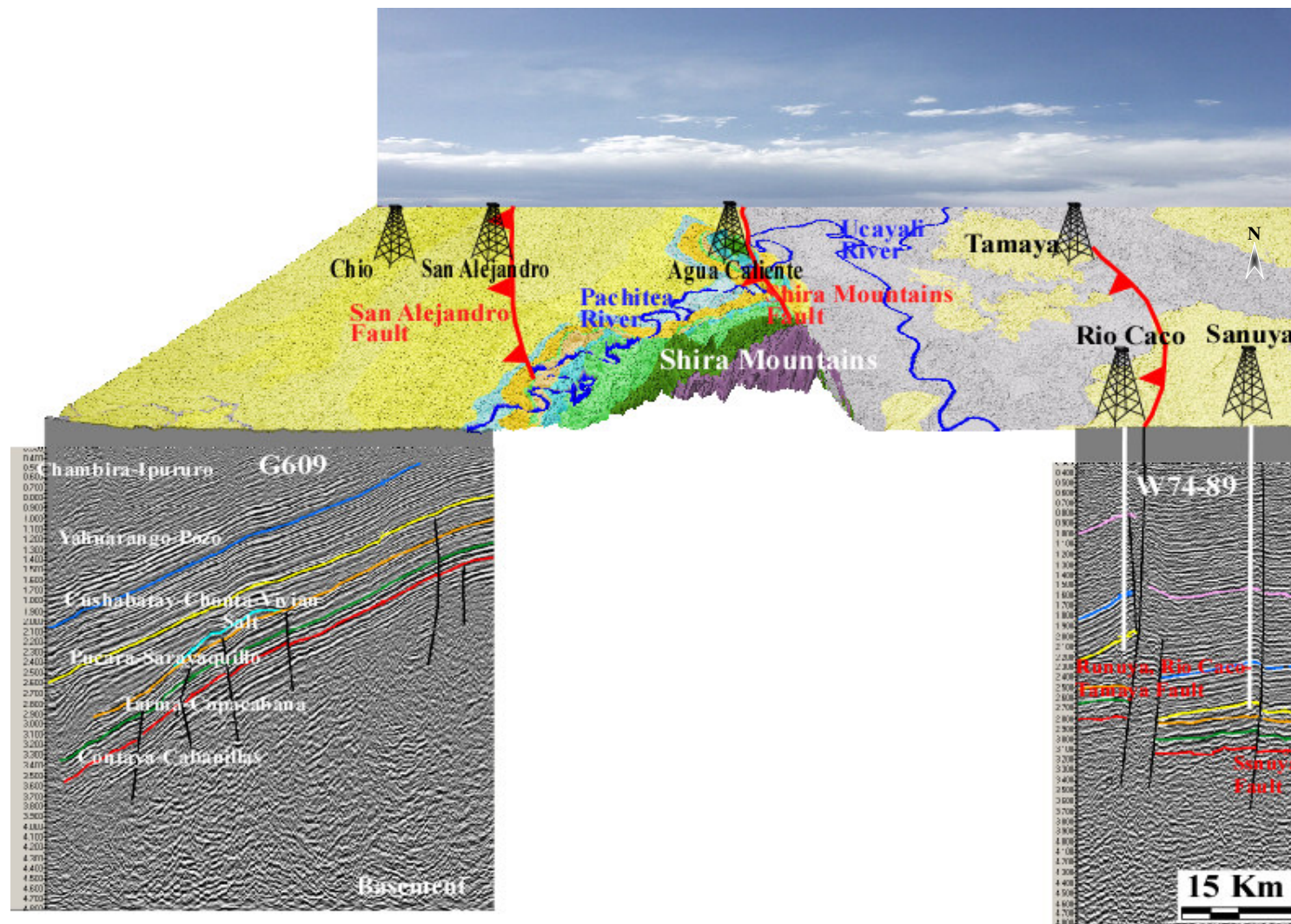


Figure 30. 3D Geologic map and seismic lines G609 and W75-89. Used for the construction of the structural profile B-B'.

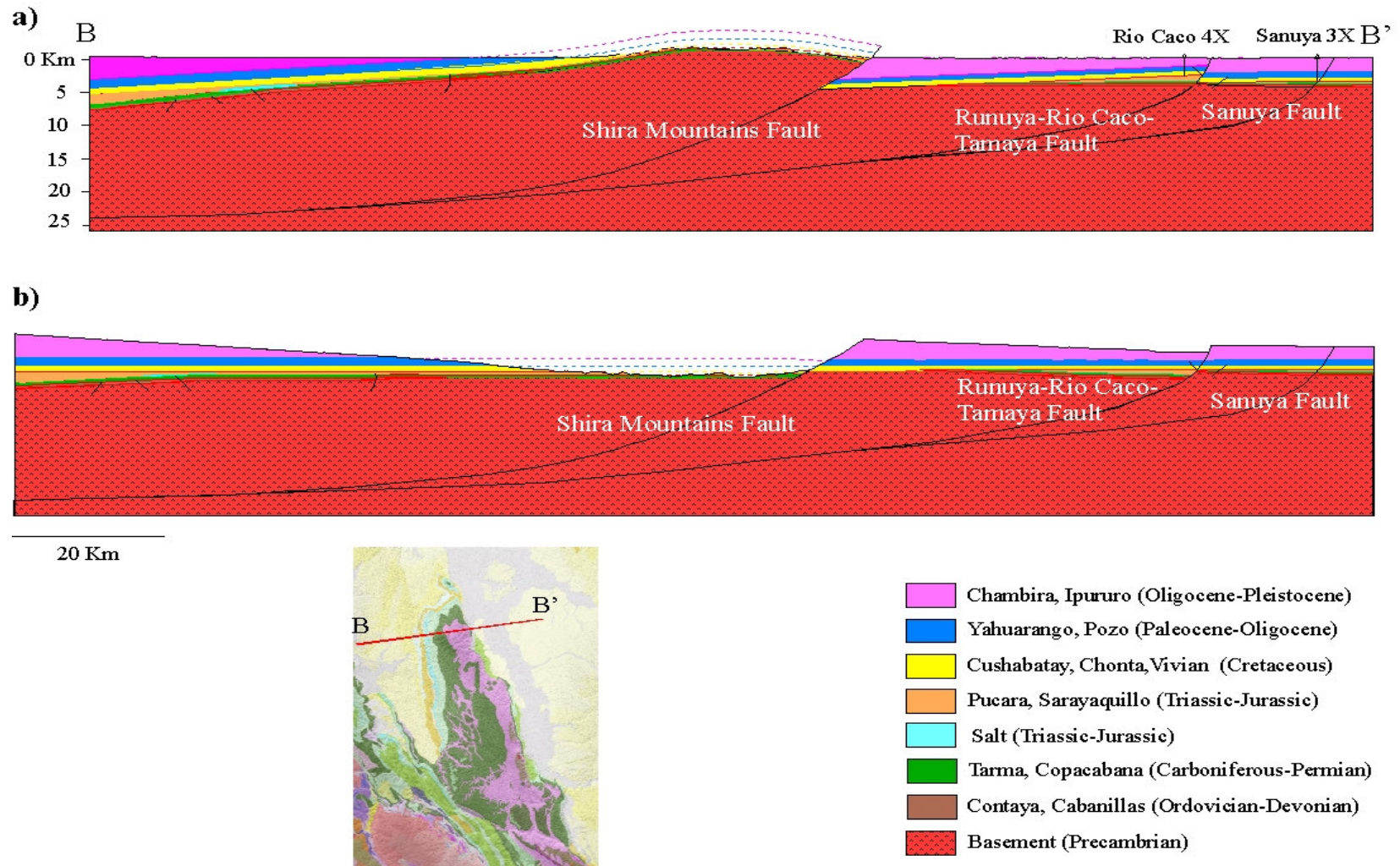


Figure 31. Balanced structural profile B-B'. a) Structural profile B-B'; b) balanced cross section to the top of Cretaceous. Illustrates the extensional nature of the all the faults.

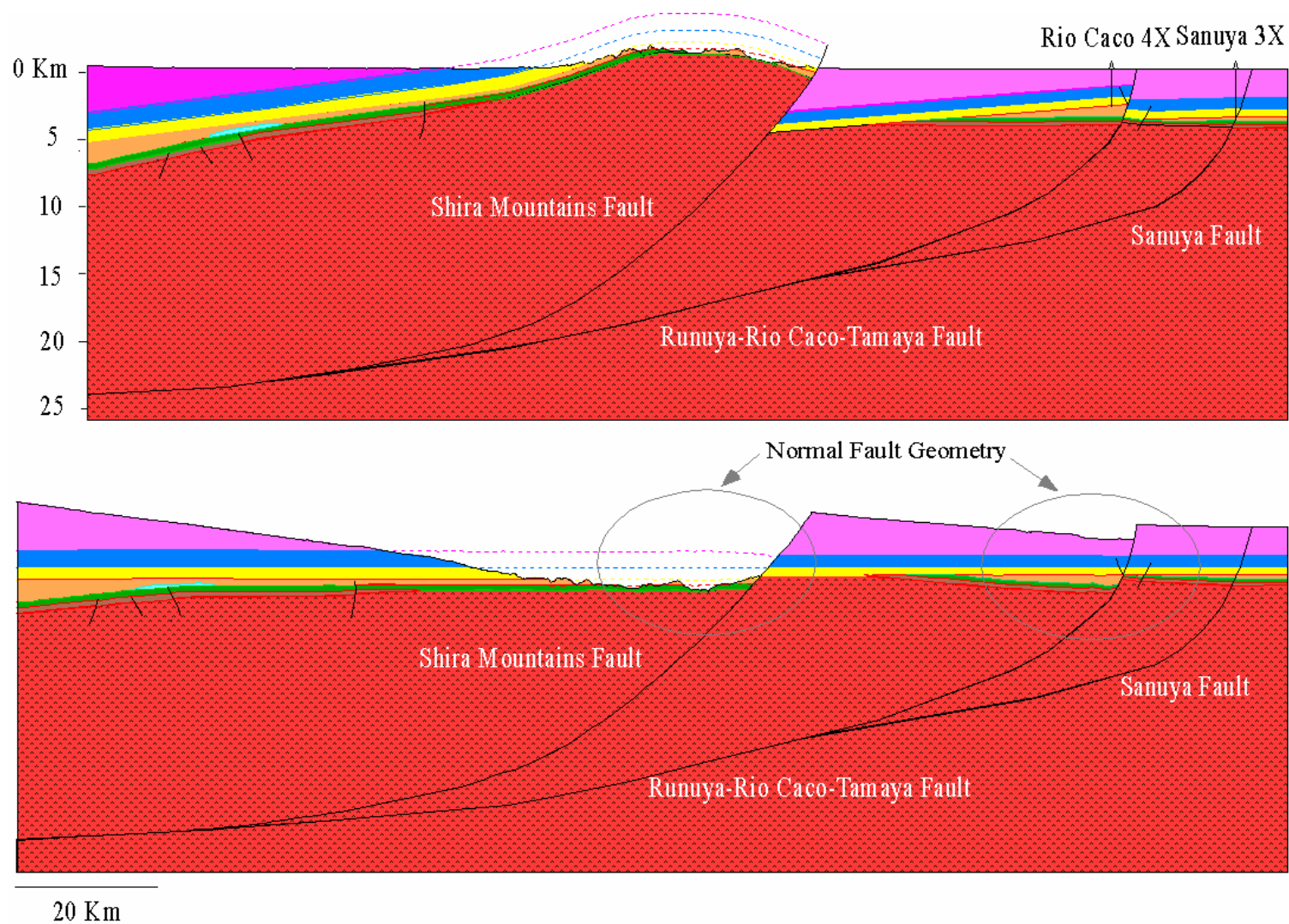


Figure 32. Balanced structural profile B-B' with vertical exaggeration. a) Structural profile B-B'; b) balanced cross section.

Total length of the balanced cross section C-C' is 192.98 km consequently the amount of shortening is 5.68 km (2.96%). This shortening is caused only by the Shira Mountains Fault only, since no other thrust or reverse faults are observed in this area..

The data used in the construction of this structural profile were:

- Seismic lines: 96ENE01, 96ENE12 and HIS15 (Figure 33)
- Wells: Oxapampa 7-1 (Figures 33, 34a and 35a)
- Geological maps: Geologic quadrangles 18M-23O INGEMMET
- Field reports

In contrast to the previous cross sections, profile C-C' shows that the Paleozoic faults are inverted much earlier probably during the compressive tectonics of the Andean Orogeny or the Peruvian phase in southern Pachitea sub-Basin close to the San Matias fault. This observation is generally consistent with Legrand et al., 2005, who suggest that the tectonic inversion affects the sub-Andean area from west to east.

The sedimentary section in the Pachitea sub-Basin dips west approximately 12° to 18°, and the units pinch out to the east toward the Brazilian Shield (Figures 33 and 34). No major compressional and extensional faulting is observed in this area in contrast to the structural profiles A-A' and B-B'. Overthrust Upper Paleozoic and Mesozoic units are observed in the western flank of San Matias Cordillera. However, this part of the profile was not balanced because there is insufficient data farther west..

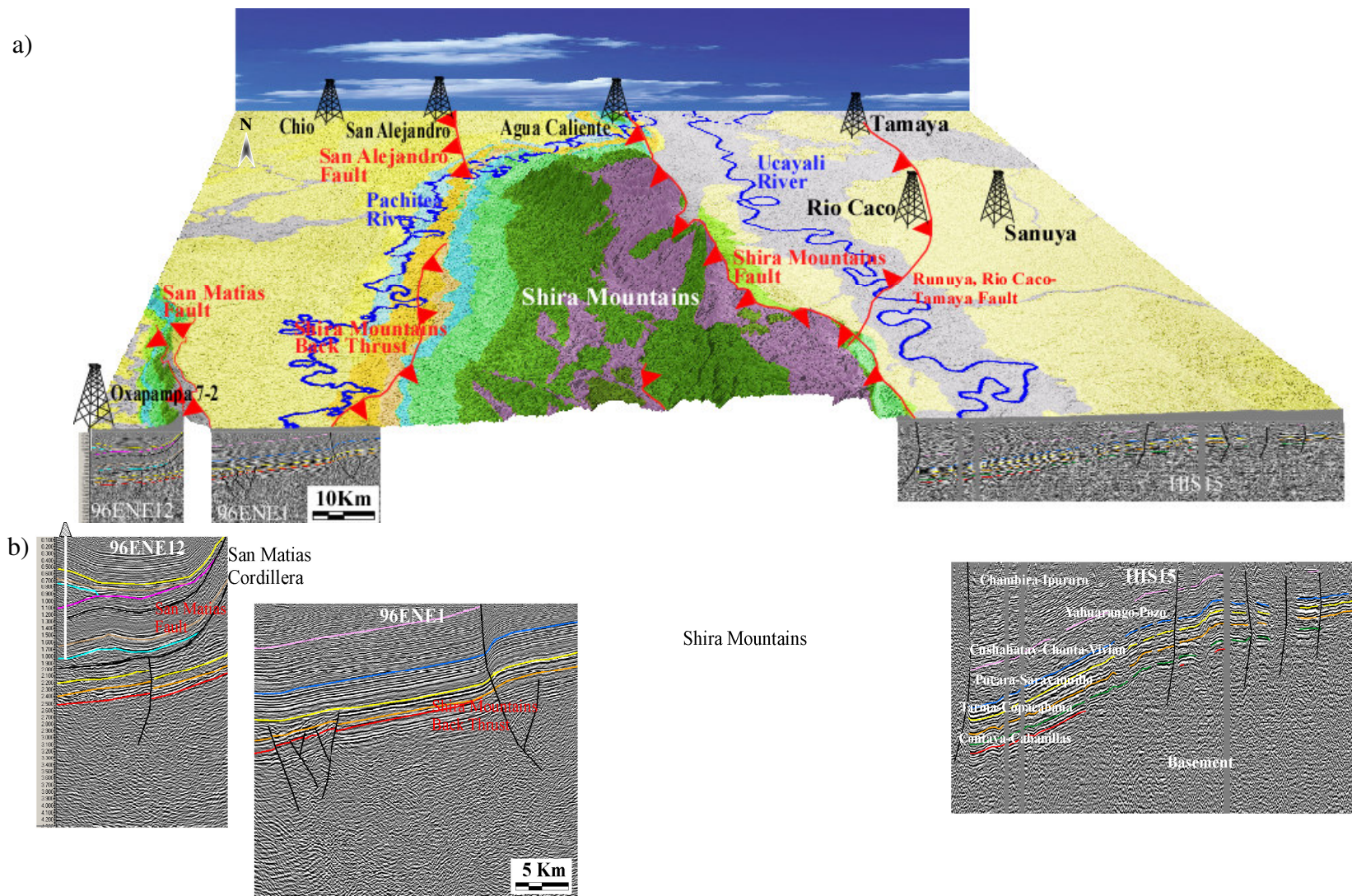


Figure 33. 3D Geologic map and seismic lines 96ENE01, 96ENE12 and HIS15. Used for the construction of the structural profile C-C’.

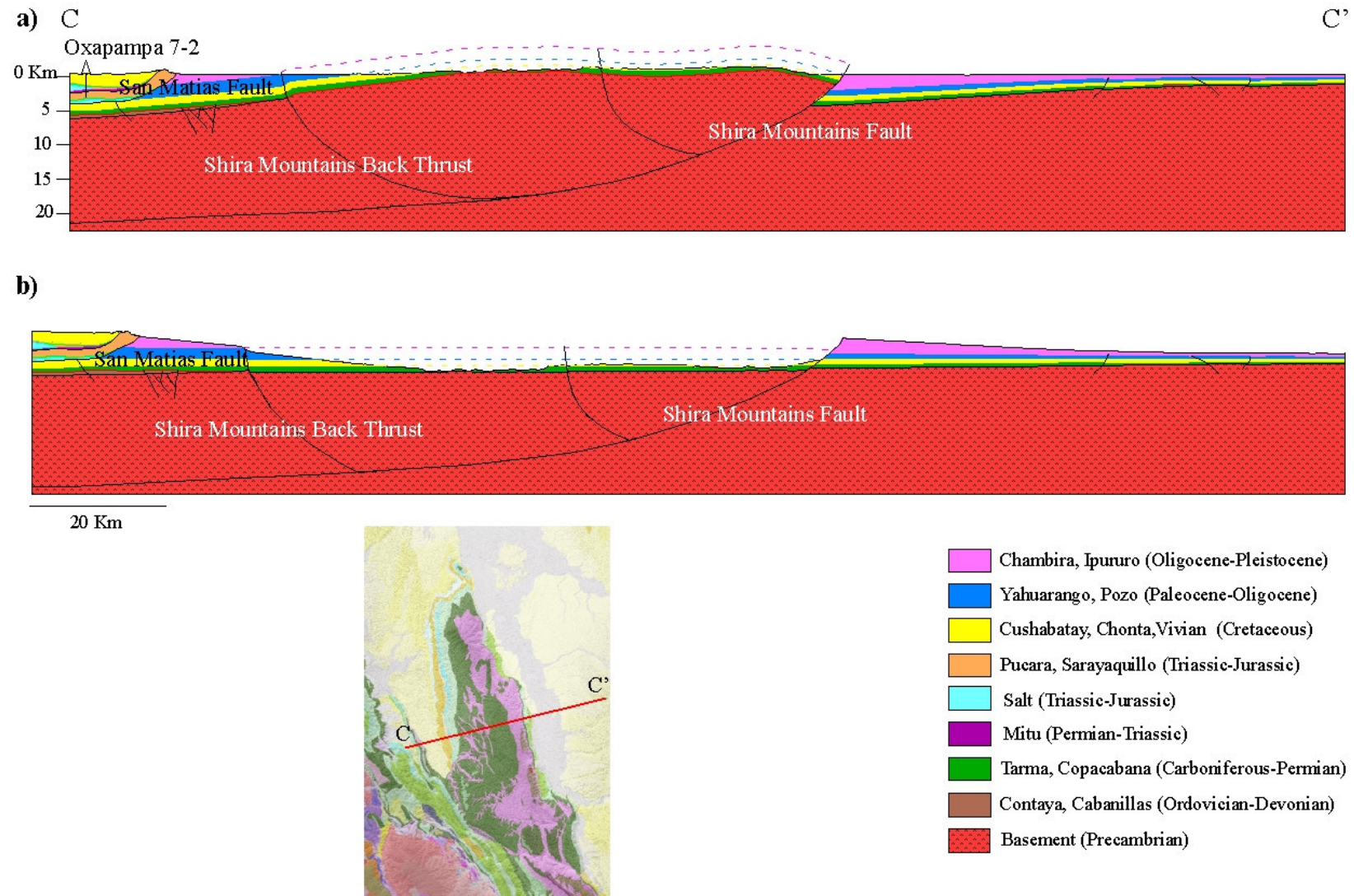


Figure 34. Balanced structural profile C-C'. a) Structural profile C-C'; b) balanced cross section to the top of Cretaceous. Illustrates the extensional nature of Shira Mountains faults and extensive erosion on the top of Shira Mountains.

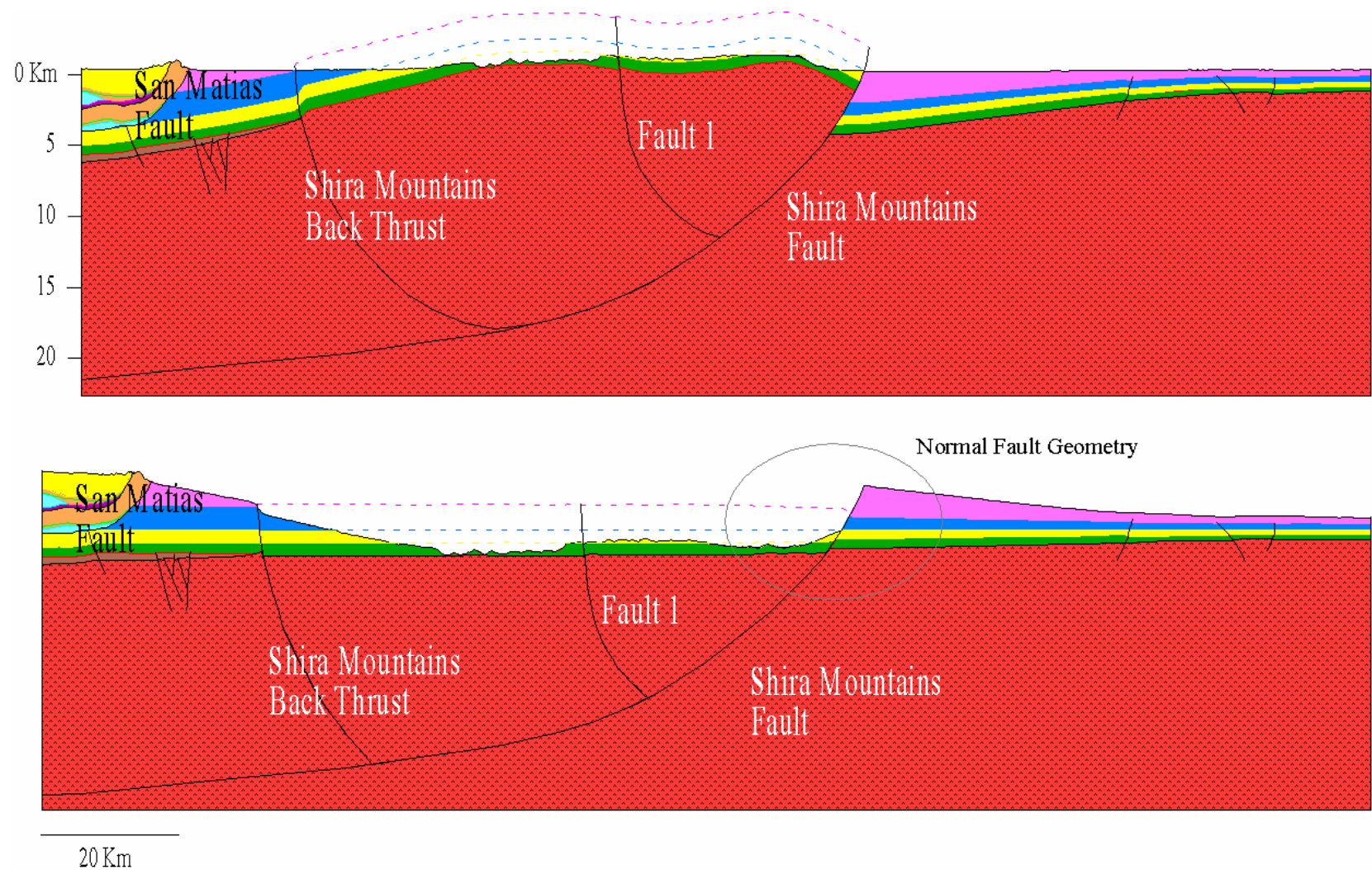


Figure 35. Balanced structural profile C-C' with vertical exaggeration. a) Structural profile C-C'; b) balanced cross section with vertical exaggeration.

The Shira Mountains are again the most important structural feature on this profile. As in profile B-B', almost the complete sedimentary section has been eroded away. This makes it difficult to establish the nature of the fault at this location. Nevertheless, a thin sequence of Permian and Cretaceous units on the hanging wall is displaced downward in comparison with the foot wall sedimentary sequences, confirming the extensional nature of the fault during this time.

Interpretation of the Detachment of Shira Mountains Thick Skinned Thrust Fault.

One of the most significant contributions of this research is to establish that the depth of the Shira Mountains fault likely detaches at a depth of ~ 20 to 25 km in the central Ucayali Basin. The most important faults included in the structural profiles were modeled using 2D Move. This software permits the shape and depth of the faults to be adjusted to model the current configuration of the different structures and stratigraphic horizons. Although this is a quite deep level for detachment, it is consistent with focal mechanisms studies that show seismicity over the 15 to 35 km depth range (Henry and Pollack, 1988).

According to Suarez, et al. (1990) the majority of the earthquakes in the overriding continental plate are concentrated in the sub-Andean region over an area roughly 100 km wide. They are concentrated within the upper 35 km, showing that brittle deformation extends here to abnormally large depths with respect to other intracontinental active belts (Figure 36).

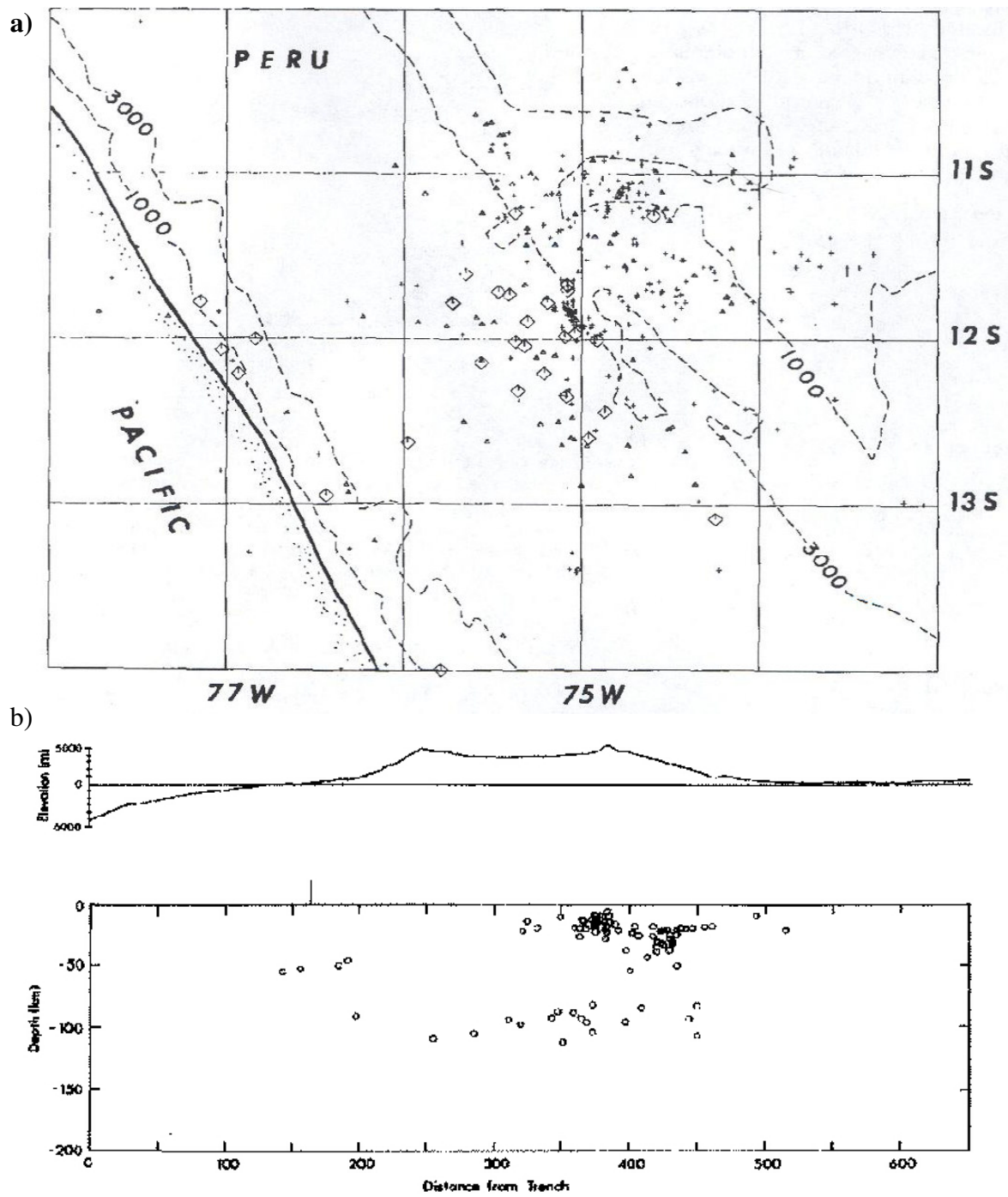


Figure 36. Epicentres and hypocentres of earthquakes in central Perú. a) Epicentres of earthquakes location; b) cross section A-B earthquakes hypocentres depth. Circles are the hypocentres. Simplified topography of the Andes is shown. (from Suarez, et al., 1990)

The fault-plane solutions obtained from seismic events in the western sub-Andes show high angle thrusting on planes oriented roughly north-south and generally dipping westward (Sandeman, 1995) coincident with the Shira Mountains fault direction and dip. More data is necessary to confirm the extent of brittle seismic deformation in the sub-Andes and its implications in the tectonic evolution of Andean type mountain belts. (Laurent and Pardo, 1974)

Timing of Tectonic Inversion

A key constraint on recent basin evolution is to determine precisely when various compressional episodes affected the region and when the inversion structures that serve as primary hydrocarbon traps developed. To do this, we examined growth stratal patterns associated with the observed structures and used biostratigraphic data at the Tamaya well to constrain the timing. Determining the fold mechanism exclusively from the final fold geometry is possible only for a limited suite of structures. The nature and time of fold-thrust interaction in shallow structures can be inferred by coupling the fold geometric analysis with the study of syntectonic sediment stratal architectures. Several factors such as axial surface activity, fold uplift, tectonic inversion, limb rotation and limb widening rates, together with sedimentation and erosion rates, control growth stratal patterns (Storti and Poblet, 1997).

Growth stratal patterns were found on several seismic lines in the eastern central Ucayali Basin, including, W74-29, W74-31, W74-53 and W74-66. These illustrate the period of time when the tectonic inversion affected the main faults in the study area (Figure 37).

The model applied for this project is based on the ratio between the uplift rate and syntectonic sedimentation rate (U/S), which in this case is assumed to be lower than 1 during the final stage of folding.. The rheological properties of growth and pre-growth strata, the gravitational stability of growth strata and the progressive volume reduction produced by compaction were not taken into account in the construction of this model (Storti and Poblet, 1997).

The progressive evolution of a self similar and sheared growth fault-propagation fold is shown in Figure 38 (Storti and Poblet, 1997). In fault-propagation folding, growth strata are passively transported downward from the anticline crest and upward from the foreland and the hinterland, thus acquiring an anticline shape (Cross and Lessenger, 1988). The anticline geometry in pre-growth units is maintained as growth continues. These are called coherent geometries because the same shape occurs in both the pre-tectonic and syntectonic units (Davies and Posamentier, 2005).

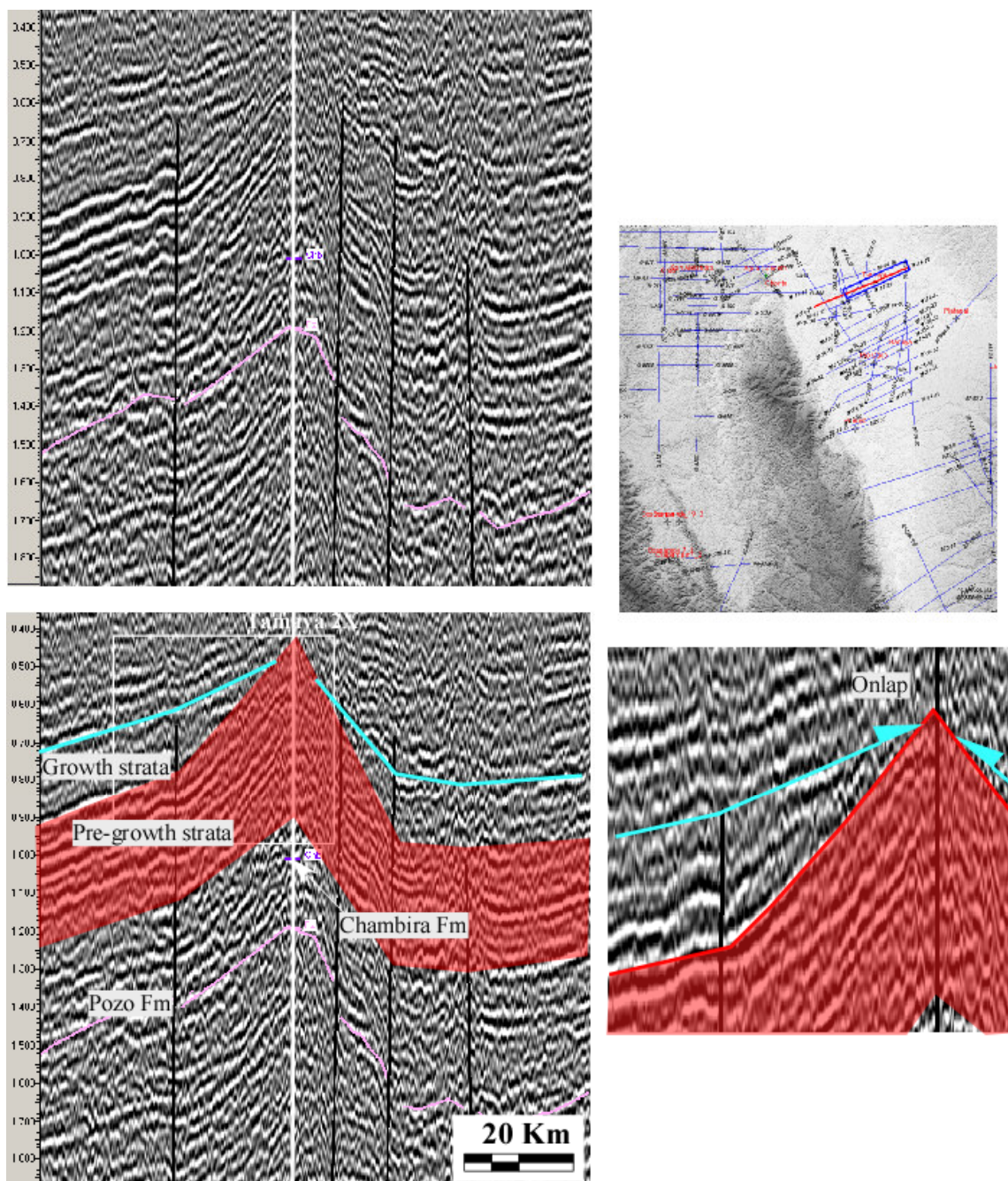


Figure 37. Seismic line W74-29. Illustrates growth stratal patterns in the northeastern central Ucayali Basin.

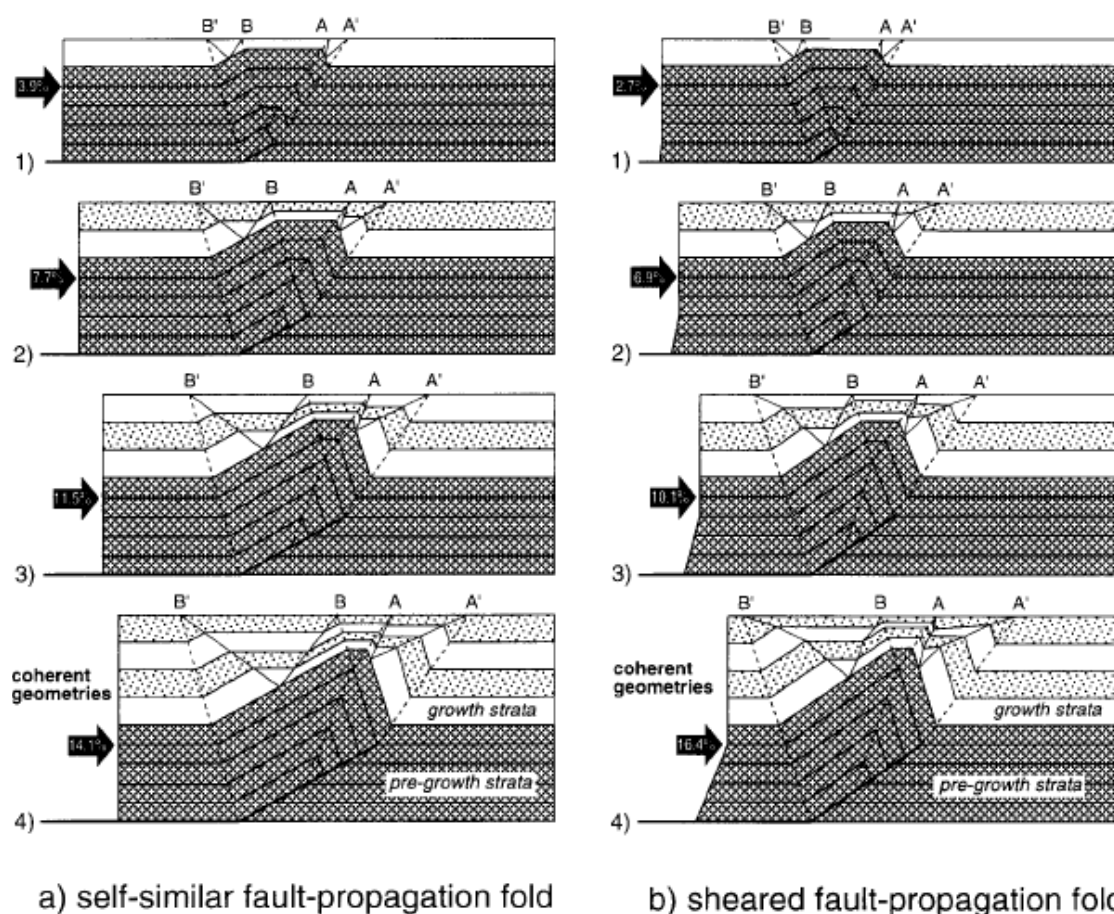


Figure 38. Self similar folding model. a) Self-similar folding; b) excess layer-parallel shear in the fold core. Forward modeled growth fault-propagation folds for uplift rate lower than sedimentation rate. (from Storti and Poblet, 1997)

To establish the time interval when these growth structures developed as a consequence the tectonic inversion, the Tamaya well plays an important roll. Growth stratal patterns are located within the Miocene-Pliocene aged Ipururo Formation at 0.8 ms depth proximately, (Figure 39) which corresponds to Upper Miocene between 7.2 to 5.3 million years interval according to the biostratigraphy of Tamaya well (Perupetro, 1980). This indicates that the inversion of the Shira Mountains fault as well as the Runuya-Rio Caco-Tamaya fault took place during the Quechua 3 compressive phase.

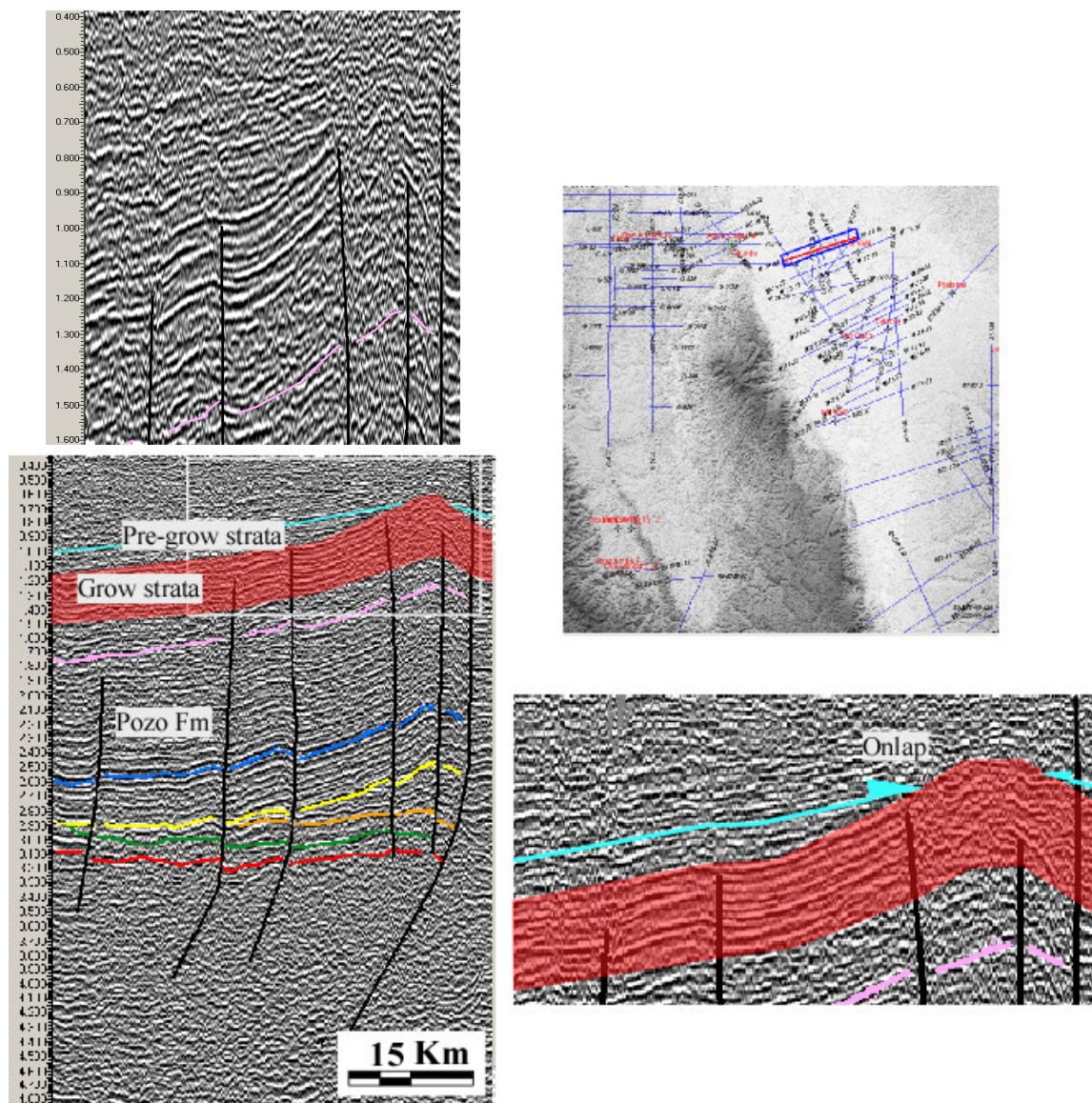


Figure 39. Seismic line W74-66. Illustrates growth stratal patterns in the northeastern central Ucayali Basin at 0.8 ms depth.

CHAPTER V

CONCLUSIONS

To establish the structural and stratigraphic history of the Shira Mountains and the central Ucayali Basin, I interpreted a 2D seismic survey and used the resultant time structure, isochore maps, well log correlations, and balanced cross sections to determine the key depositional settings and the nature and timing of major faults in the region.

The central Ucayali Basin formed in the Early Paleozoic. Repeated episodes of rifting, compression, and subduction resulted in a wide variety of sedimentary environments that record the tectonic history of the region. Extension, rifting and the resulting subsidence led to initial basin formation. The time from Albian to Maastrichtian was marked by tectonic quiescence and a major transgression, indicating slow thermal subsidence. The lack of significant tectonic deformation is clear in the seismic data where the main Cretaceous units are disturbed only by very recent compression. Major inversion and compressional tectonics affected the basin beginning in the Paleogene during the Incaic phase of the Andean orogeny, with major basin inversion beginning in the Miocene

Three main sedimentary deposits related to different tectonic settings were identified through this research. These are.

- Rift-related deposits. These deposits included the Contaya Formation, the Cabanillas Group, the Ambo Group, the Tarma Group, the Copacabana Group, the Ene Formation and the Mitu Group, and range in age from the Devonian to

the Early Triassic. They formed in half graben basins bounded by major regional normal faults.

- Post-rift related deposits. These sedimentary sequences were deposited from the Triassic to the Early Paleocene and are characterized by long periods of marine sedimentation punctuated by regressions due to minor compressive events. These deposits include the Pucara Group, the Sarayaquillo Formation, the Cuchabatay Formation, the Raya Formation, the Agua Caliente Formation, the Chonta Formation, the Vivian Formation, the Cachiyacu Formation, the Huchpayacu Formation and the Casa Blanca Formation.
- Inversion-related deposits. The inversion related deposits are more recent Cenozoic sedimentary units. The Yahuarango, Pozo, Chambira and Ipururo Formations were deposited during this phase, which was dominated by compression from the Incaic phase of the Andean orogeny. This resulted in uplift and inversion of the early rift basins.

The Shira Mountains, the Runuya – Rio Caco-Tamaya anticline, the San Alejandro anticline, San Matias anticline, the Shira Mountains fault, the Runuya-Rio Caco-Tamaya fault, the San Matias fault, and the San Alejandro fault are the most important structural features in the study area.

The reconstructed, balanced cross sections clearly show that the key faults, the Shira Mountains, the Runuya-Rio Caco-Tamaya and the San Alejandro, were initially normal faults bounding major half grabens that were inverted only very recently. The age of inversion was Upper Miocene, between 7.2 and 5.3 Ma, as demonstrated by the

timing of growth stratal patterns identified on the seismic profiles. While the main phase of inversion appears to be quite recent, deposition of the Cachiycu Formation, which onlaps the Shira Mountains, indicates an initial stage of uplift beginning as early as the Campanian.

The reconstructed cross sections balance if the Shira Mountains detaches between 21 to 24 km depth. Thus, the fault can be considered as a thick skinned thrust. Detachment of the major faults at mid-crustal levels is consistent with the regional thermal history (Henry and Pollack, 1988)

REFERENCES CITED

- Audebaud E., G. Laubacher, and R. Marocco, 1976, Coupe géologique des Andes du Sud du Pérou de l'Océan Pacifique au Bouclier Brésilien: *International Journal of Earth Science*, v. 65, n. 1, p. 223–264.
- Baby P., M. Rivadeneira, C. Dávila, M. Galárraga, J. Rosero, and J. Vega, 1997, Estilo tectónico y etapas de la deformación de la parte norte de la Cuenca Oriente ecuatoriana: VI Simposio Bolivariano Exploración Petrolera en las Cuencas Subandinas, Cartagena, Colombia, Septiembre, v. 1, p. 288-302.
- Baby P., M. Rivadeneira, F. Christophoul, and R. Barragán, 1999, Style and timing of deformation in the Oriente Basin of Ecuador: Fourth International Symposium on Andean Geodynamics, October 4-9, Goettingen, Germany, p. 68-72.
- Baby, P., W. Hermoza, M. Roddaz, N. Espurt, B. Stéphane, and R. Bolaños 2005, Geodinamica Mio-Pliocena de las cuencas subandinas Peruanas: Un mejor entendimiento de los sistemas petroleros: INGEPET 2005: International Seminar Exploration and Production of Oil and Gas, Lima, Perú, 15 p.
- Barros M. C., and E. P. Carneiro, 1991, The Triassic Juruá orogeny and the tectono-sedimentary evolution of Peruvian Oriente Basin, exploratory implications: IV Simposio Bolivariano, Exploración Petrolera en las Cuencas Subandinas, Asociación Colombiana de Geólogos y Geofísicos del Petróleo, Bogotá, Colombia, Trabajo No. 6, Tomo I.

- Bolaños, R. L., and G. D. Wine, 2003, Hydrocarbon potential of Ucayali Basin, Perú: AAPG International Conference, Barcelona, Spain, September 21 – 24, 2003, v. 87, No. 13 (Supplement).
- Carlier, G., G. Grandin, G. Laubacher, R. Marócco, and Mégard, F., 1982. Present knowledge of the magmatic evolution of the Eastern Cordillera of Perú. *Earth Science Review*, 18: 253-283.
- Cobbing, E. J., W. S. Pitcher, J. J. Wislon, J. W. Baldock, W. P. Taylor, W. McCourt, and N. J. Snelling, 1981, The geology of the Western Cordillera of northern Perú, Overseas Memoirs Institute of Geological Sciences of London, v. 5, 143 p.
- Core Laboratories Inc., 1999, Geochemical evaluation of oils and source rocks and oil-source rock correlations, sub-Andean basins, Perú, v. 1, Final Report, Interpretation and Synthesis, 78 p.
- Cross, T. A., and M. A. Lessenger, 1988, Seismic stratigraphy: *Annual Review of Earth and Planetary Sciences*, v. 16, p. 319-354.
- Davies, R. J., and H. W. Posamentier, 2005, Geologic processes in sedimentary basins inferred from three-dimensional seismic imaging: *GSA Today*, v. 15, p. 4-9.
- Debelmas, J., and J. Trottereau, 1967, Ensayo sobre los rasgos estructurales mayores y la evolución de los Andes del Perú: *Boletín de la Sociedad Geológica del Perú*, v. 40, p. 5–24.
- Dunbar, R., R. Marty, and P. Baker, 1990, Cenozoic marine sedimentation in Sechura and Pisco basins, Perú: *Palaeogeography, Palaeoclimatology, Palaeoecology*, v. 77, p. 235-261.

- Elf Petroleum Perú, 1996a, Block 66 Perú final report: Perupetro Technical Archive ITP20766, Lima, Perú, 78 p.
- Elf Petroleum Perú, 1996b, Perú block 66 geological synthesis, sedimentary geology: Perupetro Technical Archive ITP20011, Lima, Perú, 115 p.
- Elf Petroleum Perú, 1996c, Perú block 66 geological synthesis, structural geology: Perupetro Technical Archive ITP20010, 135 p.
- Farrar, E., A. H. Clark, D. J. Kontak, and D. A. Archibald, 1988, Zongo-San Gaban zone: Eocene foreland boundary of central Andean orogen, northwest Bolivia and southeast Perú: *Geology*, v. 16, Issue 1, p. 55 - 58.
- Fernandez, J. 2002, The Pucara petroleum system and pre-Cretaceous sabkha regional seal, a new hydrocarbon play in the Peruvian fold and thrust belt: IV International Seminar INGEPET, Lima, Perú, November 5 – 8, 12 p.
- Fornari M., and G. Hérail, 1991, Lower Paleozoic gold occurrences in the "Eastern Cordillera" of southern Perú and northern Bolivia; a genetic model, *In* E.A. Ladeira eds., *Brazil Gold 91*, p. 135-142.
- Gerbault, M., J. Martinod, and G. Hérail, 2005, Possible orogeny-parallel lower crustal flow and thickening in the Central Andes: *Tectonophysics*, v. 399, p. 59-72.
- Gil, W., 2001, Evolución lateral de la deformación de un frente orogénico: Ejemplo de las cuencas Subandinas entre 0 y 16 grados S: Dissertation, Universidad Paul Sabatier Toulouse III, Toulouse, Francia, 132 p.

- Gil W., P. Baby, and J. F. Ballard, 2001, Structure et contrôle paléogéographique de la zone subandine péruvienne: Sciences de la terre et des planètes, Comptes Rendus de l'Académie des Sciences, Paris, v. 333, p. 741-748.
- Gil, W., P. Baby, R. Marocco, and J. F. Ballard, 1999, North-south structural evolution of the Peruvian sub-Andean zone: Fourth ISAG, Goettingen, Germany, October, p. 278-282.
- Gutiérrez, M., 1982, Zonación bioestratigrafica del intervalo Cretaceo Superior - Terciario Inferior: Informe Inédito Perupetro, 52 p.
- Gutiérrez-Marco, J.C., J. Saavedra, and Rábano, I. 1992. Paleozoico inferior de Ibero-América. Universidad de Extremadura, 630 p., ISBN 84-604-2767-6, p. 1-19.
- Henry, S. G., and H. N., Pollack, 1988, Terrestrial heat flow above the Andean subduction zone in Bolivia and Perú: Journal of Geophysical Research, v. 93, p. 15153 - 15162.
- Hermoza, W., 2004, Dynamique tectono-sédimentaire et restauration requentielle du retro-bassin d'avant-pays des Andes Centrales: Dissertation, Université Paul Sabatier Toulouse III, Toulouse, France, 296 p.
- Hermoza, W., S. Brusset, B. Patrice, W. Gil, M. Roddaz, N. Guerrero, and R. Bolaños, 2005, The Huallaga foreland basin evolution: thrust propagation in a deltaic environment, northern Peruvian Andes: Journal of South American Earth Sciences, v. 19, p. 21 - 34.

- Higley, D. K., 2004, The Progreso Basin province of northwestern Perú and southwestern Ecuador: Neogene and Cretaceous-Paleogene total petroleum systems: U.S. Geological Survey, Bulletin 2206-B, 20 p.
- Holth, S., 2005, Deformation, erosion and natural resources in continental collision zones: Dissertation, Freien Universität, Berlin, Germany, 141 p.
- Instituto Geológico Minero del Perú, (INGEMMET), 1984–1997, Cuadrángulos Geológicos Actualizados Escala 1:100,000, 18-M-23 O.
- Jacay, J., T. Sempere, L. Husson, and A. Pino, 2002, Structural characteristics of the Incapuquio fault system, southern Perú: V International Symposium of Andean Geodynamics, Toulouse, France, p. 319-321.
- Jacques, J., 2003a, A tectonostratigraphic synthesis of the Sub-Andean basins: implications for the geotectonic segmentation of the Andean Belt: *Journal of the Geologic Society of London*, v. 160, p. 687–701.
- Jacques, J., 2003b, A tectonostratigraphic synthesis of the Sub-Andean basins: inferences on the position of South American intraplate accommodation zones and their control on South Atlantic opening: *Journal of the Geologic Society of London*, v. 160, p. 703–717.
- Jaillard, E., P. Bengtson, and A. V. Dhondt, 2005, Late Cretaceous marine transgressions in Ecuador and northern Perú: a refined stratigraphic framework: *Journal of South American Earth Sciences*, v. 19, p. 307-323.
- Jaillard, E., G. Hérail, T. Monfret, E. Díaz-Martínez, P. Baby, A. Lavenue, and J. F. Dumont, 2000, Tectonic evolution of the Andes of Ecuador, Perú, Bolivia and

- northernmost Chile, *In* Cordani, U. G., E. J. Milani, A. Thomaz Filho and D. A. Campos, 2000, Tectonic evolution of South America, Rio de Janeiro Brasil, 31st International Geological Congress, p. 481-559.
- Jaillard, E., and P. Soler, 1996, The Cretaceous to Early Paleogene tectonics evolution of the northern Central Andes and its relations to geodynamics: *Tectonophysics*, v. 259, p. 41-53.
- Jaillard, E., P. Soler, G. Carlier, and T. Mourier, 1990, Geodynamic evolution of the northern and central Andes during Early to Middle Mesozoic times: a Tethyan model: *Journal of the Geologic Society of London*, v. 147, p. 1009-1022.
- Kummel B., 1946, Estratigrafía de la región de Santa Clara: *Boletín de la Sociedad Geológica del Perú*, v. 19, p. 133-152.
- Laurent H., and A. Pardo, 1974, Ensayo de interpretación del basamento del nor-oriental Peruano: III Congreso Peruano de Geología, Sociedad Geológica del Perú, v. 48, Parte 4, p. 25-48.
- Legrand, D., P. Baby, F. Bondoux, C. Dorbath, S. Bes de Berc, and M. Rivadeneira, 2005, The 1999 - 2000 seismic experiment of Macas swarm (Ecuador) in relation with rift inversion in Subandean foothills: *Tectonophysics*, v. 395, p. 67-80.
- Leight R., and A. Rejas, 1966, Columna estratigráfica Pongo de Paquitzapango, Río Ene: Internal Report., Petroperú, 62 p.
- Marksteiner, R., and Aleman, A., 1997, Petroleum systems along the fold belt associated to the Marañon-Oriente-Putumayo (MOP) foreland basins: VI Simposio Bolivariano "Exploración Petrolera en las Cuencas Subandinas", v. 2, p. 63-74.

- Martínez M., 1975, Tectónica del área Ucayali central: Boletín de la Sociedad geológica del Perú, v. 45, p. 61-82.
- Mégard, F., 1984, The Andean orogenic period and its major structures in central and northern Perú: Journal of the Geologic Society of London, v. 141, p. 893-900.
- Mégard F., 1979, Estudio Geológico de los Andes del Perú Central: Instituto Geológico Minero y Metalúrgico del Perú. Boletín N° 8 Serie D, Estudios Especiales, 227 p.
- Mégard, F., D. C. Noble, E. H. McKee, and H. Bellon, 1984, Multiple pulses of Neogene compressive deformation in the Ayacucho intermountain basin, Andes of central Perú: Geological Society of America Bulletin, v. 95; No. 9; p. 1108-1117.
- Müller H., 1982, Evaluación potencial petrolífero cuencas Huallaga, Ucayali y Madre de Dios, Estudio palinológico del Mesozoico y Paleozoico: Cooperación Técnica Peruano – Alemana, Informe Inédito, Petroperú. 103 p.
- Navarro L., P. Baby, and R. Bolaños, 2005, Structural style and hydrocarbon potential of the Santiago basin: V International Seminar INGEPET, Lima, Perú, Nov. 8-11, 15 p.
- Petróleos del Perú, 1962, Columna estratigráfica pozo Agua Caliente: Reporte Interno, Perú, v. 1, .mapa A, 19 p.
- Perupetro S. A., 2003, Ucayali/Ene basin technical report, Lima, Perú, v. 1, 96 p.
- Quintana Minerals Perú LLC, 1998, Remaining petroleum potential of block 81 Ucayali basin Peru: Internal Report, Perupetro, v. 1, 37 p.

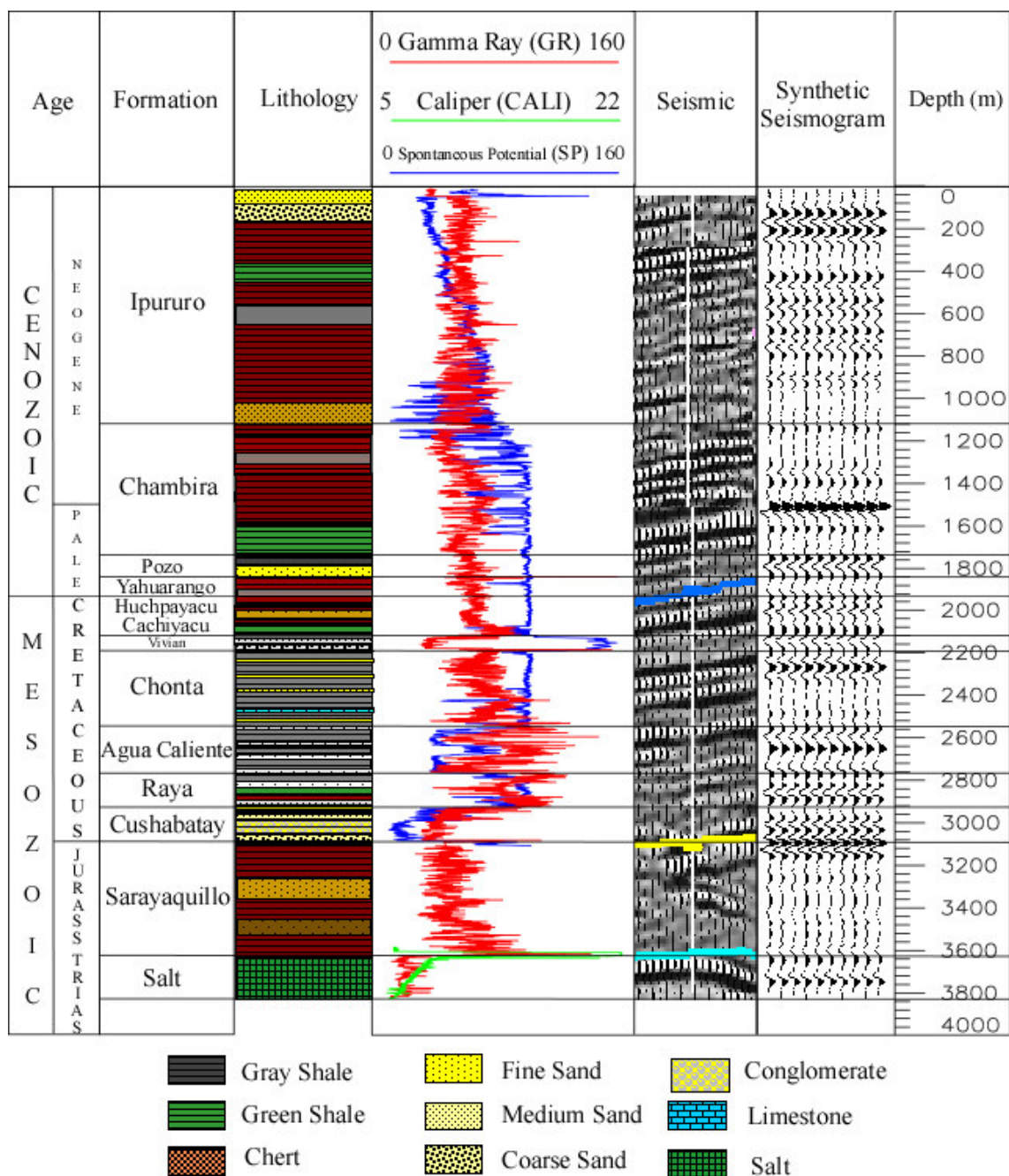
- Ramos, V.A., and Aleman, A., 2000, Tectonic evolution of the Andes, *In* Cordani, U., Milani, E.J., Thomaz Filho, A., and Campos Neto, M.C., eds., Tectonic evolution of south America: Rio de Janeiro, Brazil, p. 635-685.
- Repsol Exploration, 2002, Final well report: Mashansha 35-13-1X: Internal Report for Perupetro, Lima, Perú, v. 1, 194 p.
- Repsol YPF, 2001a, Evaluación geológica por hidrocarburos en el flanco oriental de las montañas del Sira, lote N° 34: Reporte Técnico para Perupetro, Lima, Perú, v. 1, 30 p.
- Repsol YPF, 2001b, Evaluación geológica por hidrocarburos en el flanco oriental de las montañas del Sira, lote N° 35: Reporte Técnico para Perupetro, Lima, Perú, v. 1, 36 p.
- Rivadeneira, M. B., and P. Baby, 1999, La cuenca Oriente: estilo tectónico, etapas de deformación y características geológicas de los principales campos de petroproducción: IRD (Ex ORSTOM), v. 1, 88 p.
- Roddaz, M., P. Baby, S. Brusset, W. Hermoza, and J. M. Darrozes, 2005, Forebulge dynamics and environmental control in western Amazonia: the case study of the Arch of Iquitos (Perú): Tectonophysics, v. 399, p. 87-108.
- Rojas V., 2002, REPSOL Exploration Peru, Ucayali basin block 35, Mashansha 35-13-1X, lithological samples evaluation: Internal Report, Perupetro, v. 1, 130 p.
- Sandeman, H. A., A. H. Clark, and E. Farrar, 1995, An integrated tecto-magnetic model for the evolution of the southern Peruvian Andes (13-208 s) since 55 Ma: International Geological Review, v. 37, p. 1039-1073.

- Sempere, T., G. Carlier, P. Soler, M. Fornari, V. Carlotto, J. Jacay, O. Arispe, D. Neraudeau, J. Cardenas, S. Rosas, and N. Jimenez, 2002, Late Permian-Middle Jurassic lithospheric thinning in Perú and Bolivia, and its bearing on Andean-age tectonics: *Tectonophysics*, v. 345, p. 153-158.
- Soler, P., 1989, Petrography and geochemistry of lower Cretaceous alkali basalts from the High Plateaus of central Perú and their tectonic significance: *Zentralblatt für Geologie und Paläontologie*, Stuttgart, v. (5/6), p. 1053-1064.
- Soulas, J., and P. Paris, 1977, Les phases tectoniques Andines du Tertiaire Supérieur, résultats d'une transversale Pisco-Ayacucho, Pérou central, *Comptes rendus hebdomadaires des séances de l'académie des sciences, Série D*, No. spécial, 284 p.
- Storti, F., and J. Poblet, 1997, Growth stratal architectures associated to decollement folds and fault-propagation folds. Inferences and fold kinematics: *Tectonophysics*, v. 282, p. 553-573.
- Suárez, G., J. Gagnepain, A. Cisternas, D. Hatzfeld, P. Molnar, L. Ocola, S. Roecker, and J. Viodé, 1990, Tectonic deformation of the Andes and the configuration of the subducted slab in central Peru: result from a microseismic experiment: *Geophysical Journal International*, v. 103, p. 1-12.
- Tankard, A.J., S. Suarez, and R. Wels, 1995, Petroleum basins of South America: *American Association of Petroleum Geologists, Memoir 62*, p. 101-128.

- Tassara, A., 2005, Interaction between the Nazca and South American plates and formation of the Altiplano-Puna plateau: review of a flexural analysis along the Andean margin (15-34 degrees S): *Tectonophysics*, v. 399, p. 39-57.
- Velarde P., C. Bustamante, and O. Reategui, 1978, Evaluación geológica preliminar de las sub cuencas del Ucayali y Madre de Dios: Internal. Report Petroperú, 165 p.
- Williams, G. D., C. M. Powell, and M. A. Cooper, 1989, Geometry and kinematics of inversion tectonics, *In* M.A. Cooper and G. D. Williams, eds., *Inversion tectonics: The Geological Society Special Publication 44*, p. 3–15.

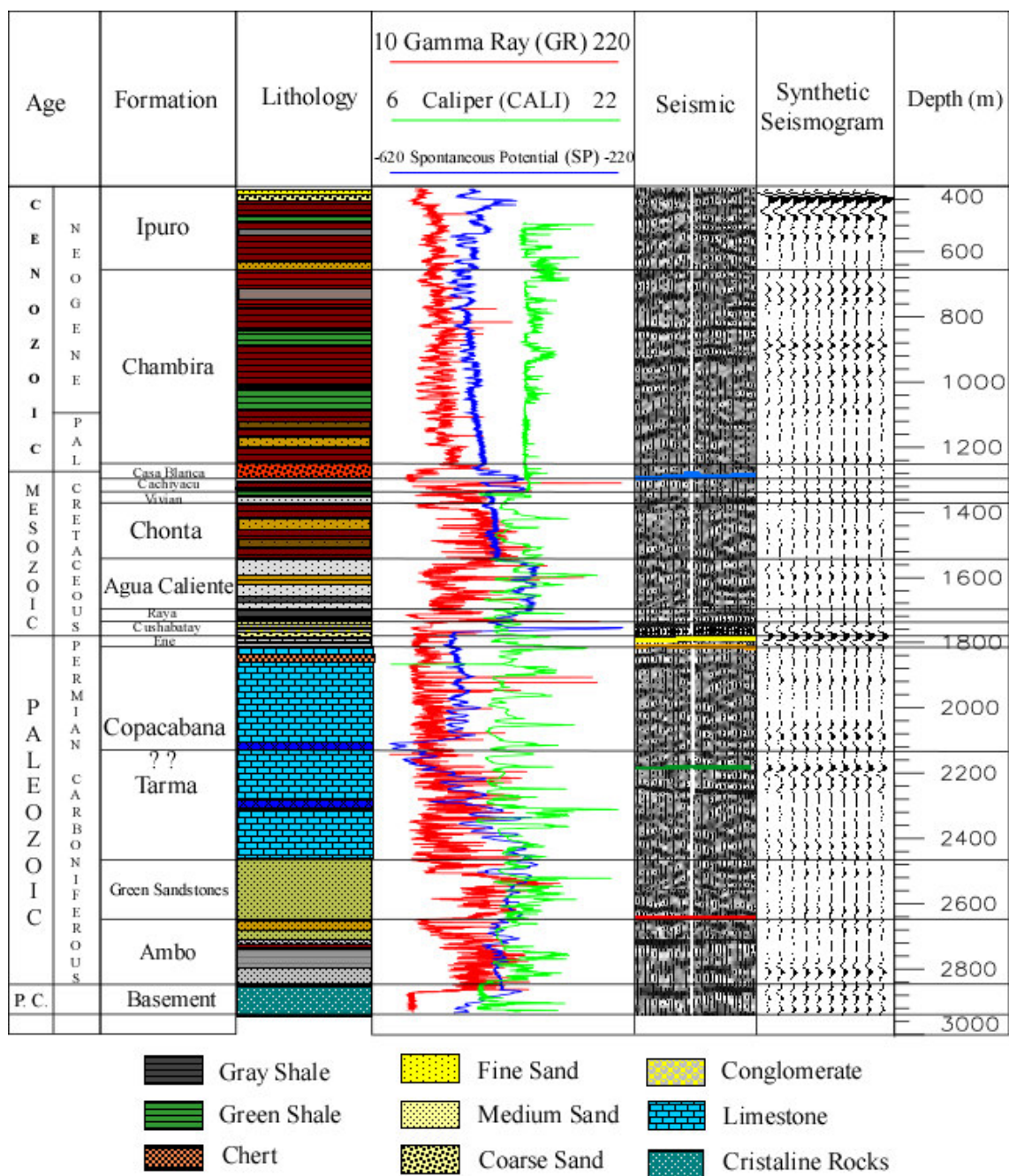
APPENDIX 1

CHIO COMPOSITE LOG



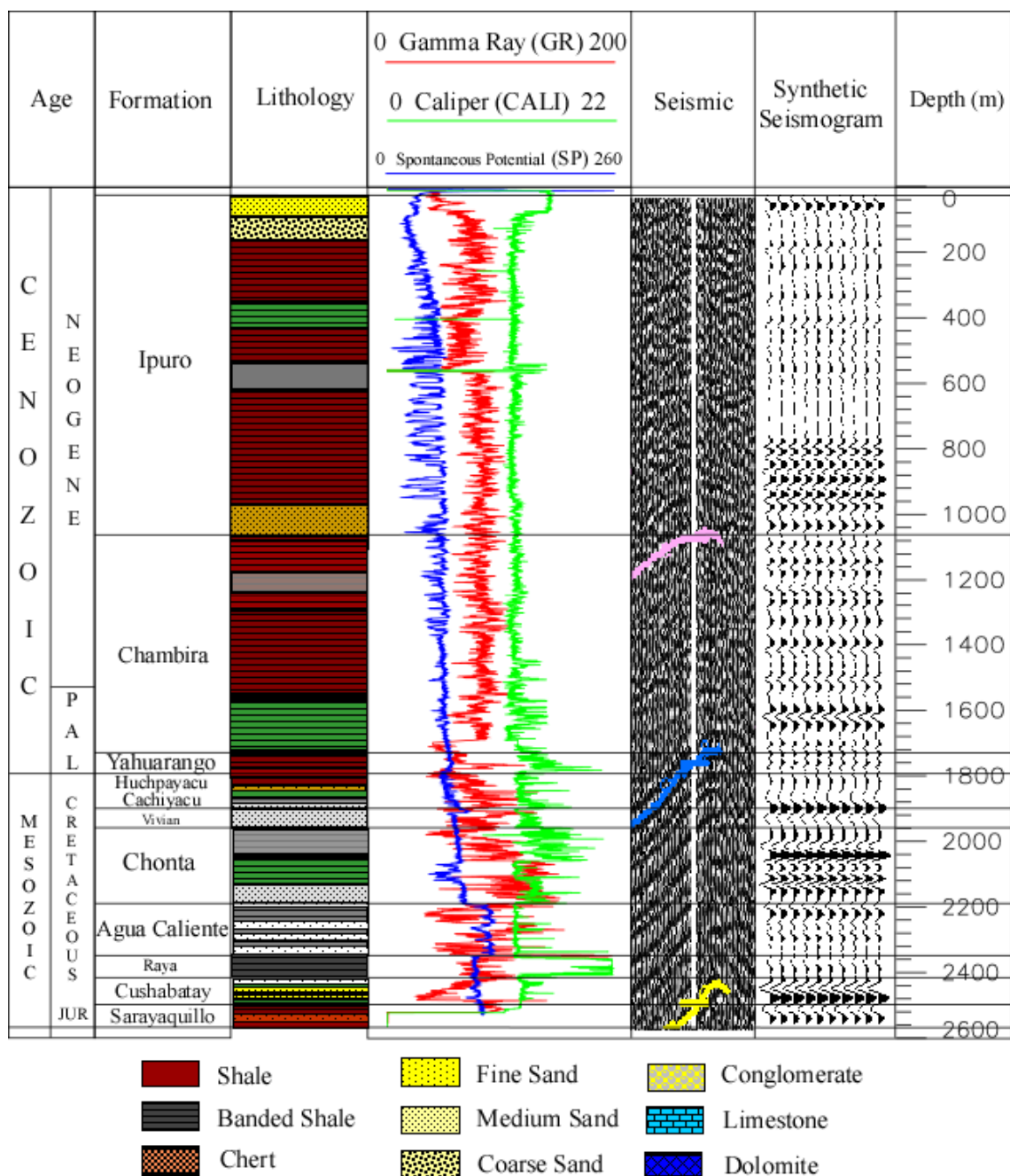
APPENDIX 2

LA COLPA COMPOSITE LOG



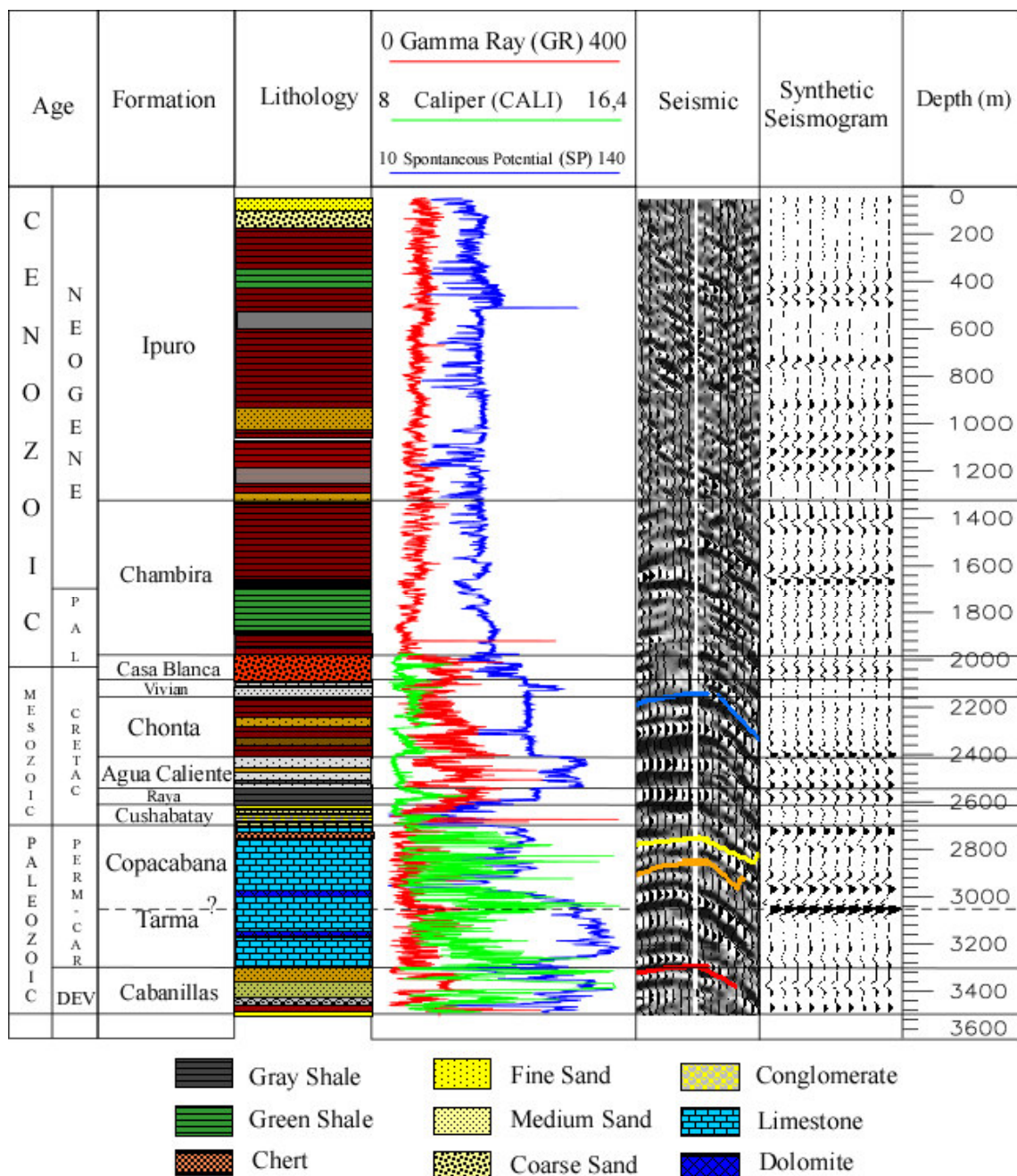
APPENDIX 3

RIO CACO COMPOSITE LOG



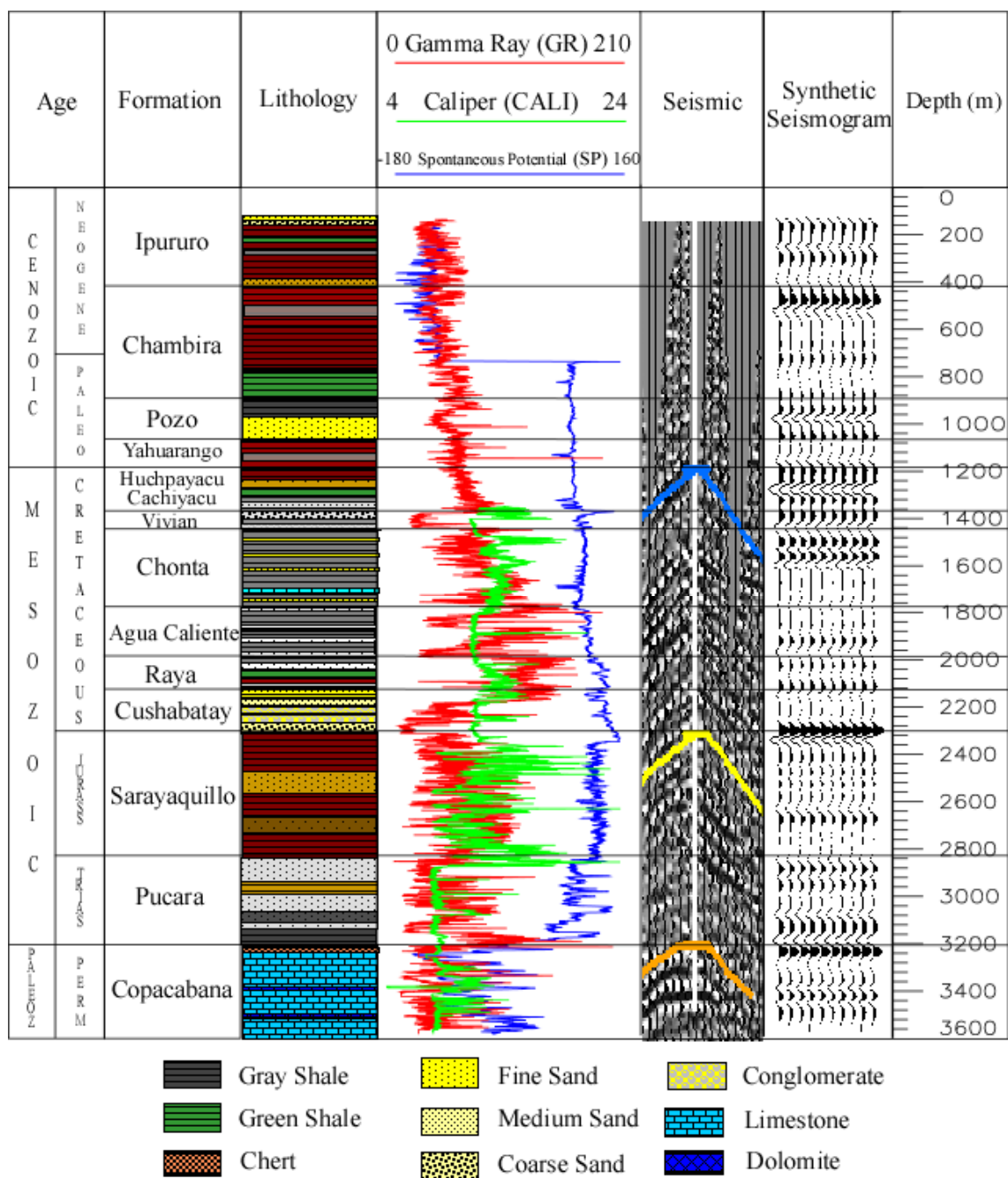
APPENDIX 4

RUNUYA COMPOSITE LOG



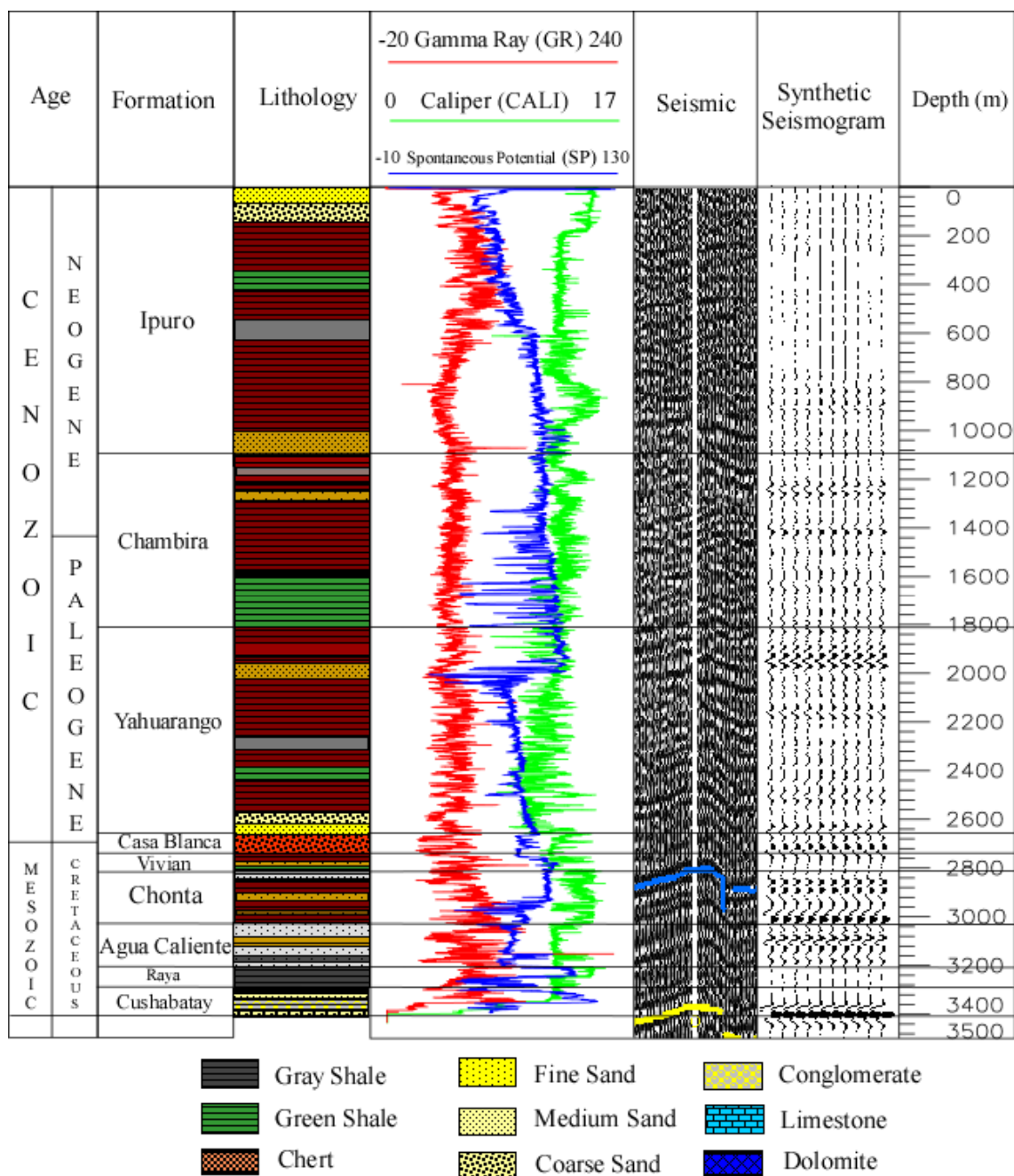
APPENDIX 5

SAN ALEJANDRO COMPOSITE LOG



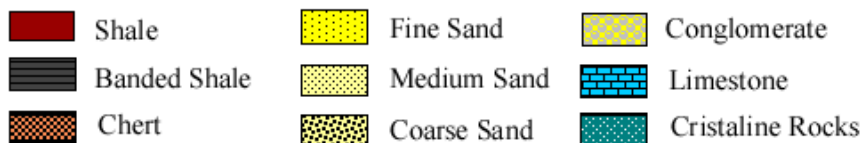
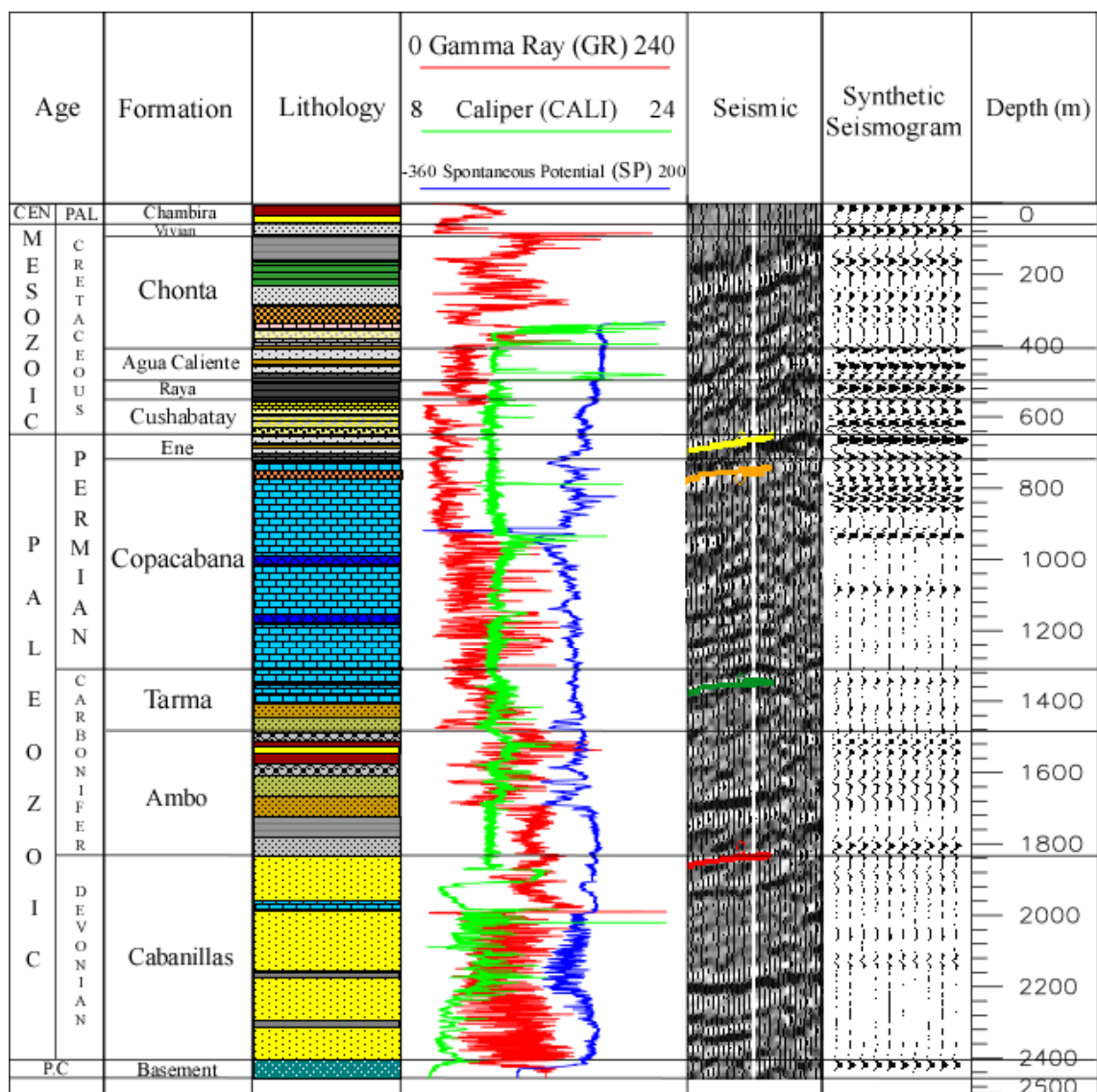
APPENDIX 6

SANUYA COMPOSITE LOG



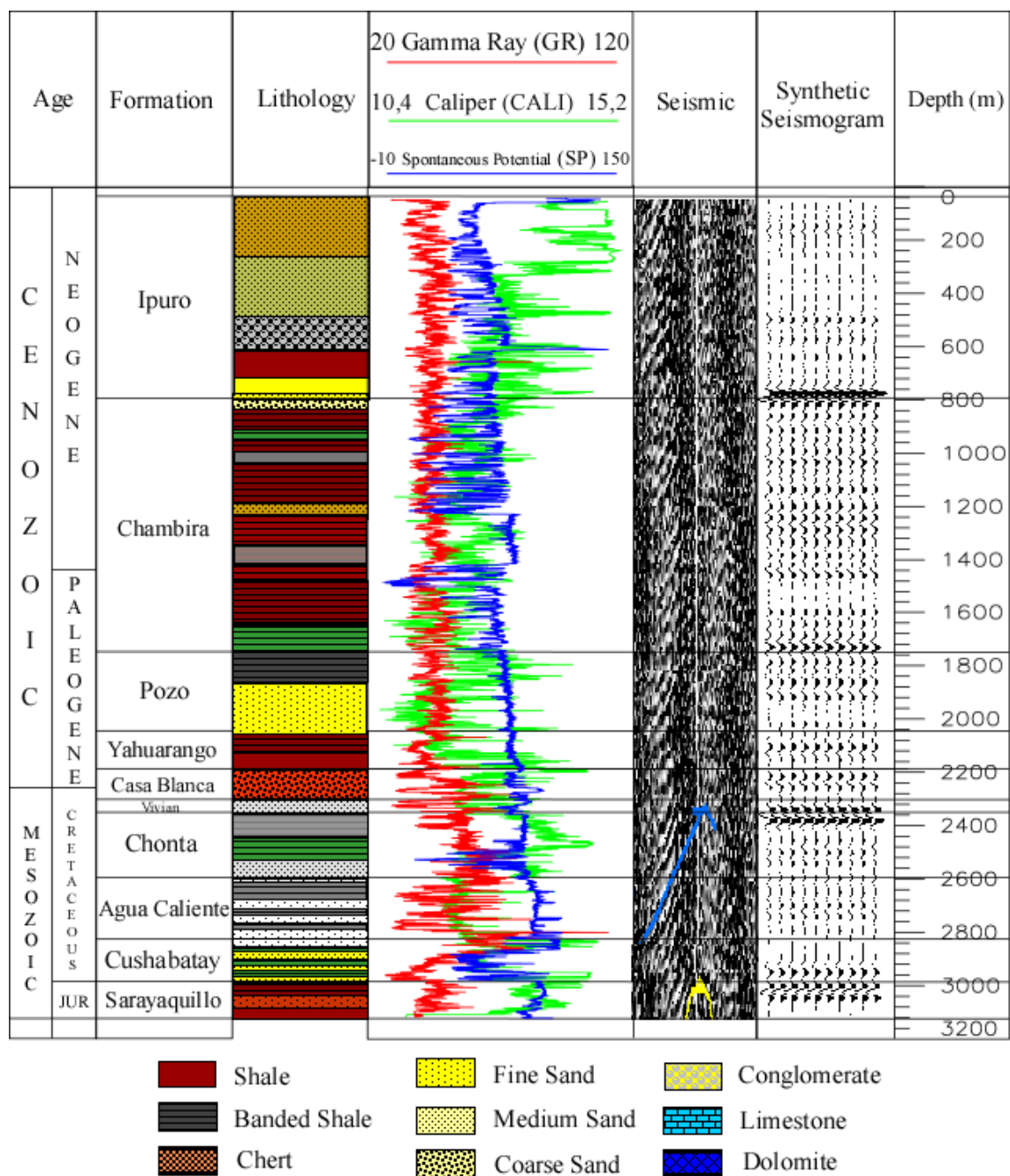
APPENDIX 7

SEPA COMPOSITE LOG



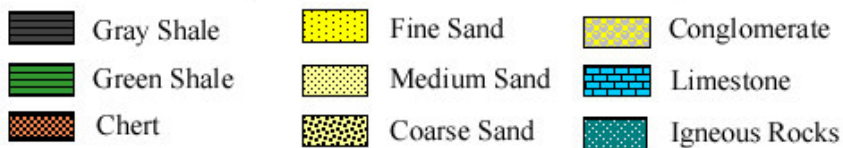
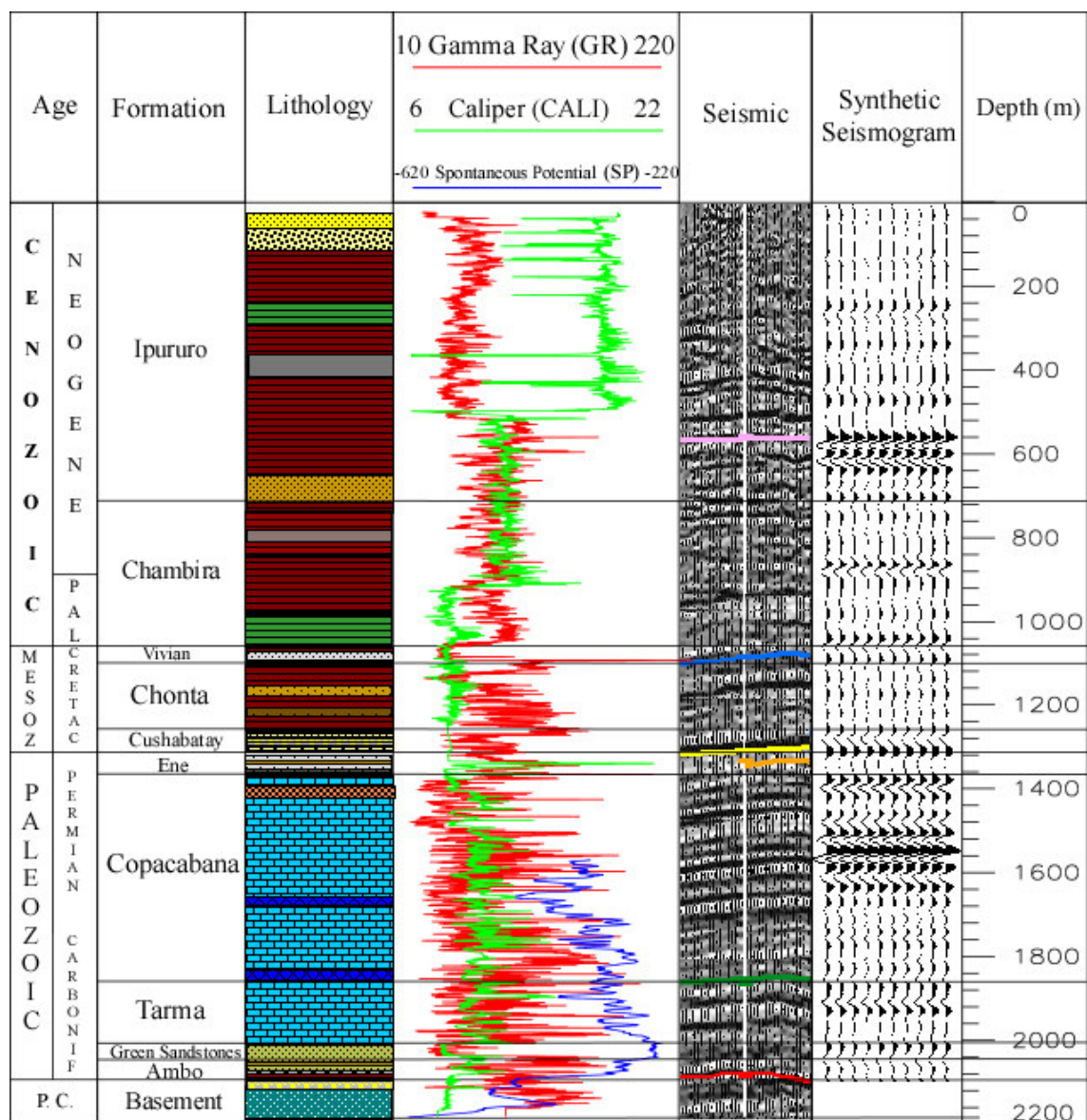
APPENDIX 8

TAMAYA COMPOSITE LOG



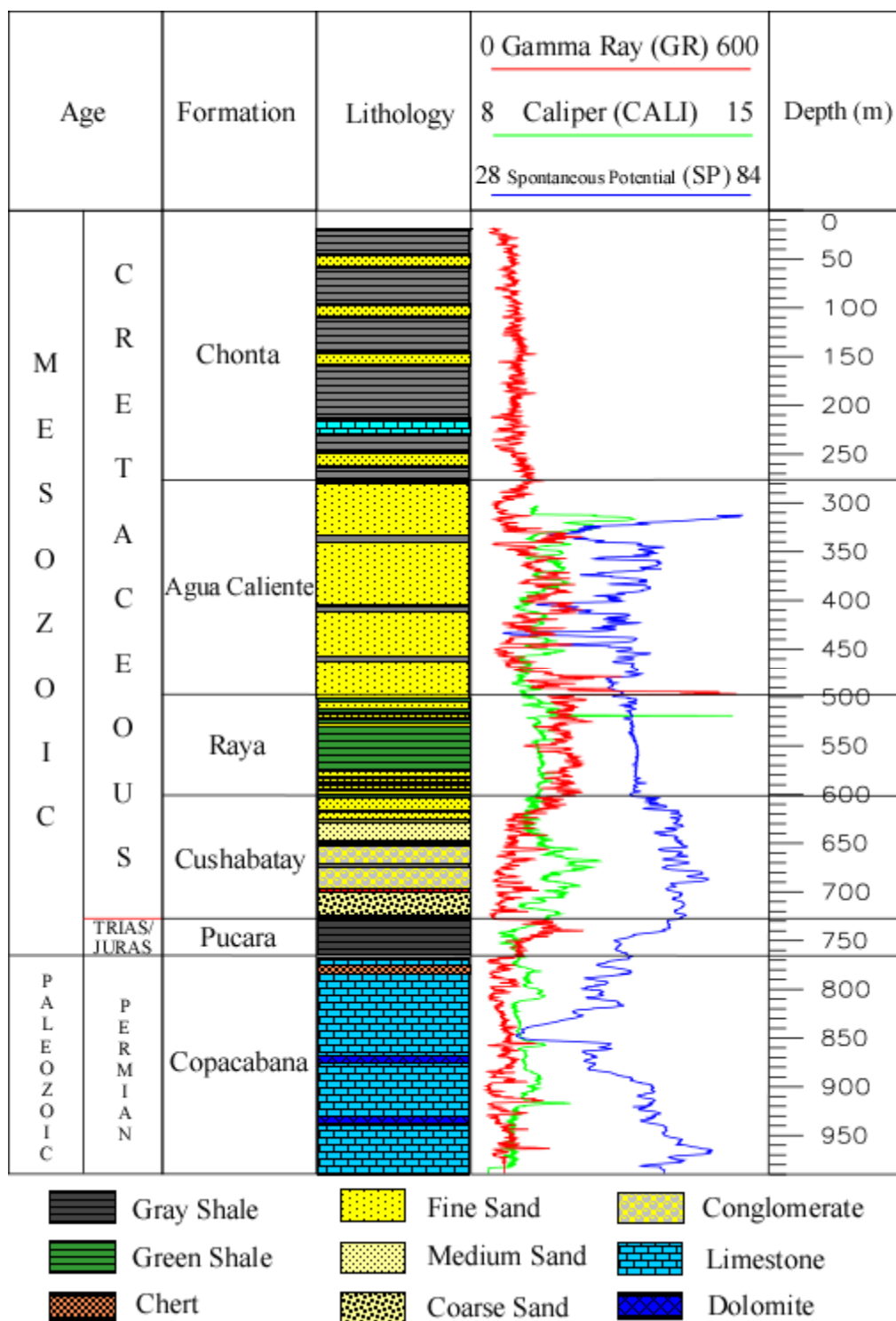
APPENDIX 9

MASHANSHA COMPOSITE LOG



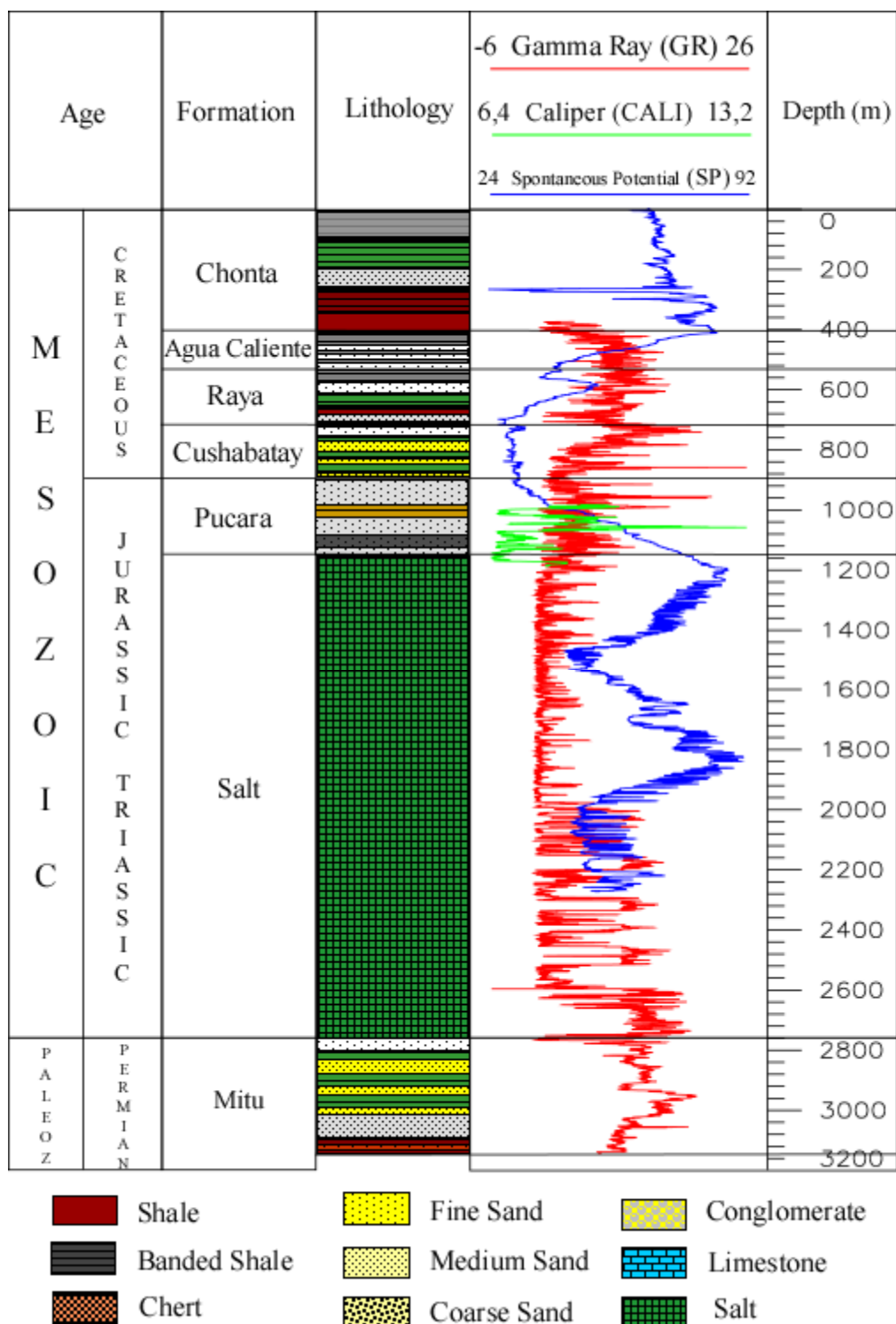
APPENDIX 10

AGUA CALIENTE COMPOSITE LOG



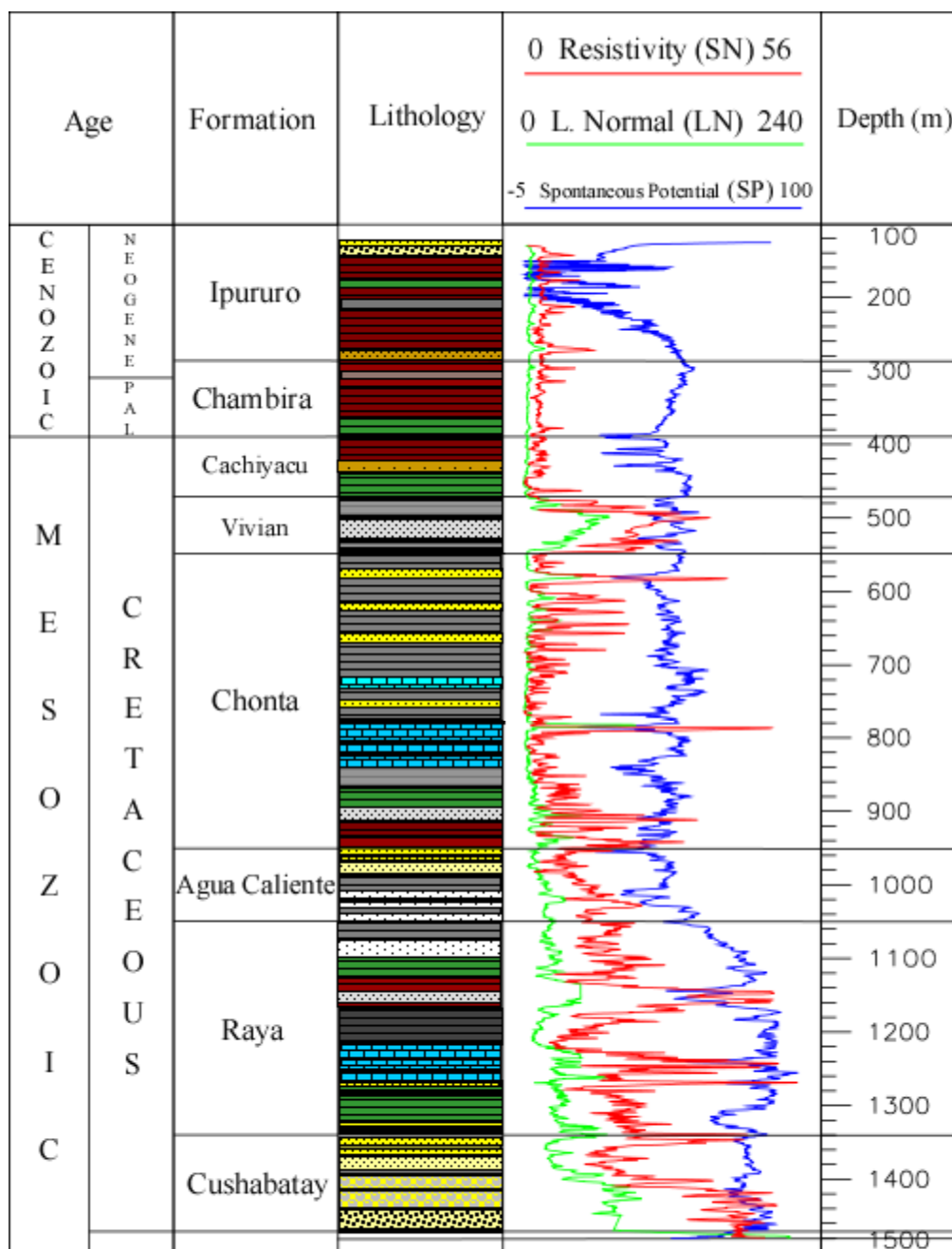
APPENDIX 11

OXAPAMPA 7-1 COMPOSITE LOG




APPENDIX 12

OXAPAMPA 19-2 COMPOSITE LOG


 Shale


 Banded Shale

 Chert

 Fine Sand

 Medium Sand

 Coarse Sand

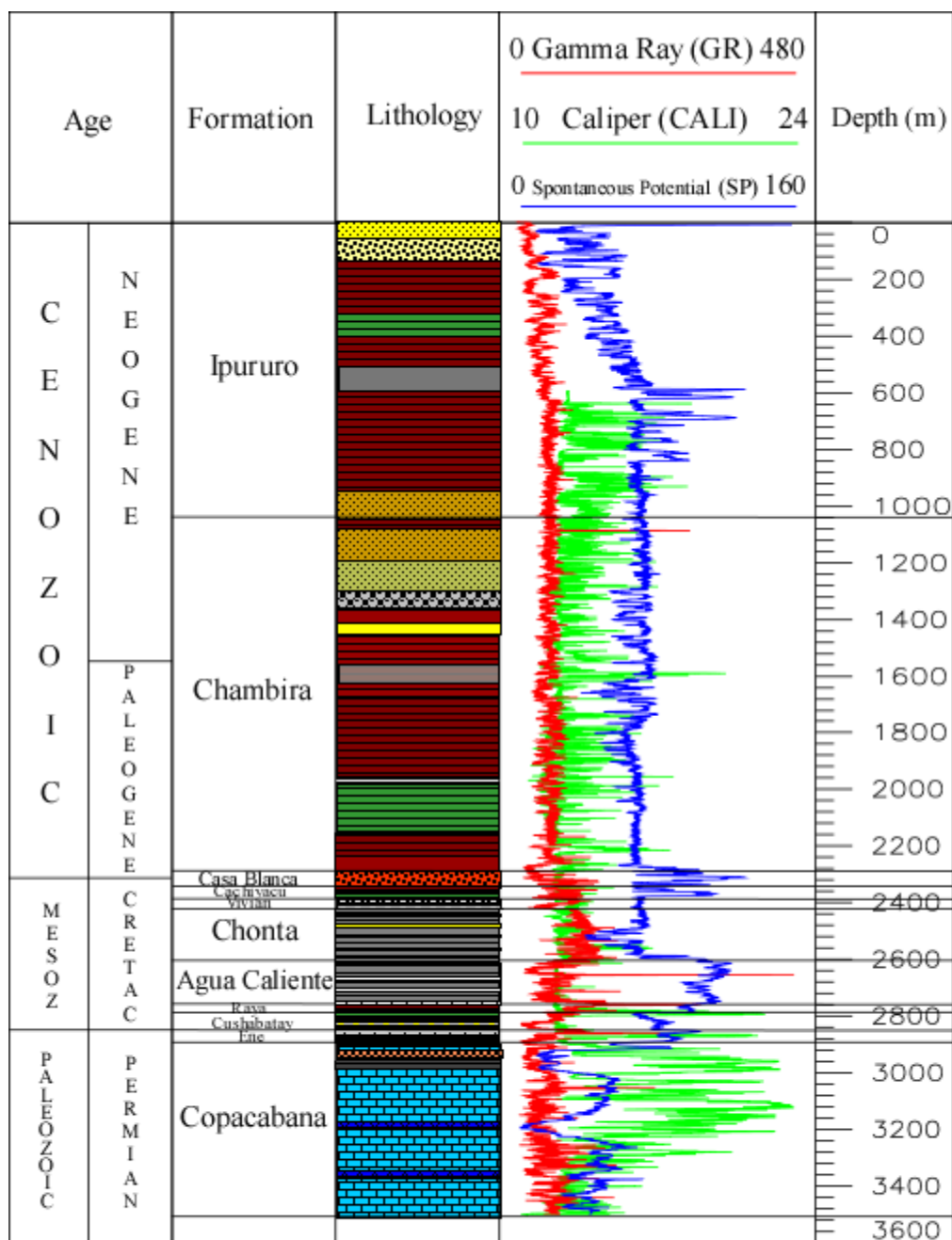
 Conglomerate

 Limestone

 Dolomite

APPENDIX 13

PLATANAL COMPOSITE LOG



Gray Shale

Green Shale

Chert

Fine Sand

Medium Sand

Coarse Sand

Conglomerate

Limestone

Dolomite

VITA

Name,	Jaime Orlando Sanchez Alvarez
Mailing Address,	4313 Eigel St. Houston, TX 77007 USA
Educational Background,	B.S. in Geology Universidad Industrial de Santander December, 1999 Bucaramanga, Colombia M.S. in Geology Texas A&M University December, 2007 College Station, TX, USA
Professional Organizations,	American Association of Petroleum Geologist (AAPG), Society of Exploration Geophysicist (SEG)